Technical Report No. 237

THE REMOTE ESTIMATION OF A GRASSLAND CANOPY: ITS BIOMASS CHLOROPHYLL, LEAF WATER, AND UNDERLYING SOIL SPECTRA

C. J. Tucker and L. D. Miller

Department of Watershed Science

Colorado State University

Fort Collins, Colorado

GRASSLAND BIOME

U. S. International Biological Program

November 1973

"Next in profusion to the divine profusion of water, light, and air, those three physical facts which render existence possible, may be reckoned the universal beneficence of grass."

Blue Grass

by John James Ingalls (1833-1900)

FRONTISPIECE. BLUE GRAMA GRASS (*Bouteloua gracilis*) SILHOUETTED AGAINST THE PRAIRIE SKY. Blue grama, the principal forage species of the shortgrass prairie, was selected for study in this thesis.

TABLE OF CONTENTS

ABSTRACT

The dynamics of a grassland ecosystem can be expressed in terms of its biomass characteristics. This involves the biomass of all its organisms from microoragnisms to plants, herbivores, carnivores, etc. The principal driving force in this biomass pyramid is the primary producer component of the system--the photosynthesizing grasses upon which all other trophic levels depend. Accurate measurements of the amount of grass biomass and its physiological status would enable more effective utilization of rangelands.

The remote sensing estimation of the grass biomass and its physiological status was initially approached by the development of a stochastic leaf radiation model. This model was used to predict the interaction of electromagnetic energy with green leaves based upon leaf structure, pigment composition and concentration, and the amount of leaf water present.

The model results have been validated by the measurement and statistical spectroanalysis of the *in situ* canopy reflectance. These statistical results expressed as a function of wavelength define the relative sensitivity between the biophysical measurements of the canopy and the resulting coding of the reflected radiation. Results of the spectroregression analysis indicate that the biomass, chlorophyll, leaf water, and underlying soil spectra can be extracted from the spectroreflectance measurements of the grass canopy of the shortgrass prairie.

ACKNOWLEDGMENTS

The author expresses appreciation to the faculty member on his committee. Special acknowledgement is given to my major professor, Lee D. Miller, for guidance during the preparation of this thesis. The assistance of Jim Smith, Joe Trlica, Freeman Smith, and Cleon Ross was appreciated during the development of the stochastic leaf model.

I was fortunate to have the able and amiable assistance of fellow students Bob Oliver, Jon Ranson, Ralph Root, Bob Pearson, Betty Clayton, Sharron Betz, and Tom Ells. The capable photographic services of R. L. Tucker and Don Skitt enabled the presentation of many microfilm figures and were likewise appreciated.

1.0 INTRODUCTION

The dynamics of a grassland ecosystem are often expressed in terms of its biomass characteristics. This involves estimates of the biomass of all of its organisms, including soil microorganisms, plants, herbivores, and carnivores. The principal state variable in this ecosystem is that component of the system which directly converts energy from the sun into bound chemical energy--the primary producers--the photosynthesizing grasses upon which all other trophic levels ultimately depend (Fig. 1) (French, 1971).

The existence of all living organisms is principally based upon the ability of the green plant to utilize the energy of electromagnetic radiation to produce carbohydrates from inorganic materials. Plant pigments, primarily the chlorophylls, enable the primary producers to utilize solar energy in the process of photosynthesis.

The organic compounds that compose the living world are directly or indirectly derived from the carbohydrates yielded by photosynthesis. This stored energy is released and utilized by organisms to drive essential metabolic processes by oxidation of organic compounds. All of the energy released during the oxidation of organic compounds is ultimately derived from energy captured by green plants during photosynthesis.

The process of photosynthesis depends upon the efficient capture of electromagnetic energy by pigments present in plant tissues.

DYNAMIC MODEL OF ECOSYSTEMS

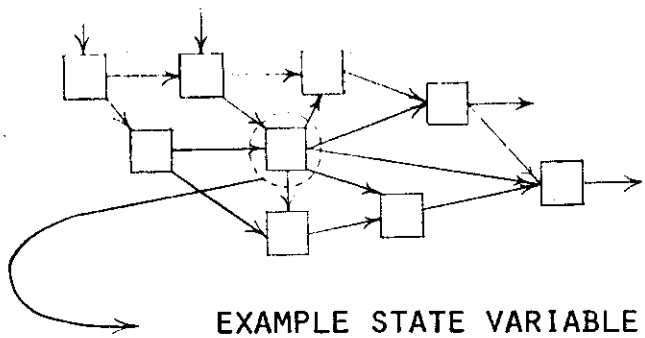

EXAMPLE STATE VARIABLE

RATE PROCESSES CAUSING INPUTS

-PHOTOSYNTHESIS

-TRANSLOCATION

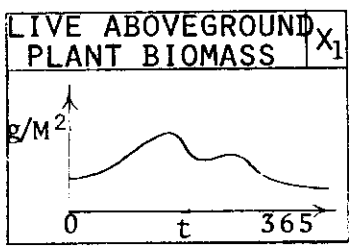

RATE PROCESSES CAUSING OUTPUTS

-HERBIVORY
-WEATHERING
-TRAMPLING
-TRANSLOCATION
-DEATH

EXAMPLE RATE PROCESS

PHOTOSYNTHESIS RATE = f

AFFECTED BY

- -LEAF AREA } STATE VARIABLES
- -SOIL MOISTURE } STATE VARIABLES
- -SOLAR RADIATION } DRIVING VARIABLES
- -TEMPERATURE } DRIVING VARIABLES

COMBINE ABOVE FEATURES IN DIFFERENTIAL EQUATION SYSTEM

$$\frac{dXi}{dt} = f\ (\text{INPUTS}) - g\ (\text{OUTPUTS})$$

OR

$$\dot{\underset{\sim}{X}} = f\ (\underset{\sim}{X}, \underset{\sim}{Z}, t)$$

$\underset{\sim}{X}$ = VECTOR OF STATE VARIABLES

$\underset{\sim}{Z}$ = VECTOR OF DRIVING VARIABLES

Figure 1. DYNAMIC MODEL OF A GRASSLAND ECOSYSTEM ILLUSTRATING THE INTERRELATIONSHIPS BETWEEN COMPONENTS (extracted from French, 1971).

Electromagnetic energy has to be absorbed before it can be used in a photobiological reaction. The process is initiated by the absorption of light energy by the photosynthetic pigments. This results in the production of carbohydrates through utilization of the absorbed energy to reduce carbon dioxide. Carbon dioxide is then chemically combined with water to yield carbohydrates (Delvin and Barker, 1970).

The ability of plants to produce carbohydrates results in energy being made available for all trophic levels. The various species of grasses, forbs, and shrubs serve as the main source of energy for other trophic levels in a grassland ecosystem. Methods to accurately and efficiently map the primary productivity over a large geographical area on a timely basis are needed. They will make available to range managers the data base necessary for efficient area management of the range resources which comprise one-sixth of the world's land area and 40 per cent of the continental United States.

Traditional methods for estimating the productivity of rangelands do not lend themselves to application over large geographical areas. These methods and other more recently proposed methods involve the measurement of herbage biomass by several ground sampling techniques. The most traditional quantitative techniques commonly used involve the hand clipping of a known area of vegetation and weighing the resulting sample. The usefulness of clipping as a sampling method is limited by two characteristics. First, it is a slow, tedious and time-consuming operation. Second, clipping is a destructive sampling procedure which prevents sampling the same plot

on a repetitive basis. Several nondestructive sampling methods are available and include the ocular estimation procedure (Pechanec and Pickford, 1937), the point quadrat method (Warren Wilson, 1963), the capacitance meter (Van Dyne *et al*, 1968), the β-attenuation technique (Mitchell, 1972), and the multispectral method (Pearson and Miller, 1972).

The spectral method of range vegetation analysis used measurements of the solar energy reflected from the vegetation canopy in the 0.30 to 3.0 μm region of the electromagnetic spectrum from ground, aircraft or satellite based remote sensors. The variation with wavelength in this reflected solar spectrum when compared with the spectrum of incident solar energy contains coded information on the amount, type, and vigor of the vegetative canopy present. Proper decoding of this spectrum has been used to map the spatial distribution of the vegetative biomass of a grassland. It should also map the vegetation in terms of chlorophyll and leaf water content, thereby describing the functioning mass of the vegetation present in the grassland canopy. Spectral methods of analysis have been applied from aircraft for several years with great success (Colwell, 1969) and have recently been applied via the Earth Resource Technology Satellite (ERTS). Aircraft and satellite platforms afford scientists a synopic base with which to analyze the vast grassland areas of the world. It is reasonable to believe that satellite based remote sensing endeavors will make as much of an impact upon resource management as the TIROS, NIMBUS and ATS weather satellites have made upon weather forecasting. The periodic remote sensing

measurement of characteristics of rangeland vegetation from satellites and aircraft will provide spatial inputs to management models to represent primary productivity and its dynamics. It is difficult to imagine that this essential spatial information can be measured by any other means on a timely basis.

The purpose of the research reported here has been to determine if the amount of graminous herbage (the grass biomass) and information about its physiological status can be measured by remotely sensed spectral information in the .350 to .800 μm region of the spectrum. Initially this was approached by the development of a leaf radiation model based upon physiological and physical properties of leaves. This leaf model, based upon leaf structure, pigment content, and water content, was used to predict the interaction of electromagnetic energy with green leaves. The mathematically modeled effect of these characteristics upon leaf spectroabsorptance, spectroreflectance, and spectrotransmissance has in turn been validated by their measurement and statistical analysis for the canopy. The specific modeling and validation measurement approaches of this research are best understood if a review of the current methods used in measuring and estimating grassland vegetative characteristics is made. The next section entitled BACKGROUND reviews the physiological and ecological significance of chlorophyll, leaf water, and canopy biomass and the various methods used to measure or estimate these characteristics.

2.0 BACKGROUND

2.1 Chlorophyll and its *In Situ* Estimation

The ability of chlorophyll molecules to harness the energy of the sun to reduce carbon dioxide and ultimately produce carbohydrates is the basis for life. The primary productivity or photosynthetic rate of plants depends upon chlorophyll content, incident radiation, water, nutrients, and genetic response coupled to controlling driving variables. The photosynthetic rate can be modeled knowing these characteristics. Genetic variability is excluded to a greater extent when a particular plant species is selected for analysis. The effects of nutrients and driving variables can be considered as a function of site location. The solar irradiance is also a function of location (i.e. latitude), atmospheric conditioning, and time of year. The water and chlorophyll content of leaves depends almost entirely upon short term environmental conditions (temperature, radiation, precipitation, etc.) and are directly interrelated.

Ecological evaluation of the significance of chlorophyll ranges from the hypothesis that the chlorophyll content of different plant communities is approximately the same (Gessner, 1949) to the other extreme hypothesis that marked differences exist between the chlorophyll content of different plant communities (Ovington and Lawrence, 1967). Comparison of the oven-dry weight and chlorophyll content in six forest and thirteen native herbaceous stands in central Minnesota

showed strong positive correlations (Bray, 1960). Additional study of these same stands suggested that an apparent correlation between chlorophyll content and the annual accumulation of dry matter existed. This indicated that the annual productivity of an ecosystem might be estimated from chlorophyll extracts (Bray, 1966).

The solar energy flux, chlorophyll content, and resulting photosynthetic rate have been considered theoretically. It has been suggested that chlorophyll content of a plant community might be used to estimate the net organic matter production (Anderson, 1967). Unfortunately, the chlorophyll content of plant canopies is troublesome to measure, does not account for losses through death and herbivory, and cannot be readily sampled and compared between species. The main difficulty is the complexity introduced by tree or plant canopy geometry which makes it very tedious to accurately sample the chlorophyll present in the ecosystem.

The use of *in situ* spectrometric methods for estimating chlorophyll potentially provides a technique whereby chlorophyll in the entire plant canopy may be assayed. Spectrometric methods for measuring chlorophyll concentrations have been reported for algae, citrus leaves, and agricultural crops (Arvesen *et al*, 1971; Duntley, 1972; Mueller, 1972; Benedict and Swidler, 1961; Carnenas and Gausman, 1971; Gausman *et al*, 1971). These methods use spectroradiometric measurements of a leaf, canopy, or ocean profile which have been related to chlorophyll content by a least squares regression approach. The current limiting factor in applying this technique to all vegetative types and surfaces is the high leaf area index (LAI)

of some forest vegetation canopies. For example, in a prarie ecosystem this type of measurement currently provides excellent results because of the simplicity of the vegetation canopy and its low LAI as compared to a coniferous or deciduous forest where the multiple leaf layering and more complex structure *may* not permit such measurements. A forest canopy does, however, contain chlorophyll and intercepts solar radiation. Therefore, a related method for spectrometric estimation of the chlorophyll in the *in situ* forest canopy may yet be designed.

2.2. Leaf Water and its *In Situ* Estimation

Photosynthesis of a shortgrass prairie canopy is quite dependent upon the availability of soil water derived from precipitation. Most growth of the blue grama (*Bouteloua gracilis*) component of this system occurs during the early summer when temperatures are high and soil water is not limiting (Bement, 1968). Development of non-destructive techniques to readily estimate leaf water should enable the rate of photosynthesis for blue grama to be modeled through coupling of the leaf water measurement with measurements of the canopy or air temperature, solar irradiance, and leaf area index. Several spectro-optical and photographic methods have been used to remotely estimate the water content or water stress in natural plant and crop canopies. Earlier studies using remotely measured spectroradiance for this specific purpose dealt with the measurement of plant vigor by near infrared black and white photography (Gibson *et al*, 1965; Eastman Kodak Co., 1968). Reductions in plant vigor

are discernible in this 0.7 to 1.0 μm spectral region on commercially available infrared film due to a corresponding decrease in the spectroreflectance of the plant canopy in this spectral region (Knipling, 1967). Numerous studies have outlined this same general approach using Ektachrome infrared film to measure vegetation vigor (Tarkington and Sorem, 1963; Fritz, 1967).

The vigor of a functioning vegetation canopy is highly dependent upon the water status of the leaves. Leaves with non-limiting leaf water concentrations retain their turgidity and internal structure and as leaves become dehydrated, turgidity and the internal cellular water volumes decrease. This causes a marked decrease in reflectance in the photographic infrared (1.7 to 1.0 μm) because of changes in the internal scattering mechanisms responsible for leaf reflectance (Knipling, 1970). Leaf water decreases which are insufficient to cause changes in cellular volume do not significantly affect spectroreflectance in the spectral region of 0.400 to ∿1.300 μm.

The leaf water status of vegetation can be measured directly from spectroradiance in the ∿1.300 to 2.600 μm region of the electromagnetic spectrum. The absorption spectrum of water in the tissue directly controls the spectroreflectance of the leaf at these wavelengths. The presence of strong water absorption bands in this region of the spectrum is based upon accepted physical principles (Curcio and Petty, 1951). This relationship has been investigated and the spectroreflectance of leaves have been statistically related to their leaf water content for several crop and forest species (Thomas *et al*, 1967; Sinclair, 1968; Carlson, 1969 and 1971; Olson, 1969).

An excellent study for the relationship between spectroreflectance of crop canopies and leaf water content for corn, soybeans, and sorghum leaves was recently completed (Carlson, 1971). Emphasis in this research was placed upon correlating field measured spectroreflectance and leaf water at the wavelengths of maximum water absorption. Spectroreflectance measurements were integrated over the sensitive wavelength intervals and regressed against relative leaf water concentration. Correlation coefficients (r) of .99, .97, and .98 were obtained for integrated reflectances from 1.00 to 2.50 μm regressed against relative leaf water content for corn, soybeans, and sorghum respectively. r values of .98, .97, and .97 were calculated for the specific reflectances at 1.450 μm regressed against the same relative leaf water content values for the same three species respectively.

The effect of leaf water upon the energy absorption of the leaf is also supported by theoretical considerations. Extinction coefficients for water (Curcio and Petty, 1951) have been used to express the equivalent water thickness (EWT) of a leaf and to predict that thickness of water which can account for the absorption spectrum of the leaf in the 1.4 to 2.5 μm spectral region (Allen *et al*, 1968; Allen *et al*, 1969; and Gausman *et al*, 1970). The calculated values for EWT were in close agreement with the measured amounts of water in the leaves (Gausman, 1970).

2.3 Biomass and its *In Situ* Estimation

Studies by scientists in the Grassland Biome program have placed emphasis on understanding, explaining, and predicting the intraseasonal dynamics of grasslands. Priorities, in order of decreasing importance, were placed on measuring and modeling the dynamics of biomass, energy, nitrogen, phosphorus, sulfur and subsequently other elements which move through the system (French, 1971). Highest priority was placed on measuring and modeling biomass dynamics, or the biological mass per unit area of a certain species, class, or group of organisms. This was necessary to quantitatively characterize the various components and energy flow at any point in the system (Fig. 1). The easy and efficient measurement of above ground plant biomass was a high priority. The energy flow and nutrient cycling through the primary producer compartment of the system is affected by the state variable of leaf area and the driving variables solar radiation, soil water, and temperature. These factors to a large degree control the biomass and energy available to other trophic levels in the ecosystem. Techniques for accurate estimation or measurement of above ground biomass are therefore basic to the approach undertaken by investigators in the Grassland Biome.

2.3.1 Ocular Weight Estimation Method

The ocular or visual method of biomass estimation is the visual observation of several permanent and temporary plots by a trained observer. The sacrifice plots are clipped and weighed to develop the regression relationship needed to correct estimates of the biomass on

the permanent plots. The equipment needed to conduct this type of inventory includes a pair of shears, plot marking materials, a small scale, and some paper sacks in which to store the herbage clipped. It was suggested (Pechanec and Pickford, 1937) that the technician making the survey spend several days checking estimates on the same type of vegetation for which future estimation is to be made. This period of training may be profitably extended to a week in the case of entirely untrained individuals. The visual or ocular estimation procedure suffers from human variations among estimators, is limited in geographical extent of its application, and does not directly characterize the vegetation in physiological terms.

2.3.2 Point Quadrat Method

The point quadrat or point frame method involves the calculation of leaf area index (LAI) by determining the average number of pin contacts with the vegetative canopy for a slender, cylindrical, sharp-pointed rod. The rod is lowered from a quadrat or frame into the vegetation at a fixed angle with reference to the ground surface (Levy, 1933; Goodall, 1952; Philip, 1965; Warren Wilson, 1959, 1960, 1963). Modifications to the basic techniques (Warren Wilson, 1963) have been made for more efficient operation in the shortgrass prairie (Knight, 1970). These modifications include the addition of an electric motor to speed smooth pin penetration and withdrawal from the plant canopy, pins 2.5 cm apart, and three pin angles of 8°, 32.5°, and 65° from the vertical. The LAI was determined by the equation:

$$LAI = .89\ f_{8°} + .462\ f_{32.5°} + .453\ f_{65°}$$

where f_n is the average number of contacts per pin for the respective angle n in measured degrees from the normal to the soil surface. The LAI values can be converted to herbage biomass by the double-sampling method explained earlier (Warren Wilson, 1963; Knight, 1971). The advantages of the point frame method are that accurate LAI measurements and leaf angle distributions can be determined and the sample plot is not disturbed and can be remeasured again at any time. The major disadvantages are the substantial amount of time involved in determining the LAI of each sample plot (especially if it is a heavy grass canopy) and the resulting lack of area-wide data.

2.3.3 Capacitance Meters

Capacitance meters were developed to measure the mass of the vegetation between two or more metallic probes of a specially designed capacitor which are inserted into the vegetation canopy (Fletcher and Robinson, 1956). The capacitance meter utilizes the concept that there is a significant difference between the dielectric constant of air (a dielectric constant of 1), and that of the leaf water present in vegetation (a dielectric constant of ∿80). The capacitance measured is proportional to the leaf water present between the device's capacitance probes. Accurate measurements of green functioning biomass as it correlates to the leaf water present are possible in a short period of time (Van Dyne *et al*, 1968). The double sampling method is used to convert the capacitance readings of the leaf water present into herbage biomass. The advantages of

this method include its accurate measurements of green functioning vegetation and simplicity of use. The principal disadvantages of capacitance meters are the weight of the device and the ground currents caused by the variations in soil water in the near-surface soil layers and that it does not lend itself to adaptation to aircraft surveys.

2.3.4 β - attenuation Technique

This method of herbage biomass estimation is based upon the attenuation of a stream of beta particles by the mass of the vegetation canopy present on a plot (Teare, Mott and Eaton, 1966). The beta particles are emitted by radioactive nuclides and their attenuation by this vegetation mass is measured by a detector placed on the plot. The degree of attenuation between the emitting source and the detector is a function of the herbage biomass intersecting and attenuating this field. Initial results have predicted the herbage biomass of a shortgrass prairie accurately and account for 90 per cent of variation in clipped control sample plots (Mitchell, 1972). The technique is accurate, precise, relatively inexpensive, and nondestructive. Specific limitations and disadvantages of this method have not yet been established. However, care must be observed in handling the radioisotopes and variation in low yielding plots is great. Also, the technique is not readily used from aircraft.

2.3.5 Spectral Methods

Spectro-optical methods for estimating the herbage biomass are based upon the interaction of the vegetative canopy with natural

solar or artificial electromagnetic energy. A spectrum of incident electromagnetic energy which strikes a vegetation canopy is 'coded' or modified in a spectral or wavelength sense by the various physical or biological characteristics of that canopy. The resulting spectroradiance returned or reflected from the canopy after this interaction can be analyzed or decoded to yield information concerning the herbage biomass present, the relative amounts of green and standing dead vegetation, the leaf water concentration, and the amounts of certain plant pigments present. Various related spectral methods have been developed for remotely estimating the biomass and vegetation status in natural grasslands and rangelands (Miller *et al*, 1970; Miller and Pearson, 1971; Pearson and Miller, 1972; Tucker *et al*, 1973). These methods have been field tested with a ground-based, hand-held radiometer-calculator system, trailer mounted telescopic spectrometer, and by automatic computer analysis of multispectral aircraft imagery (Pearson and Miller, 1972, 1973a, 1973b). The key advantages of these various spectral assay techniques is that they can be exploited from the ground, aircraft, or from satellite platforms in combinations to map the spatial distribution of biomass and other biophysical characteristics of the vegetation canopy. Comparisons between recurrent measurements might enable estimates of the primary productivity to be made, although the effect of other factors such as heavy biomass, solar angle, and cloud conditions on spectroradiance must be evaluated.

3.0 EQUIPMENT DESCRIPTION

In situ measurements of spectroabsorptance, spectroreflectance, and spectrotransmissance (0.2 μm to 1.6 μm) of blue grama grass yielded data that might be used to model the vigor of these plants. Spectroabsorptance was not measured directly but was calculated from measurements of spectroreflectance and spectrotransmissance. These measurements and calculations were accomplished using the unique field spectrometer designed and constructed for the IBP Grassland Biome Program to test the feasibility of measuring plant cover and above ground biomass spectro-optically (Pearson and Miller, 1971). A brief description and summary of the spectrometer system follows to assist the reader in understanding the methods for measuring the spectral curves used in this study. These field spectrometer subsystems are grouped and reviewed in three categories: spectroradiometer; computer controlled digital data acquisition system; and trailer and logistical support equipment.

3.1 Spectrometer Hardware

The spectroradiation measuring instrument used in the field spectrometer system was an EG&G model 580-585 spectroradiometer (Fig. 2). This instrument consisted of the following modular subsystems:

1. A reflective telescope with a variable field of view from 7.5' to 2° and an on-axis viewing eyepiece through

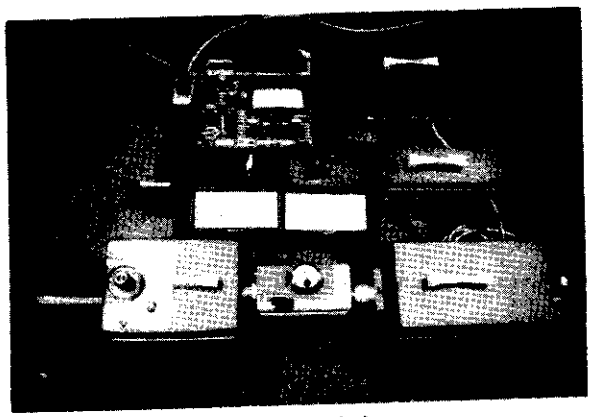

(a)

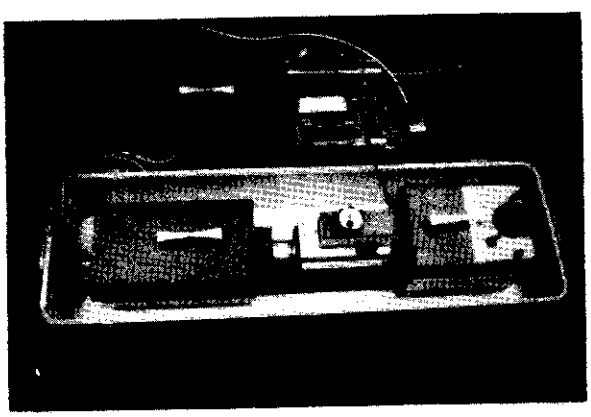

(b)

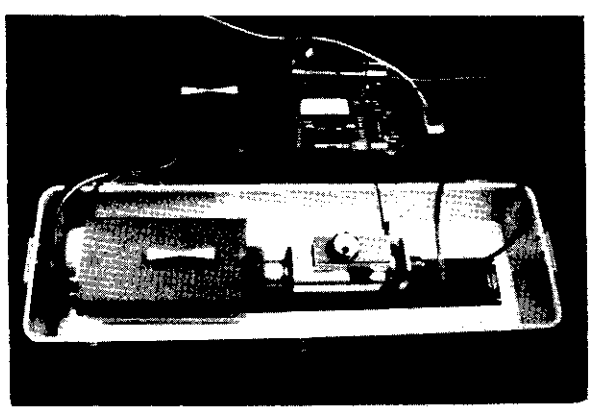

(c)

Figure 2. MODULAR SPECTRORADIOMETER SYSTEM. (a) composite view showing all available modules and components; (b) system as configured for use in the trailer; and (c) system as configured for use at a remote location.

which the operator could see the exact area for which spectroradiance was collected by the telescope.

2. A monochromator housing which accepted one of the three gratings used to cover the spectral region of 0.18 μm to 1.6 μm. Each grating had an attached wavelength transducer with an output voltage proportional to the angular position of the grating or the wavelength measured.
3. A high sensitivity detector head housing an S-10 photomultiplier detector sensitive from approximately .2 μm to .8 μm and associated power supply.
4. A high sensitivity detector head housing an S-1 photomultiplier detector sensitive from approximately 0.7 μm to 1.6 μm, a separate power supply and a cooling controller.
5. A readout unit which contained a six decade low level current amplifier which measured the detector current.
6. A fiber optics probe of one meter in length with a 3mm diameter viewing port which replaced the telescope module to measure irradiance in very small areas and at difficult viewing angles. This spectroradiometer, as presently configured, could measure spectroradiance with a band width or spectral resolution of 1 per cent of the wavelength set on the grating over the range of 0.2 μm to 1.6 μm.[1]

---

[1]The manufacturer now has available another detector and grating module which will extend the measurement range to 3.0 μm.

3.2 Computer Controlled Data Acquisition System

The large number of spectroradiance measurements taken by the spectroradiometer in scanning a single curve were sampled, stored, and subsequently reduced to yield curves which were plotted, printed, and punched on-line in the field using a computer digital data acquisition system (Fig. 3). This Hewlett Packard system consisted of:

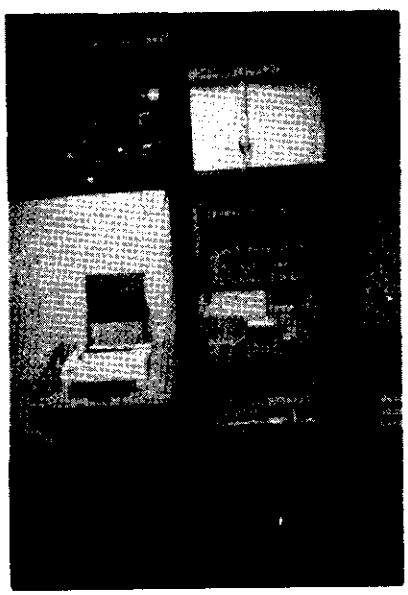

Figure 3. COMPUTERIZED DIGITAL DATA ACQUISITION SYSTEM. The system is shown in a rack used for laboratory operation indoors during the winter months.

1. A model 2114A general purpose digital computer with 8192 words of 16 bit memory.
2. A low level analog-to-digital converter for conversion of the analog signals from the spectroradiometer and other analog input sensors to digital computer input with 12 sensitivity ranges from 10 mv to 10 v and an

A/D conversion rate of 10KHz.

3. A multiplexer for selecting, under program control, the analog input channel to be digitized at a maximum switching rate of 10KHz.
4. A model ASR-33 teletype for keyboard input and printed output from the computer.
5. A high speed punched paper tape reader used primarily for program input to the computer.
6. A high speed paper tape punch for recording the processed data for subsequent transfer to the central University computer system.
7. An analog X-Y plotter interfaced to the computer and used to plot the raw spectral curves as they were measured or the reduced curves produced by the computer.
8. Internal to the computer were a crystal controlled time base generator for time reference, a digital-to-analog output conversion card to drive the X-Y plotter, and a power failure interrupt to maintain software integrity during power failure in the field.
9. A digital multimeter for system maintenance and testing.

The software used with the computer was written in any one of four languages (FORTRAN, ALGOL, Basic, and Assembler). A main program in FORTRAN controlled the experimental procedure and the data collection used in these experiments and subsequently output the reduced spectroradiometer measurements to the teletype, high speed paper tape punch, and X-Y plotter. The X-Y display allowed a

continual monitoring of the experiments as the curves were collected. The data curves were inspected as they were obtained and the data collection hardware was adjusted in the field to yield satisfactory and meaningful results.

3.3 Spectrometer Trailer

A specially designed 13.5 foot trailer housed all the equipment in the field (Fig. 4). It contained a work counter at the rear for the spectroradiometer, a reinforced platform for the computer data acquisition system, a teletype area and numerous special storage cabinets and closets. The trailer had both heating and air conditioning equipment to maintain the ambient temperature of 72°F. The air conditioner was large enough to provide a positive pressure gradient from the inside to outside during the summer to keep dust out of the trailer and out of the optical and electronic equipment which it housed. A separate, portable 3.5 kw alternator supplied operating power when the trailer was used more than 100 feet from a line power source.

The spectroradiometer could also be housed in a protective fiberglass box and taken up to 90 meters from the trailer into the field for detailed study of light flow into the grassland community with the fiber optics probe. The sampling by the data acquisition system of the instruments in this remote configuration and the voice communications to the trailer were handled by a multiconductor geophysical data cable housed on spools in a locker on the rear bumper

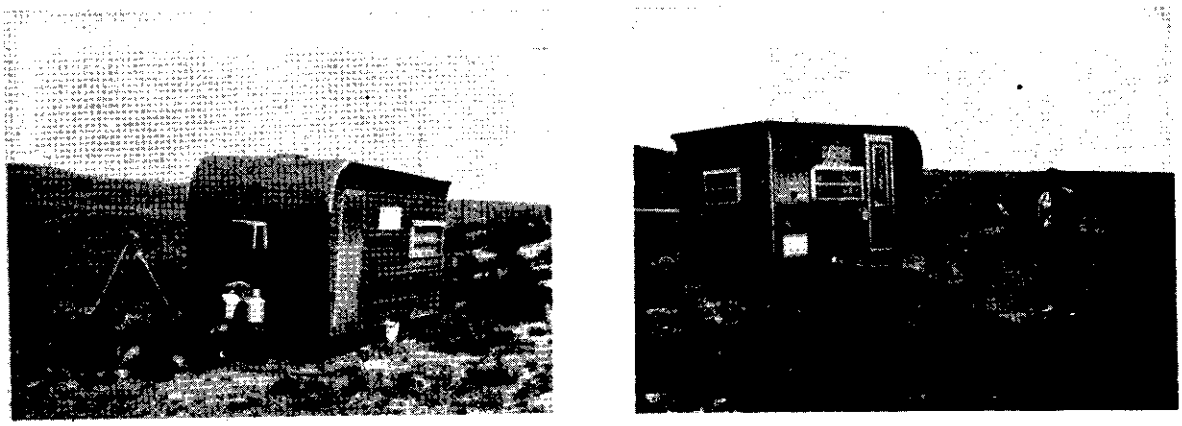

(a) (b)

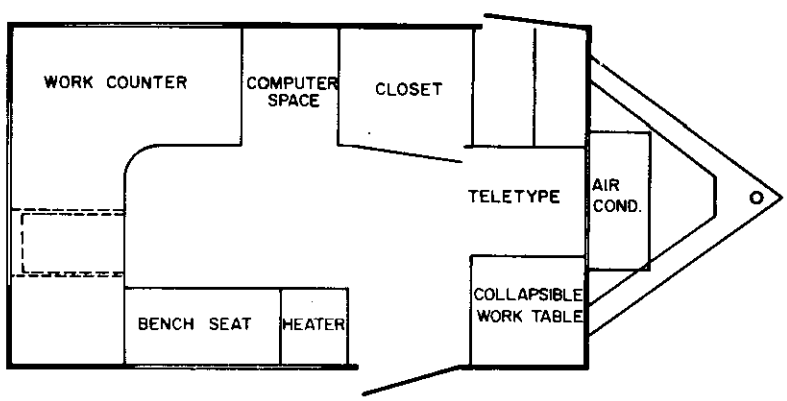

(c) floor plan

Figure 4. FIELD SPECTROMETER TRAILER AND SUPPORT EQUIPMENT. A tripod-mounted, first surface mirror (a and b) was used to fold the horizontal field-of-view of the spectroradiometer down onto the sample. A 3500 watt power plant supplies field power. A cable locker (not shown) has been added atop the rear bumper to store the trailer's main power cable (90 m), and a remote site power cable (90 meters), and a remote site data and communication cable.

of the trailer. A power cable to service this remote operation was also stored in this locker.

3.4 General Spectrometer Operation

Normally, the spectroradiometer was housed inside the trailer and telescopically views the *in situ* plant or grass-plot through a small hole in the side of the trailer (Fig. 5). The horizontal view

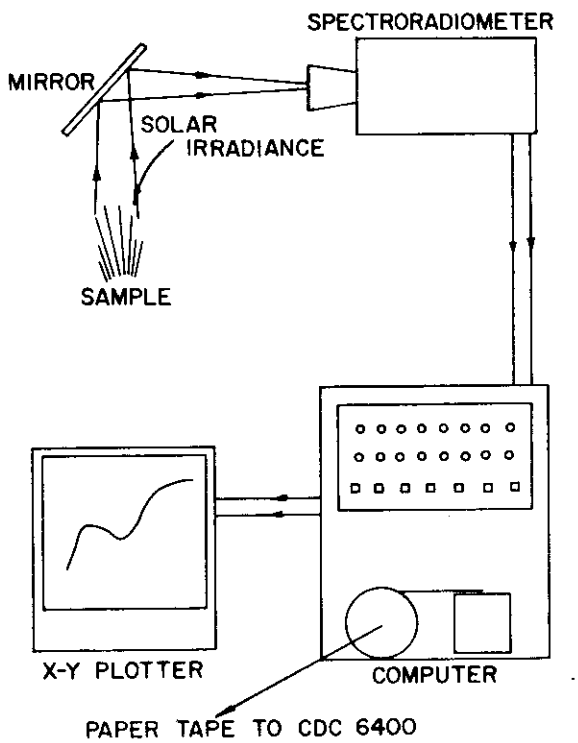

Figure 5. SCHEMATIC OF FIELD SPECTROMETER IN OPERATION. The spectroradiometer and digital data acquisition subsystems are shown diagrammatically as used in a field situation.

of the telescope was folded down normal to the ground's surface or at some other angle of incidence by a mirror mounted on a tripod.

The tripod and mirror were positioned so that they did not cast a shadow onto the sample and they blocked only a negligible portion of the indirect solar irradiance which would have reached the sample plot. The telescope had a variable field of view from 7.5' to 2° in five steps, allowing the selection of a wide number of field-of-views. The upper size limit of the sample area measured was limited by the dimensions of the available folding mirror to approximately 50 cm.[1] At present, larger folding mirrors would not be practical as they have continually blown over and broken. Measuring larger areas could be accomplished by looking directly at them from a high vantage point such as a tower. The lower size limit of the sample area which could be measured by the telescope was approximately 2 mm, as the eyepiece did not focus closer than 2 meters and the operator could not determine the area viewed.[2]

The detector in the spectroradiometer output an analog signal proportional to the spectroradiance collected from the sample at the wavelength determined by the angular position of the interference grating. A second analog signal was output proportional to the gain setting of the detector amplifier. The wavelength transducer, mounted on the grating, output a third analog signal

---

[1]This would be a circle of approximately 50 cm in diameter or 1/4 square meter if the view were folded or projected normal to the ground surface, e.g., the mirror is at a 45° angle to the ground surface. The 50 cm would be the limiting size or minor axis of the ellipse viewed at the sample in oblique views which are not normal to the ground surface.

[2]Measurement of the spectroradiance of small areas could be accomplished using a microscope module available from the manufacturer which could be attached to the fiber optics probe.

proportional to its angular position which was the wavelength of the detector output. The wavelength transducer had a knob atop it which was turned by hand to rotate the grating and scan the spectrum across the detector or to set off a particular wavelength on the detector. While the operator scanned the spectrum by turning this knob, the computer, under program control, sampled the output of the wavelength transducer, converted the analog signal to digital computer words at a rate of 10 KHz. This digital value of the wavelength was tested by the software to see how much it had changed from the previous wavelength at which the prior spectral value was taken. If the output had changed by a wavelength increment input via the teletype, the software stored this new wavelength and converted and stored the output of the detector and its gain setting. These incoming values could be multiplied by a stored tabular detector sensitivity curve to yield a calibrated curve of spectroradiance for the sample viewed by the telescope at the angle of inclination determined by the mirror angle. The measured values, with or without conversion to spectroradiance, were stored for comparison with the next curve to be measured, listed on the teletype, punched on paper tape, or plotted on the X-Y plotter.

4.0 MEASUREMENT PROCEDURE

4.1 Spectroreflectance

Spectroreflectance measurements were made in the field with reference to an aluminum panel painted with $BaSO_4$.[1] This reference panel was placed on a small stand a few inches above the test plot to avoid crushing the sample plants. A spectroradiance curve was read from this reference panel and stored in the computer core (Fig. 6). Upon completion of the scan, the panel was removed and a

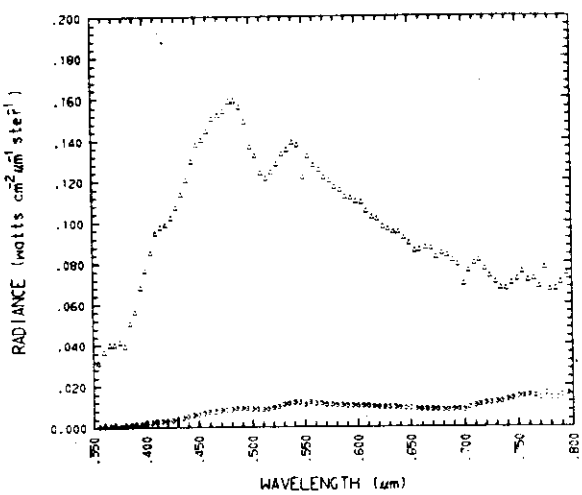

Figure 6. SPECTRORADIANCE OF THE WHITE REFERENCE PANEL AND THE PLANT CANOPY. Measured normal to a reference panel coated with barium sulfate (△) and an *in situ* sample plot of 1/4 m^2 of blue grama (*B. gracilis*) (⊙) of medium cover with some dead leaves. Julian day 242. 12:43 hours, MST, 1971.

---

[1] $BaSO_4$ or barium sulfate has recently been adopted as the standard of laboratory reflectance replacing freshly smoked MgO_2.

spectroradiance curve was measured immediately for the same plot (Holmes, 1966). This second curve was ratioed as it was taken on a matching wavelength basis to the white panel curve which was just measured and stored. The ratio was plotted on-line on the X-Y plotter and punched on tape as bidirectional spectroreflectance (Fig. 7).

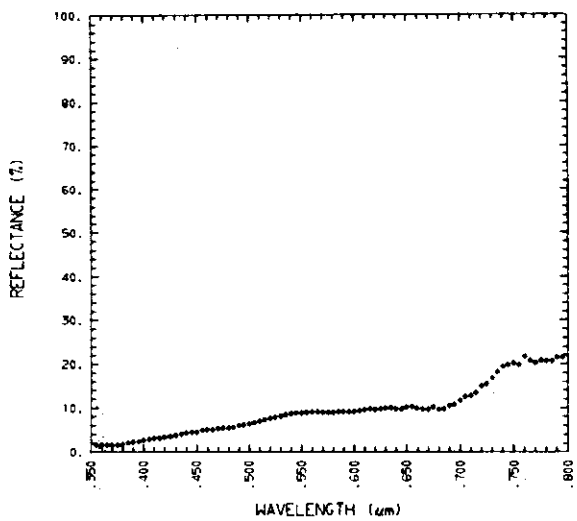

Figure 7. SPECTROREFLECTANCE OF THE PLANT CANOPY. Spectroreflectance curve of an *in situ* sample plot of 1/4 m^2 of blue grama (*B. gracilis*) of medium cover with some dead leaves. This curve is the ratio of the two spectroradiance curves in Figure 6. Julian day 242. 12:43 hours, MST, 1971.

Note that any detector sensitivity functions or intensity calibration problems were eliminated in this ratioing process but careful calibration in wavelength must be preserved.

Bidirectional spectroreflectance is the spectroreflectance of a surface measured at a particular angle of view. The field spectroreflectance of an *in situ* grassland sample plot is a function of the angle of measurement of the plot with respect to the normal. More

vegetation and less soil show in an inclined view of the plot which changed its spectroreflectance. Thus, spectroreflectance is an angular property of the surface. All the measurements of bidirectional spectroradiance and spectroreflectance in this paper were normal to the ground surface and plant canopy.

4.2 Spectrotransmissance

Spectrotransmissance measurements were made by replacing the telescope module of the spectroradiometer with the fiber optics probe. A reference measurement of the incident spectroirradiance at the sample surface was made by aiming the 3 mm diameter viewing port of the probe at the source of the irradiance, e.g., the sun (Fig. 8).

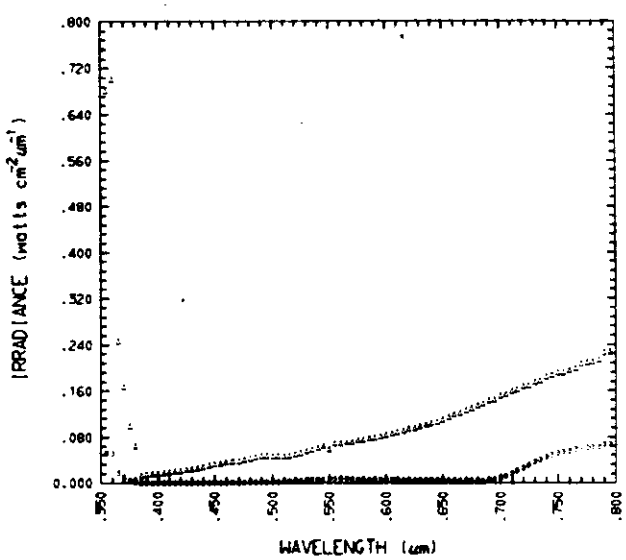

Figure 8. SPECTROIRRADIANCE AT LEAF SURFACE AND PASSING THROUGH THE LEAF. Measured spectroirradiance (△) and the spectroradiance passing through a single blade of blue grama (*B. gracilis*) (○).

This spectroirradiance curve was read at the sample position and

stored in the computer core as a function of wavelength just as was done with the white panel reference curve. Upon completion of the scan of the spectrum of the energy source, the plant material being measured was placed over the viewing port and the energy transmitted was measured as a function of wavelength (Fig. 8). This second curve was ratioed on a matching wavelength basis as it was taken to the reference curve of spectroirradiance presented to the plant material which was just measured and stored. The resulting spectrotransmissance is plotted on-line on the X-Y plotter, punched onto paper tape, and printed as needed on the teletype (Fig. 9). A

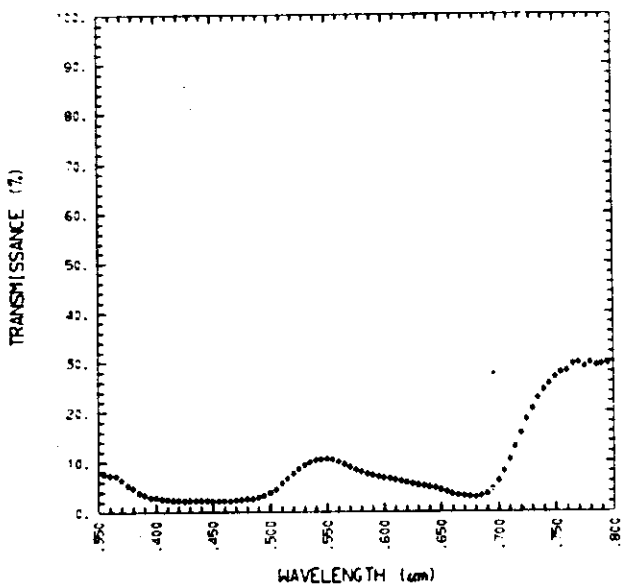

Figure 9. SPECTROTRANSMISSANCE OF A SINGLE BLADE OF BLUE GRAMA (*B. gracilis*). This curve is the ratio of the two spectral curves in Figure 8.

procedure which was similar in general approach was used to measure the total plant canopy *in situ* in the field (Pearson and Miller, 1971).

4.3 Spectroabsorptance

Spectroabsorptance is calculated from the measurements, under steady state conditions, of spectroreflectance and spectrotransmissance using the following: spectroabsorptance (α) + spectroreflectance (ρ) + spectrotransmissance (τ) = 1, (i.e. $\alpha + \rho + \tau = 1$). Therefore, spectroabsorptance = 1 - spectroreflectance - spectrotransmissance (i.e. $\alpha = 1 - \rho - \tau$) (Fig. 10 and 11). This method

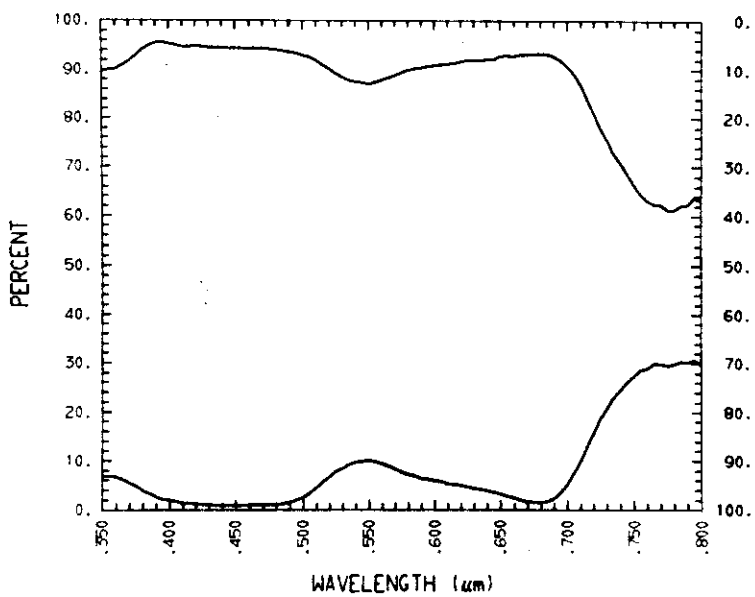

Figure 10. SPECTROABSORPTANCE, SPECTROREFLECTANCE, AND SPECTROTRANSMISSANCE OF A SINGLE BLADE OF BLUE GRAMA. Spectroreflectance (ρ) is plotted with reference to the left axis and spectrotransmissance (τ) is plotted with respect to the right axis. The interval between these two curves is the spectroabsorptance (α) from the equation: $\alpha_\lambda + \rho_\lambda + \tau_\lambda = 100$.

of measuring spectroabsorptance in the field was validated by remeasuring materials whose spectroabsorptance curves had been measured in the laboratory and reported in the literature (Tucker and Miller, 1973).

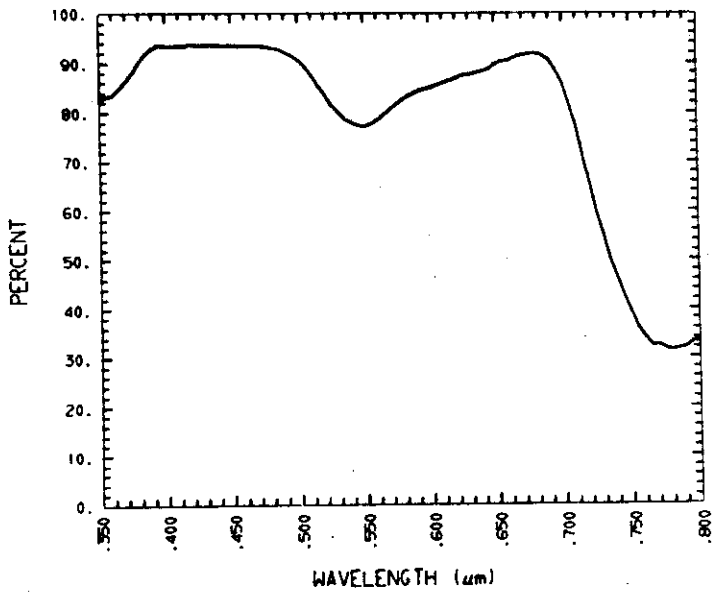

Figure 11. SPECTROABSORPTANCE OF A SINGLE BLUE GRAMA BLADE. This curve is the sum of the two curves shown in Figure 10 at each wavelength subtracted from 100. Note the order of magnitude changes in the curve with respect to wavelength.

The spectro-optical measurement methods just described have been used to validate leaf modeling efforts reviewed in the next section. These same procedures were also used to measure canopy spectroreflectance of 1/4 m^2 plots of blue grama grass (*B. gracilis*) discussed in the final validation portion of this study. The measurements provided the data used to develop the statistical relationships among the biophysical characteristics of *in situ* blue grama and associated spectroreflectance.

5.0 BIOPHYSICAL FACTORS CONTROLLING THE SPECTRO-OPTICAL CHARACTERISTICS OF A LEAF

5.1 Introduction

Knowledge of how solar energy, more specifically solar spectroirradiance, interacts with the grassland vegetation canopy is necessary to design measurement schemes to quantify the physical and biological parameters responsible for these interactions in natural shortgrass prairie. The grass blades or leaves are the functional unit in this complex interaction with electromagnetic energy and a close similarity among shortgrass prairie species exists (Tucker and Miller, 1973). Incident solar spectroirradiance interacts with leaves and results in three distinct solar energy states: absorbed, reflected, and transmitted (Fig. 12). The absorption, reflection and transmission of electromagnetic energy by leaves is a function of the wavelength of that energy. The terms spectroabsorption, spectroreflection, and spectrotransmission are used to denote these spectro-optical parameters of the leaf as wavelength functions. Four principal leaf characteristics or state variables determine the three spectro-optical characteristics of the leaf and the related energy states:

1. Internal leaf structure or the histological arrangement of tissues and cells is responsible for the diffusion or internal scattering of incident solar spectroirradiance.

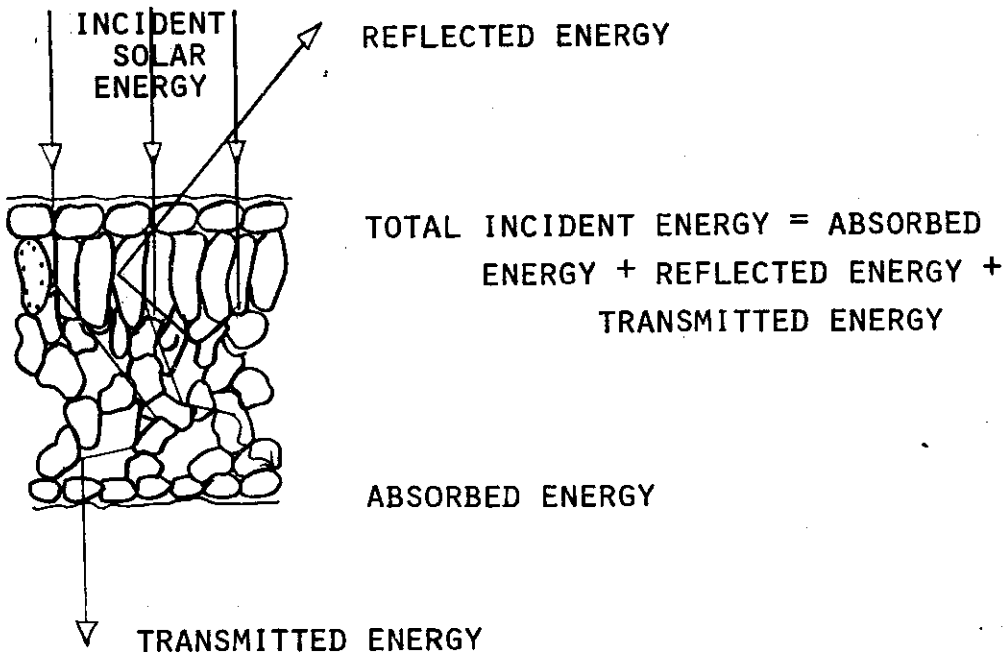

Figure 12. SOLAR ENERGY INTERACTION WITH A LEAF CROSS SECTION. Diagrammatic representation of the complex interaction between the solar energy spectrum and a typical leaf cross section.

Spectroabsorptance, spectroreflection, and spectrotransmission are thereby determined by the mean optical path length of incident energy (Willstatter and Stoll, 1913; Maestro, 1935; Gates *et al*, 1965; Sinclair, 1968; Allen *et al*, 1968; Allen *et al*, 1969; Gausman *et al*, 1970; Knipling, 1970; and Allen and Richardson, 1971).

2. The pigment composition, concentration(s), and distribution(s) control the absorption of ultraviolet and visible spectroirradiance (Allen *et al*, 1968, 1969; Salisbury and Ross, 1969; Knipling, 1970; Gausman *et al*, 1970; Gates

et al, 1965; Gates, 1970; Allen and Richardson, 1971; Woolley, 1971).

3. The concentration and distribution of leaf water controls the absorption of spectroirradiance in the infrared region of the spectrum (Gates *et al*, 1965; Allen *et al*, 1968; Allen *et al*, 1969; Gates, 1970; Gausman *et al*, 1970; Knipling, 1970; Allen and Richardson, 1971; Woolley, 1971).
4. The surface roughness characteristics and the refractive index of the cuticular wax of the upper epidermis control the spectroreflectance from this surface (Bennett and Porteus, 1961; Eglinton, 1962).

A high degree of correlation existed between spectroabsorptance, spectroreflectance, and spectrotransmissance with a correlation coefficient (r) value of .986 between spectrotransmissance (τ_λ) and spectroreflectance (ρ_λ) for blue grama for 91 data points at varying wavelengths. The same high correlation existed between spectroabsorptance (α_λ) and spectroreflectance (ρ_λ), and spectroabsorptance (α_λ) and spectrotransmissance (τ_λ) due to the linear relationship of these three spectro-optical characteristics (Fig. 12) given by $\alpha_\lambda + \rho_\lambda + \tau_\lambda = 1$.

The high intercorrelation between these three optical properties of the leaf substantiated the reports in the literature that they are determined by the same characteristics of the leaf. The high correlation coefficient (r value) between spectroreflectance and spectrotransmissance allowed a stochastic leaf model based upon leaf structure, leaf pigments, leaf water, and epidermal properties

to be constructed to predict the three interrelated spectro-optical characteristics of a leaf with computer simulation techniques. This quasi-deterministic/stochastic leaf model demonstrated the feasibility of using these spectro-optical characteristics of a leaf and subsequently the plant canopy to estimate the biomass, chlorophyll, and leaf water present in the shortgrass prairie canopy.

5.2 Background

The interaction between solar energy and leaves was first explained by the Willstätter and Stoll theory (1913). The development of this theory used an albino maple leaf (*Acer negundo* L.) and based its hypothesis upon internal geometrical optics of the leaf. The basic validity of the Willstätter and Stoll theory (1913) has been recently substantiated, with minor variations, by other investigators (Allen and Richardson, 1971). The key components of Willstätter and Stoll's original hypothesis are worthy of brief review.

> Incident solar energy, normal to the epidermis, passes through the platelike epidermal cells of the albino maple leaf and enters the densely packed cylindrical palisade parenchyma cells arranged roughly parallel to the incident radiation. The radiation passes through this cell layer into the spongy mesophyll of the leaf. Here the cells are ovoid to round in shape, are not densely packed, and are interspersed with intercellular air spaces. In the *absence* of absorption, the spongy mesophyll causes internal scattering of the incident radiation resulting from multiple reflections from the cells and refractions due to the refractive index differences between the hydrated cell walls ($\sim$1.3) and the intercellular air spaces (1.0). This nature of the spongy mesophyll causes the scattered radiation to be diffused within the leaf. A portion of this scattered radiation escapes through the lower epidermis and is

> designated as transmitted energy. The other fraction diffuses upward and escapes through the upper epidermis.[1]

The Willstätter and Stoll theory (1913) was based on an albino leaf to emphasize the interactions in the absence of pigment or water absorption. The normal leaf, however, is characterized by the absorption of incident energy by pigments and water within its structure.

The interaction of electromagnetic energy with leaves in the visible and near infrared region of the spectrum has received a great deal of attention by other investigators (Clark, 1946; Gates and Tantraporn, 1952; Gates *et al*, 1965; Steiner and Guterman, 1966; Myers and Allen, 1968; Sinclair, 1968; Allen *et al*, 1969; Allen *et al*, 1970; Gates, 1970; Gausman *et al*, 1970; Knipling, 1970; Allen *et al*, 1970; Allen and Richardson, 1971; Gausman, 1971; Woolley, 1971). This interval of the electromagnetic spectrum from 0.4 to 2.8 μm has received almost all the attention in these earlier studies of the spectro-optical properties of leaves. Spectroradiometric equipment is commercially available and sensitive in this region and 90 per cent of the incident solar irradiance occurs within this spectral region (Knipling, 1970). Below .4 μm in the ultraviolet and in the infrared beyond 2.8 μm, leaf absorption is quite high ($\geq$ 90 per cent) and transmission and reflection are quite low (Gates and Tantraporn, 1952; Wong and Blevin, 1967) (Fig. 13).

The spectro-optical characteristics of a leaf from 0.4 to 2.5 μm can be subdivided into three wavelength subsections each

---

[1]Paraphrased from A. Willstätter and K. Stoll in Untersuchungen über die Assimilation der Kohlensäure (Berlin: Verlag-Springer, 1913), pp. 122-127.

essentially controlled by a different leaf characteristic (Fig. 13).

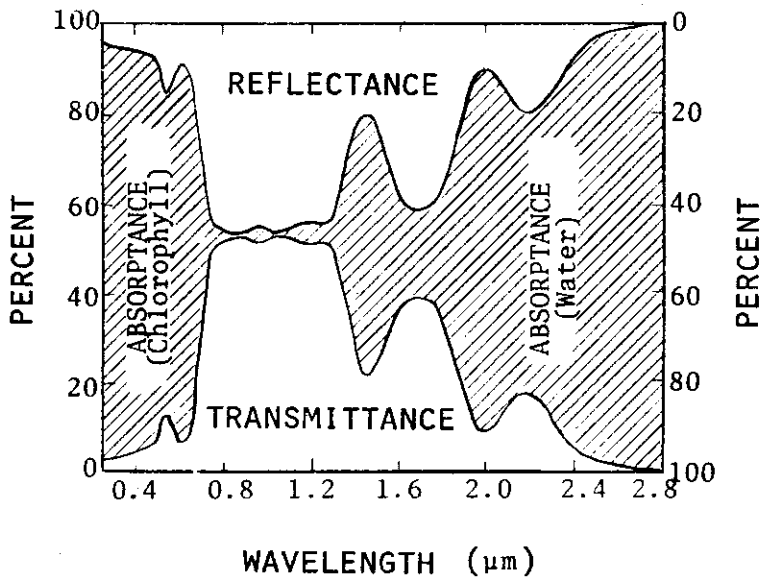

Figure 13. TYPICAL SPECTROABSORPTANCE, SPECTROREFLECTANCE, AND SPECTROTRANSMISSANCE OF A PLANT LEAF. Note the high spectroabsorptance due to plant pigments (predominantly the chlorophylls) in the visible region, the lack of spectroabsorptance and resulting high values of spectroreflectance and spectrotransmissance in the .8 to 1.3 µm region, and the high spectroabsorptance due to leaf water in the 1.3 to 2.8 µm region (extracted from Knipling, 1970).

The region from .40 to .70 µm is influenced by the absorption due to plant pigments; the area from 0.70 to 1.30 µm is characterized by the lack of absorption and high values for reflection and transmission; the region from 1.30 to 2.8 µm shows the effects of absorptance by the water in the leaf tissue (Fig. 13).

5.3 Scattering of Incident Radiation in Leaves

Scattering of electromagnetic (EM) radiation in leaves is a complex phenomenon caused by the complex cytoplasmic contents, irregular cellular shapes, and various geometric organizations of tissues. Two principal types of scattering occur in leaves: Rayleigh scattering; and diffuse scattering. Rayleigh scattering occurs for particles of sizes equal to or less than the wavelength of the incident energy and is roughly proportional to the inverse forth power of the wavelength (λ^{-4}) for these conditions (Fig. 14). The extent

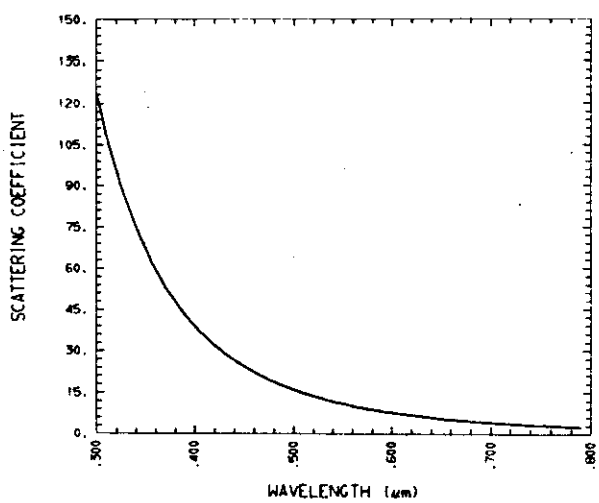

Figure 14. RAYLEIGH SCATTERING COEFFICIENTS PLOTTED AS A FUNCTION OF WAVELENGTH FOR PARTICLES SMALLER THAN THE WAVELENGTH OF THE INCIDENT RADIATION. The scattering coefficient shown is the inverse fourth power of the wavelength. Note the order of magnitude changes that occurs within a short wavelength range over this narrow portion of the electromagnetic spectrum.

of Rayleigh scattering in functioning leaves remains unresolved in the literature. Some Rayleigh scattering must occur because of the dimensions of various cellular organelles. Chloroplasts, for

example, are 4 to 6 μm in length and 1 to 2 μm thick. The thickness of the chloroplast unit membrane is ∿.03 μm and is typical of the other unit membranes in the leaf (Esau, 1965). Various other organelles such as mitochondria, lysosomes, etc. and macromolecules such as proteins and lipids probably also cause Rayleigh scattering. The extent of, and the exact causes for Rayleigh scattering in functioning leaves has not been resolved.

Diffuse or refractive-reflective scattering occurs within functioning leaves in addition to Rayleigh scattering and is independent of wavelength. This type of scattering is caused by refractive index differences between hydrated cells and adjacent intercellular air spaces and is compounded by the irregular shapes and organization of cells. Both of these scattering processes play a role in establishing the spectro-optical characteristics of a green leaf and should be considered when modelling leaf energy processes.

5.3.1 Rayleigh Scattering

Rayleigh scattering is a complex phenomenon which depends on the size of the scattering particles, their shape, and the differences in the index of refraction between the particles and suspending medium. The transmission (τ_λ) at any wavelength for small independent isotropic particles can be expressed as:

$$\tau_\lambda = \frac{32\pi\ 3_c\ Mn_{o_\lambda}^{\ 2}}{3N^4} \left(\frac{n_\lambda - n_{o_\lambda}}{c}^{\ 2} \right) \qquad (1)$$

where: c is the concentration of particles in grams per milliliter,

M the molecular weight,

N Avogradro's number,

n_o the refractive index of the medium, and

n the refractive index of the solution (Oster, 1948).

Particles approaching the wavelength of the incident electromagnetic radiation are scattered according to this Rayleigh equation. The scattered wavelets from the various surfaces of the particles interfere due to the fixed positions of the scattering particles and the orientation of these surfaces and this results in greater scattering of light in the direction of the incident beam than in other directions (i.e., back toward the source). Forward scattering is proportional to the shape of the particles, being greatest for spheres and smallest for thin rods (Oster, 1948). Particles of a size greater than the wavelengths of the incident electromagnetic radiation yield scattering which is no longer proportional to λ^{-4} but to λ^{-4+k}, where k = 1.0 for rods, 1.74 for coils, and 2.0 for spheres (Fig. 15). This scattered light will also be a superposition of the wavelets from various parts of the same particles (Oster, 1948).

The Rayleigh scattering coefficients plotted against wavelength showed order of magnitude differences that occurred within a short wavelength range for particles smaller than the wavelength of the incident radiation (Fig. 14) and for particles greater than or equal to the wavelength of the incident radiation (Fig. 15).

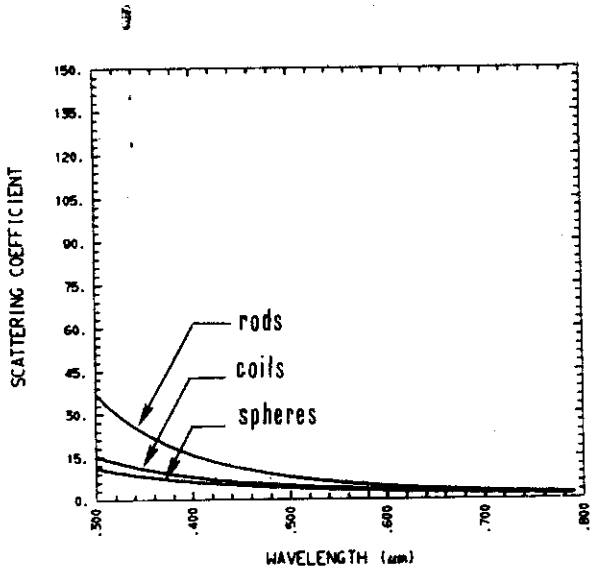

Figure 15. RAYLEIGH SCATTERING COEFFICIENTS PLOTTED AS A FUNCTION OF WAVELENGTH FOR PARTICLES LARGER THAN THE WAVELENGTH OF INCIDENT RADIATION. The scattering coefficients are no longer proportional to the inverse fourth power of the wavelength, but are proportional to λ^{-4+k}, where k = 1.0 for rods, 1.74 for coils, and 2.0 for spheres (Oster, 1948). Note the marked effects that particle shape can have upon Rayleigh scattering.

5.3.2 Diffuse Scattering

The internal mechanism for diffuse scattering was first suggested by Willstätter and Stoll (1913) and has recently been elaborated on and revised by several authors. Near infrared spectroreflectance has been mathematically related to the number of intercellular air spaces or lacunae in leaf mesophylls (Allen *et al*, 1969; Guasman *et al*, 1970; Gausman, 1971). The infiltration of the intercellular airspaces by a leaf in water resulted in much lower near infrared spectroreflectance further substantiating the effect of this component on internal scattering (Knipling, 1970).

Attention has recently focused on the cellular constituents responsible for the surface roughness and diffusing nature of

electromagnetic radiation interactions within and between adjacent leaf cells. These characteristics have been attributed to the cell wall roughness (Sinclair, 1968). Cellular membranes reflected more near-infrared radiation at .850 μm than the cytoplasm and the middle lamella reflected more radiation at this same wavelength than the cell walls (Gausman, 1971). Cell walls are composed primarily of cellulose, the middle lamella is abundant in calcium pectate and cellular membranes are composed of a protein-lipid-protein sandwich arrangement (Esau, 1965). Differences in spectroreflectance at .850 μm between cell walls, the middle lamella, and cell walls could be due to chemical compound differences (Gausman, 1971). Cytoplasmic constituents (macromolecules, proteins, lipids, etc.) are too small to cause an appreciable amount of scattering due to their surface roughness (Allen, 1964). Some internal scattering results from the cellular organelles although to date there has been no consensus of opinion on this matter in current research. The majority of internal scattering results from the irregular surface shapes of cells and the intercellular airspaces with this mechanism occurring in *both* the palisade parenchyma and spongy mesophyll although relative frequencies for these cell areas are not known.

5.4 Plant Pigments

The strong spectroabsorptance by healthy functioning green leaves in the photo ultraviolet and visible region of the electromagnetic spectrum (.3 to .7 μm) is caused by pigments present in

the leaf tissue. Most of this absorption is due to chlorophyll a, chlorophyll b, and the carotenoids (Salisbury and Ross, 1969). Attenuation of incident electromagnetic energy by plant pigments and leaf water concentration can be described by the Lambert-Beer law:

$$T_\lambda = H_\lambda \, e^{-\alpha_\lambda x} \qquad (2)$$

where: T_λ = resulting intensity of incident energy transmitted through the medium at a given wavelength,

H_λ = intensity of incident energy presented to the medium at a given wavelength,

α_λ = coefficient of absorptance for the medium at the given wavelength of incident energy,

x = thickness of the medium, and

e = Napier's number $\tilde{=}$ 2.71.

Relative pigment concentrations vary between and within species. One report stated that ∿65% of the total pigments are chlorophylls and that 35% are carotenoids (Gates *et al*, 1965). Another report indicated that ∿75% of the pigments are chlorophylls and ∿25% are carotenoids for most species (Anderson, 1967). Chlorophylls and carotenoids, therefore, account for the great majority of total pigment absorption in the green, functioning leaf. The absorption of incident electromagnetic energy by anthocyans, psycobilins, and other lesser pigments are quite low in such leaves (Ross, 1973). The chemical nature of chlorophylls and carotenoids will be briefly reviewed as these properties pertain to modeling the radiation exchange of a leaf.

5.4.1 Chlorophyll

The chlorophyll molecule is a porphyrin derivative with a cyclic tetrapyrrolic structure with one pyrrole ring partially reduced. The tetrapyrrolic nucleus contains a nonionic magnesium atom held by two covalent and two coordinate bonds. Chlorophyll a and b are very similar, with chlorophyll a having a methyl group at position 3 while chlorophyll b has an aldehyde group at this same position. The chlorophyll molecules in their natural state are bound to proteins in the chloroplast to form a lipoprotein complex (Delvin and Barker, 1971).

All plants possess chlorophyll a while chlorophyll b is found in lesser quantities in all higher plants and in two of the algae divisions. Chlorophyll a and b closely resemble each other in molecular structure but definite differences in their physical and chemical properties have been observed (Salisbury and Ross, 1969; Delvin and Barker, 1971). The absorption spectra for the two pigments differ with chlorophyll a having maximum absorption at .430 and .662 μm while the corresponding maxima for chlorophyll b occur at .453 and .642 μm (Fig. 16). Chlorophyll a and b within the living leaf (*in vivo*) cell have their absorption maxima at .010 to .015 μm longer wavelengths than the same pigments in the organic solvents used for their extraction (*in vitro*) (Salisbury and Ross, 1969). Their *in vitro* absorption spectrum is also broadened and flattened relative to wavelength. Chemical environment effects upon molecular structure cause these changes for chlorophyll in the organic solvent used for extraction (Allen, 1964). Thus, the chlorophyll extinction

spectra have been shifted .10 μm to longer wavelengths and a concentration of .012 mg/cm^{-2} total chlorophyll (a + b) for a healthy, live leaf are used for model calculations in the next section. Nothing has been done, however, to compensate for magnitude differences between *in vivo* and *in vitro* extinction coefficients in this model.

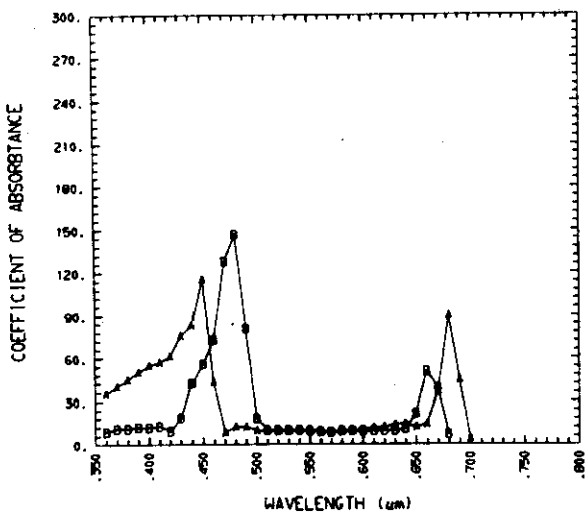

Figure 16. COMPARISON BETWEEN COEFFICIENTS OF ABSORPTANCE FOR CHLOROPHYLL A AND B. These *in vitro* absorptance curves have been shifted .010 μm to longer wavelengths as suggested in the literature (Salisbury and Ross, 1969).

5.4.2 Carotenoids

The carotenoids belong to that large group of compounds called the terpenoids and are divided into two classes, the carotenes which are hydrocarbons and their oxygen derivatives the xanthophylls. The carotenoids comprise ∿20 to 30% of the total leaf pigments and have typical leaf concentrations of .005 to .025 mg/cm^2 for mature leaves

(Anderson, 1967). The principal carotenoids of higher plants are leutin, β - carotene, violaxanthin, and neoxanthin which comprise 40%, 25%, 15%, and 15% respectively of the total carotenoid concentration (Delvin and Barker, 1971). The extinction coefficients for β - carotene and leutin are very similar (Fig. 17).

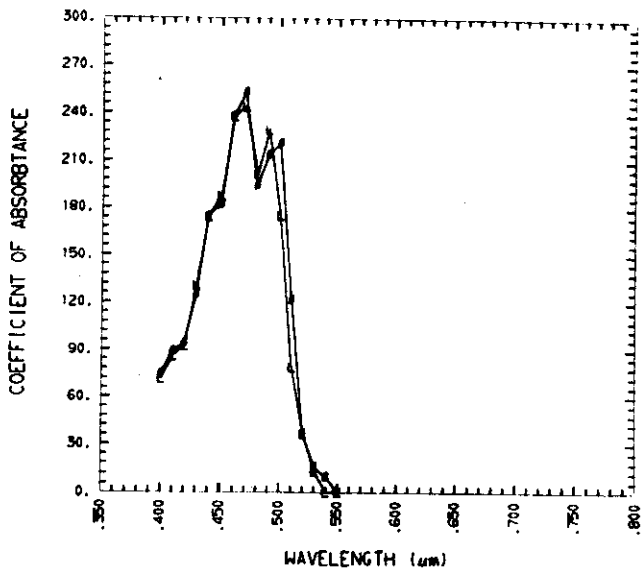

Figure 17. EXTINCTION COEFFICIENTS FOR β CAROTENE (β) AND LEUTIN (L). Note the similarity between the spectral characteristics of the coefficients of absorption for these two carotenoid compounds. The input data has been shifted 0.010 μm to longer wavelengths as suggested in the literature (extracted from Salisbury and Ross, 1969).

Chemical environment complexing in an extract also causes minor structural shifts in these pigment molecules as with chlorophyll. This results in slightly different *in vivo* versus *in vitro* attenuation of light energy (Allen, 1964). The *in vivo* shift to longer wavelengths for the absorptance maxima is approximately the same as that for the chlorophylls (Ross, 1973). The extinction

coefficients used for the carotenoids in the modeling effort have been shifted .010 μm to longer wavelengths based upon this information. Because of the similarity between the absorption coefficients of β - carotene and leutin (Fig. 17), only the absorption coefficients for leutin were used. The entire carotenoid content of .004 mg/cm^{-2} was therefore assumed to be leutin in the model.

5.5 Leaf Water

Spectroabsorptance in the near-infrared region (1.3 to 2.8 μm) of the spectrum is caused by absorption (extinction) by leaf water molecules. Water in the leaf tissue is very transparent to visible electromagnetic energy but significantly attenuates near infrared energy (Fig. 18). These absorption coefficients for water as a

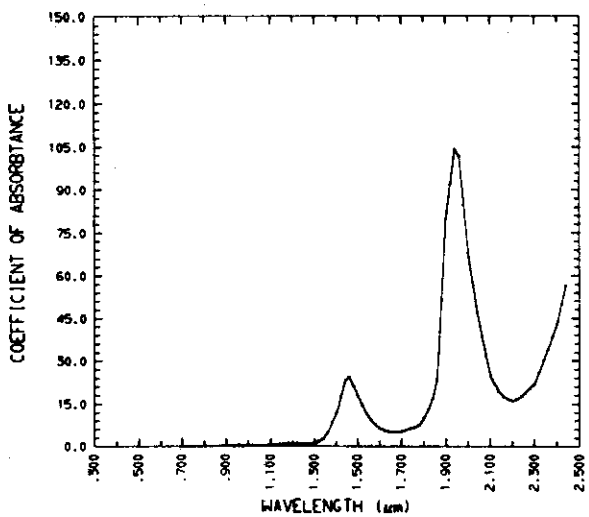

Figure 18. COEFFICIENTS OF ABSORPTANCE FOR PURE LIQUID WATER AT 20°C (extracted from Curcio and Petty, 1951).

function of wavelength are used exactly as they are reported in the literature (Curcio and Petty, 1951).

5.6 Cuticle Characteristics

The cuticle of leaves is generally thought to be nearly transparent to incident radiation. A small amount of electromagnetic radiation is reflected from the upper cuticular surface while the majority is transmitted into the interior of the leaf (Gates, 1970). The small amount of cuticular reflection is probably caused by refractive differences between air and the cuticular wax coating (Eglinton, 1962) and the upper epidermal cell layer. Although, ultrastructural surface roughness and characteristics could also be contributing to this type of initial reflection. The exact causes of the cuticular reflection remain unresolved at the present time. The simulation model of the leaf attributed .01 of the incident radiation to cuticular reflectance and .99 of the incident radiation entered the leaf.

6.0 SPECTRO-OPTICAL MODELS OF LEAVES

6.1 Background

Reports on two general types of spectro-optical leaf models occur in the literature. Both of these types of leaf models were developed by researchers in the USDA/ARS at Weslaco, Texas. One is essentially a geometric ray tracing model (Allen and Richardson, 1971) and the other is a plate type of model based upon four optical constants of leaves (Allen *et al*, 1969, 1970, 1971; Gausman *et al*, 1970). The plate type models have received the most attention in the literature and will be reviewed first.

6.1.1 Plate Models

The flat plate model was used to explain the spectroreflectance of a corn leaf over the spectral range of 0.5 to 2.5 μm (Allen *et al*, 1969). The external and internal surfaces of the corn leaf are considered as diffusing surfaces for a compact leaf which has few intercellular air spaces in the leaf mesophyll. The flat model for compact leaves has also been expanded to the noncompact case accounting for the presence of many intercellular air spaces in the mesophyll (Allen *et al*, 1970; Gausman *et al*, 1970).

The model for the compact leaf represents a transparent plate (Fig. 19) with rough plane-parallel surfaces of a thickness D and a unit incident isotropic irradiance H_λ originating from medium 1

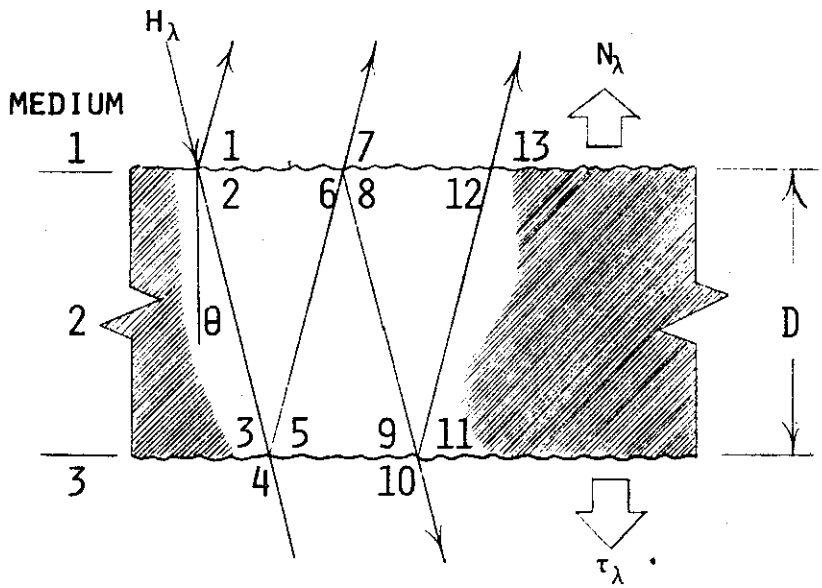

Figure 19. DIAGRAMMATIC REPRESENTATION OF THE FLAT PLATE MODEL FOR A COMPACT CORN LEAF. Compact refers to the absence of intercellular air spaces. H_λ = spectral irradiance, N_λ = spectral radiance, τ_λ = transmitted spectral energy, and D = leaf thickness. The arrows represent the resultant E-M rays as they interact with the compact corn leaf (extracted from Allen *et al*, 1969).

(e.g. the atmosphere) (Allen *et al*, 1969). The incident irradiance interacts with the rough upper surface of the transparent plate, passes into medium 2 (e.g. the leaf) with thickness D, strikes the other rough plane-parallel surface interface between media 2 and 3 (e.g. the atmosphere) and is subsequently reflected (N) or transmitted (T) with no absorption occurring for this wavelength of isotropic light. Media 1 and 3 are air while media 2 represents the compact corn leaf. Monotomic transmissance at an interface between media i and j will be denoted as τ_{ij} and the corresponding reflectance is given at that wavelength ρ_{ij}, which, in the *absence of absorption*, equals $1 - \tau_{ij}$. Multiple reflections of the isotropic

radiance within the semi-transparent plate are referred by the numbers 3, 5, 6, 8, 9, 11, 12, 14, and .... (Fig. 19). Medium 2 has an absorptance coefficient of α, the relative index of refraction between air and the plate (e.g. between mediums 1 and 2 or 3 and 2) is denoted as n_λ and the sumbol τ represents the transmissance of the plate (medium 2). Reflectance and transmissance can be expressed as sums of an infinite series.

The compact flat leaf model has been applied with considerable accuracy to the interaction between isotropic radiation and corn leaves represented by the semi-transparent plate (Allen *et al*, 1969).

The flat plate model has been modified and extended to the noncompact case (Allen *et al*, 1970, 1971; Gausman *et al*, 1970). Noncompact refers to the presence of many intercellular air spaces in the leaf mesophyll. Adaptation of the flat plate model to noncompact leaves treated the leaf as a stack of N identical elementary compact layers of cells separated by air spaces with a total compact layer thickness D. The number of air spaces between the plates is N-1. The same model used in the compact case is used for the noncompact leaf along with four other parameters: an effective index of refraction between the plates; an effection absorption coefficient; an equivalent water thickness; and the assumed number of compact layers. The model parameters for the effective index of refraction and the effective absorption coefficient are optical constants which vary with wavelength. The equivalent water thickness and the number of compact layers specify the internal structure of the leaf.

The four needed parameters or optical constants can be calculated if the diffuse reflectance and transmissance of the leaf are known. The compact flat plate model is used in addition to Fresnell's Law for the interaction between compact layers and the intercellular air spaces. The extention of the compact flat plate model to non-compact leaves has explained the approximate equality of leaf reflectance and transmissance measured by instruments for single leaves. Predicted values for the equivalent water thickness (D) are in close agreement with measured values (Allen *et al*, 1970).

6.1.2 Ray Tracing Model

A model based on the optical geometry of the leaf has been developed at the USDA/ARS station (Allen and Richardson, 1971). The basic geometric theory involved is an extension of that of the Willstätter and Stoll theory (1913). The optical system is an unconventional one which is not centered and has no optical axis. This optical system treats interactions between components as diffuse and not specular, is restricted to 2 dimensions, and the structural surfaces are sequences of intersecting circular arcs. The geometrical arrangement is specified by the curvature and the center of curvature for each interface, a periodic structure of sequential replications, and a laterally infinite system. The two media are air and hydrated cells with indices of refraction of 1.0 and 1.4 respectively. The restriction to only 2 dimensions is advantageous because the internal structure of typical leaves cannot be represented accurately with 3 dimensional spherical surfaces (Allen and Richardson, 1971).

The geometric abstraction and representation of a black maple leaf (*Acer negundo* L.) has been accomplished using this optical system model and evaluated using computer simulation (Allen and Richardson, 1971). The model is based upon refraction, reflection, and absorption theory. Incident rays are traced to an intersecting surface where the ray divides into a reflected and a refracted component unless the ray is emerging from the highest index medium at a critical or greater than critical angle and no refraction occurs. The resulting interaction components are determined by Fresnel theory. Absorption occurs in the hydrated cell medium according to the Lambert-Beer law and the process continues until all resultant rays of the incident ray have been absorbed or have escaped from the optical-geometric system as diffuse reflectance and/or transmissance (Allen and Richardson, 1971). Accurate predictions of the reflected, transmitted, and absorbed incident energy have been reported using this simulation technique.

6.2 Stochastic Spectro-Optical Leaf Model

6.2.1 Description of the Model

The stochastic leaf model compartmentalizes a leaf to represent the energy states, cell parts, and interval scattering mechanisms (Fig. 20). Four energy states are represented in 6 compartments:

1. The solar input to the model.
2. Specular reflection from the cuticle.
4. The absorption in the palisade parenchyma.

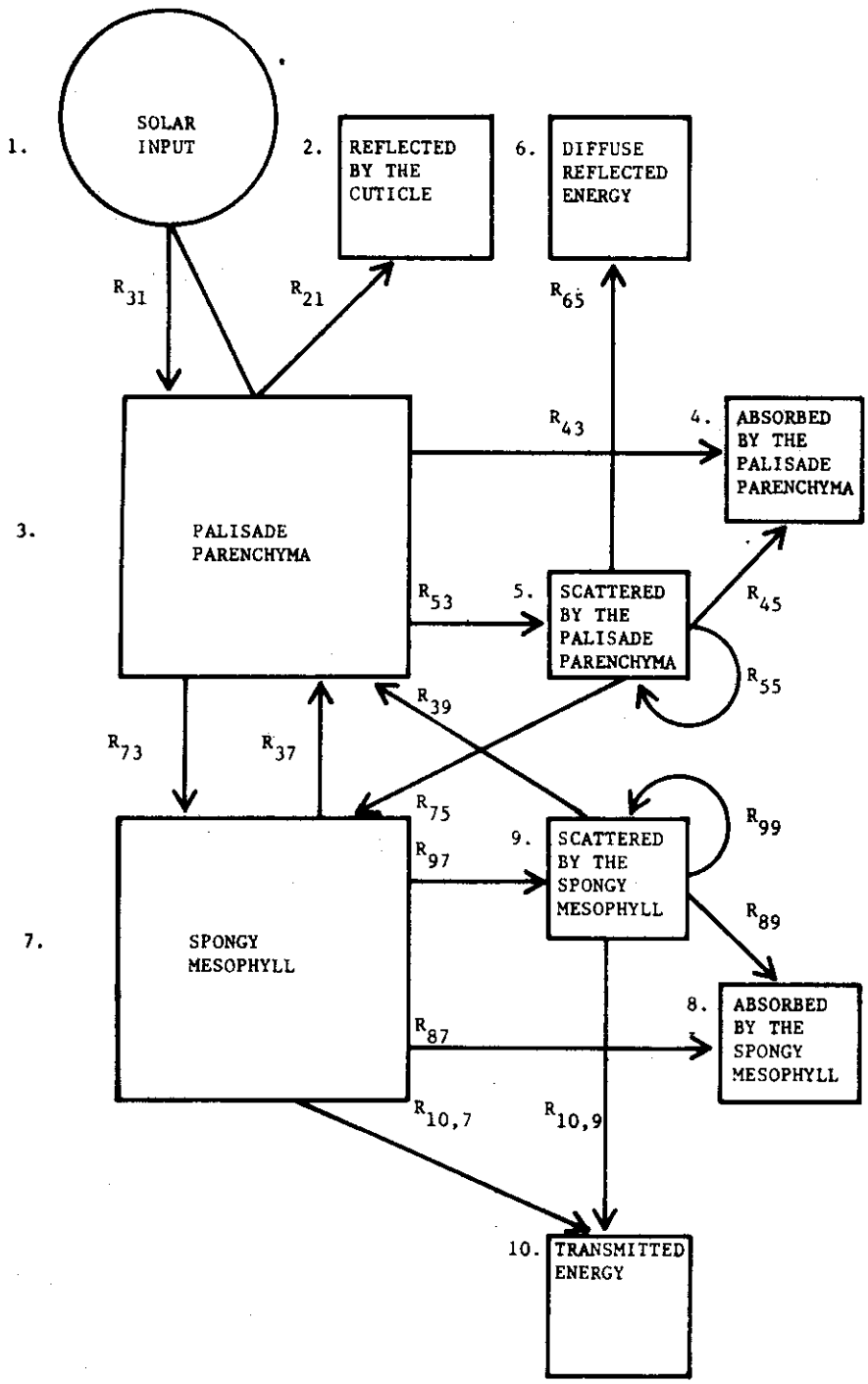

Figure 20. COMPARTMENT MODEL OF A LEAF OPTICAL SYSTEM. The arrows between compartments represent the flow rates and the direction of flow. The processes or leaf cellular aggregates are indicated within the compartments.

6. Diffuse reflected energy.

8. The absorption in the spongy mesophyll.

10. Diffuse transmitted energy.

Two cellular aggregates are represented by two compartments:

3. The palisade parenchyma.

8. The spongy mesophyll.

Two scattering mechanisms are represented by two compartments:

5. The scattering occurring in the palisade parenchyma.

9. Scattering occurring in the spongy mesophyll.

The arrows between compartments are flow functions and also indicate the direction of flow (Fig. 20). The model accounts for all incident electromagnetic energy (0.35 to 2.5 μm) entering the system and which ends up either being reflected, transmitted, or absorbed. The model is represented as a Markovian process and evaluated using the Markov chain approach. The flow rates are expressed as probabilities in the Markov chain transition matrix and the energy values at any given time are stored in a state vector. This approach is not new as a substantial amount of theory exists on the use of Markov chains to model radiative transfer (Preisendorfer, 1965).[1]

The transfer of energy within the leaf is approximated by the compartment diagram (Fig. 20) and the Markov chain approach is justifiable because of the discrete spaces represented in the leaf optical system diagram. The radiative interactions within the leaf are considered as a random walk process (Gates, 1970) and therefore

---

[1]Chapter 13 in this source is entitled: Markov chains and radiative transfer.

probabilities can be assigned according to the various interactions possible. Success in this modeling approach is the calculation and justification of accurate probabilities to represent the flow between and within compartments.

Quasi-deterministic expressions have been derived from the literature, adapted to the diagrammatic representation of the leaf model, and evaluated in terms of modeling success. An attempt was made to derive every possible probability calculation from valid data available in the literature. Values for the extinction coefficients for chlorophyll a, chlorophyll b, leutin, β - carotene, and water were available (Curcio and Petty, 1951; Salisbury and Ross, 1969; Devlin and Barker, 1971). Values for chlorophyll concentrations, carotenoid concentration, water concentration, leaf thickness, and leaf structure were also available (Esau, 1965; Anderson, 1967; Gates, 1970; Allen *et al*, 1971). Where no specific data was available, assumptions were made following a series of consultations (Ross, 1973; Smith, 1973; Trlica, 1973).

The stochastic model entitled LFMOD1[1] was written in FORTRAN and is essentially a matrix multiplication routine within a loop where each iteration of the loop corresponds to a wavelength interval. At each iteration of this main loop calculated or estimated probabilities of interaction are assigned (Table 1 and 2). At each wavelength, using the various probabilities which have been calculated, the state vector is multiplied times the Markov chain

---

[1] LFMOD1 was selected to represent LeaF MODel version 1.

Table 1. TABLE OF PROBABILITIES USED IN LFMOD1. R_{ij} = flow function from compartment j to compartment i, $\alpha(I)$ = extinction coefficient for material I, X = thickness of material, PP = thickness of palisade parenchyma, SM = thickness of spongy mesophyll, and e = Napier's number.

$$R_{43} = \sum_{i=1}^{4} \left[1.-e^{-\alpha(I)X_{PP}}\right]$$

$$R_{45} = R_{43}/2.$$

$$R_{87} = \sum_{i=1}^{4} \left[1.-e^{-\alpha(I)X_{SM}}\right]$$

$$R_{89} = R_{87}/2$$

$$R_{53} = R_{73}(1.-R_{43})/2$$

$$R_{97} = 1.-R_{87}$$

$$R_{65} = \left(R_{53} * \frac{PP}{PP + SM}\right)/2.$$

$$R_{75} = \left(R_{53} * \frac{SM}{PP + SM}\right)/2.$$

$$R_{55} = 1. - R_{45} - R_{65} - R_{75}.$$

$$R_{10\ 9} = .08$$

$$R_{39} = .12$$

$$R_{21} = .01$$

$$R_{31} = .99$$

$$R_{99} = 1. - R_{39} - R_{10\ 9} - R_{89}$$

$$R_{22} = R_{44} = R_{66} = R_{88} = R_{10\ 10} = 1.$$

$R_{ij} \neq$ one of the above, then transition probability = 0.0

Table 2. ASSUMPTIONS USED IN CALCULATING THE VARIOUS PROBABILITIES.

1. The distribution of chlorophyll a, chlorophyll b, the carotenoids, and water between the palisade parenchyma and spongy mesophyll cells is proportional to cellular density. No cellular concentration differences exist between individual palisade parenchyma and spongy mesophyll cells for these four materials.

2. Incident radiation is normal to the leaf epidermal surface.

3. 1% of the incident radiation is specularly reflected by the cuticle.

4. The upper and lower epidermal layers are transparent to radiation.

5. Rayleigh scattering is not considered.

6. A chlorophyll a to chlorophyll b ratio of 3 to 1 exists in the leaf with a .012 mg cm^{-2} total concentration present.

7. 25% of the pigment composition are carotenoids or .004 mg of total carotenoids are present with β - carotene representing 35% of this, Lutein 45% and neoxanthin 20% of the total. The entire carotenoid concentration was assumed to be leutin due to the similarity between the extinction coefficients for these three carotenoids.

8. The leaf has a thickness of .020 cm.

9. The water content is 70%, hence the equivalent water thickness is .014 cm.

10. The incident radiation does not saturate the pigment systems.

11. Internal scattering is diffuse and not specular.

12. Leaf temperature is assumed to be 20°C.

transition matrix until a steady state is reached. Steady state occurs when all the incident energy has been reflected, transmitted, or absorbed by the leaf (Fig. 21). Normally, 25 to 50 matrix

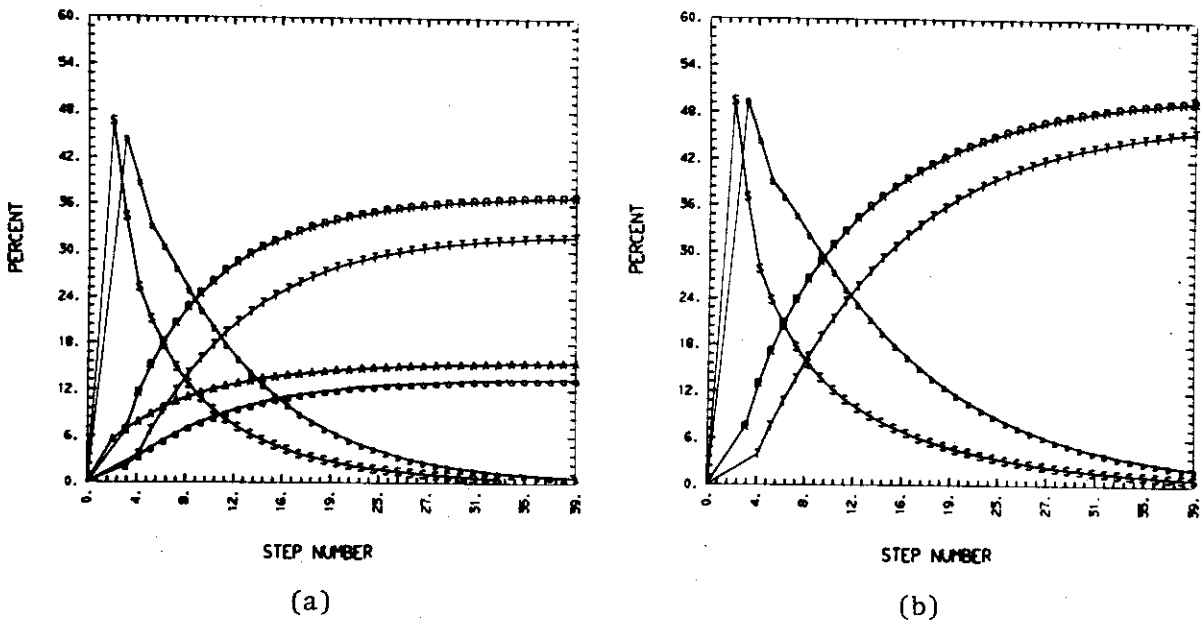

Figure 21. ITERATIVE RESPONSE OF STOCHASTIC MODEL TO INCIDENT RADIATION. Radiative flux plots at two wavelengths showing the interactions occurring as the predictions proceed to a steady state. (a) the interleaf radiative flux at .50 μm and (b) the interleaf radiative flux at .80 μm. A = absorbed in palisade parenchyma; S = scattered in palisade parenchyma; R = reflected; a = absorbed in spongy mesophyll; s = scattered in spongy mesophyll; T = transmitted. Note the differences in magnitude and similarity in form between wavelengths.

multiplications are necessary to reach a steady state. The model outputs a tabular and microfilmed summary (Fig. 22) of the predictions after evaluating the 216 iterations representing the spectral range of .35 μm to 2.50 μm at a wavelength increment of .010 μm.

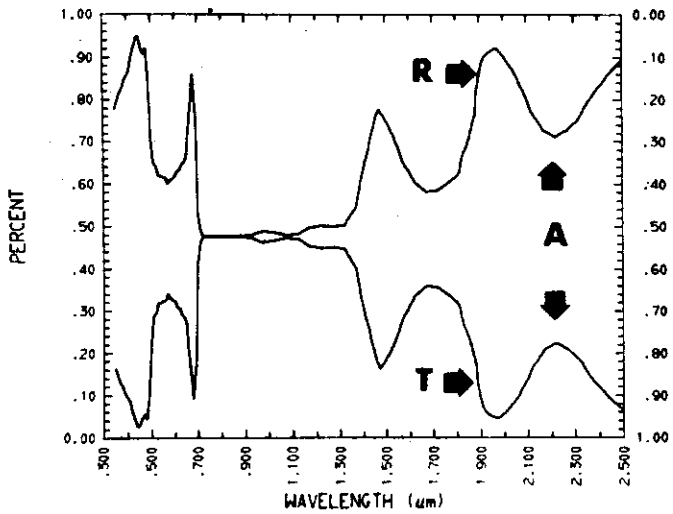

Figure 22. PREDICTED SPECTRO-OPTICAL FUNCTIONS OUTPUT FROM LFMOD1. Model predictions of the spectro-optical characteristics of a black maple (*Acer negundo*) leaf from .35 to 2.50 µm based upon leaf structure; chlorophyll, carotenoid, and leaf water content; and specular properties of the cuticle. R = reflected (plotted against right axis); T = transmitted; and area between R and T is A, the absorbed energy.

6.3 Results Obtained with the Model

The Willstätter and Stoll (1913) theory of radiative interaction within leaves was based upon the existence of distinct scattering differences between the palisade parenchyma and spongy mesophyll. This implies that somewhat different physical and biological processes are occurring in each tissue or compartment with respect to transfer and absorption of incident E-M energy for a black maple leaf (*Acer negundo*). The same type of leaf was selected for the preparation of a stochastic model because it had

been used by Willstätter and Stoll (1913) in their original explanation of the interaction between plant leaves and electromagnetic radiation in the visible portion of the spectrum and more recently it has been used in the optical-geometrical model (Allen and Richardson, 1971). Prior studies concerning the structure, thickness, and other optical parameters of black maple made it suitable for use to validate the new model. No reports of measured spectroreflectance for black maple over a sufficient wavelength interval could be found but curves were available for individual silver maple leaves and were used for comparison with the model predictions (LARS Purdue, 1969).

Prediction of the spectroreflectance, spectrotransmissance, and spectroabsorptance by the stochastic model varied in accuracy with wavelength with good predictions in the near infrared from 0.70 to 2.50 μm. Relatively poor predictions were achieved for the ultraviolet-visible region from .35 to .70 μm using the model (Fig. 23). The results of the model will be discussed separately for these two regions of the spectrum.

The model predictions for all three spectral functions were very similar to actual measured values in the 0.70 to 2.50 μm region of the spectrum (Fig. 23). These results demonstrate the validity of the abstraction of a leaf into a Markovian stochastic process when representative biophysical leaf characteristics are available. The predictions of the model in this region could be separated into two effects and their interaction(s):

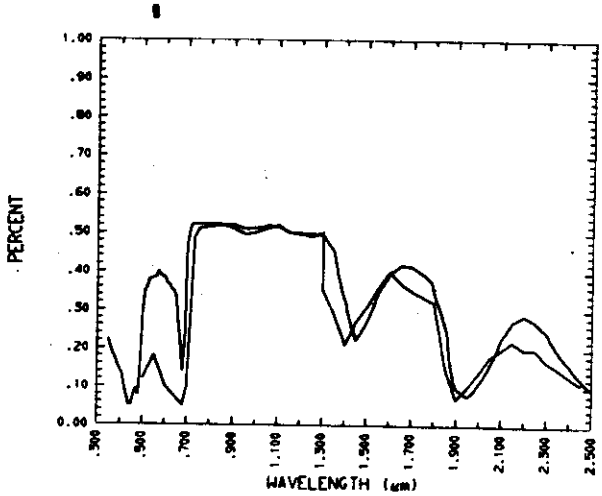

Figure 23. COMPARISON OF THE SPECTROREFLECTANCE MODELED FOR BLACK MAPLE (*Acer negundo*) AND MEASURED VALUES FOR SILVER MAPLE (*Acer saccharum*). Note the close similarity between the two spectrorefelctance curves. The silver maple curve was extracted from LARS Purdue (1969).

1. The 0.70 to 1.30 μm interval of the model was a region where limited absorption occurred and most of the incident radiation (90 - 99%) was either transmitted or reflected. Predictions of these spectro-optical characteristics in the absence of absorptance was highly dependent upon the diffuse internal scattering mechanism described by the model. The significant similarity between the prediction of the model and actual measured values supports the validity of these approximations of leaf scattering mechanisms.

2. The absorption by leaf water of incident spectroirradiance in the 1.30 to 2.50 μm interval is also accurately predicted. The model predictions were validated for

reflected, transmitted, and absorbed radiation on a wavelength basis based upon the interaction between the internal scattering mechanism and the spectral extinction coefficients for pure liquid water. It is reasonable to conclude that only slight differences existed between the spectral extinction coefficients for pure liquid water and the actual *in vitro* coefficients for the water in leaf.

The general character of the predicted spectroreflectance curves approximates actual measured values (Fig. 23). There is discrepancy, however, between predicted and measured values particularly in .50 to .68 μm spectral region. The low values for the extinction coefficients resulted in unrealistically higher values for the modeled leaf spectroreflectance in this interval and were probably caused by inaccuracies in the chlorophyll and carotenoid extinction coefficient values obtained from the literature. The reported values are low because of the chemical complexing which occurs for the pigments in the extraction solvent (acetone, dimethyl ether, ethanol). Structural alterations of the chlorophyll molecules results from the solvent environment used in its laboratory assay and this alters the true *in vivo* extinction curve for these pigments (Allen, 1964). Thus, the extinction coefficients used in this model did not represent the *in vivo* situation and such extinction coefficients are not available. The reported values for extinction coefficients in the .50 to .68 μm region of the visible spectrum are particularly suspect. It is clear that *in vitro* these

extinction coefficients for the chlorophylls and carotenoids cannot account for energy attenuation measured in healthy green leaves in the green region of the spectrum.

The Markov chain approach to modeling the spectro-optical system of a leaf has been used to accurately predict the interaction between functioning green leaves of *Acer negundo* and spectroirradiance (0.35 to 2.5 μm) of normal incidence. The modeled results indicated that the *in vitro* extinction coefficients for extracted chlorophyll a, chlorophyll b, and leutin were slightly different from the *in vivo* situation. This was supported by reports of possible pigment complexing in the organic solvents used for extraction when compared to the undisturbed pigments in a functioning leaf. The Willstätter and Stoll (1913) hypothesis concerning the mechanisms for radiative interaction within leaves has thus been substantiated by modeling with a few minor variations. The model has been used in predicting the effects that biomass, chlorophyll, and leaf water concentrations have on the spectroreflectance and spectroradiance of a plant canopy. Interpretation of the effect of the biophysical state variables in the model in an *in situ* field situation will be the subject of the balance of this report.

Several changes are contemplated to LFMOD1 to improve its immediate utility and accuracy. These include the incorporation of routines to allow non-normal incident radiation; the inclusion of Monte Carlo methods to approximate the variation in leaf structure, pigment concentrations, and leaf water content in a lateral dimension; and thorough revision of the FORTRAN code to increase program

efficiency and decrease execution time. Currently the model is being used to determine and evaluate the use of *in vitro* extinction coefficients for the plant pigments.

7.0 SPECTROREGRESSION ANALYSIS METHOD

An analytic method has been developed which enables the relationship to be determined between the spectroreflectance of a blue grama sample plot and the biophysical characteristics of that plant canopy such as total biomass, green biomass, brown biomass, total chlorophyll (a + b), and the leaf water concentration. The relationship was checked by computing a series of statistical values over the visible and photo infrared spectral range (.35 to .8 μm). A least-squares regression approach was used where the simple, linear correlation coefficient (r) and the coefficient of determination (r^2) were calculated at 91 of .005 μm intervals between .350 and .800 μm. Each of the 91 regressions resulted in output of an analysis of variance table, standard error of the estimate, and the equation of the linear regression. These statistics, expressed as functions of wavelength, defined the relative sensitivity on a spectral basis between the various biophysical characteristics of the sample plot and their spectroreflectances.

Numerous spectroreflectance curves (∿1600) for the grassland vegetation canopy have been collected in the field using the field spectrometer (Pearson, *et al*, 1973; Tucker, *et al*, 1973b). A subset of this data base was selected for the tests using the spectroregression analysis methods. This consisted of the spectroradiance and spectroreflectance of 1/4 square meter plots of *in situ* blue grama

grass measured in an irrigated and nitrogen fertilized area of the ecosystem stress area (ESA) at the Pawnee Intensive Site (Appendix B). Twenty-four plots measured in July and forty measured in September of 1971 were selected for analysis.

7.1 Effects of the Source of Spectroirradiance

The *in situ* spectroreflectance of each sample plot was measured twice using natural sunlight on cloudless days and again using an artificial light source.[1] The spectroreflectance curves for the same specific sample plot for the two types of illumination were quite similar with coefficient of determinations (r^2)>.93 for all but six of the 40 plots measured (Table 3). The spectroradiances from the sample plot were quite different between the two sources of irradiance. The solar irradiance yielded much higher spectroradiances from the near ultraviolet through the visible spectrum while the irradiance of the artificial lights produced a twofold greater spectroradiance between ∿.720 μm and .800 μm (Fig. 24).

The source of the spectroirradiance had a definite effect on the accuracy of the measurement of the spectroreflectance for the spectral interval measured. Higher incident energy values yielded higher signal to noise ratios yielding accurate reflectance measurements for that respective portion of the spectrum. Spectrocorrelation results for solar spectroirradiance showed less noise bias as

---

[1] The artificial light source consisted of ten 150 watt GE Cool-Ray lights pointed down and inward ∿100 cm from a stand surrounding the sample plot in the form of a ring. Solar irradiance was excluded by a black felt skirt.

Table 3. THE MEASURED BIOPHYSICAL CHARACTERISTICS OF THE CANOPY PRESENT ON EACH SAMPLE PLOT. The following data characterizes the in situ vegetation canopy of the 40 sample plots of blue grama grass (B. gracilis). All measurements were made between September 1 and 5, 1971 immediately after the spectroreflectance of the undisturbed sample plot was measured.

Plot Number	Total Wet Biomass (g/m^2)	Total Dry Biomass (g/m^2)	Dry Green Biomass (g/m^2)	Dry Brown Biomass (g/m^2)	Leaf Water (g/m^2)	Total Chlorophyll (A+B) Wet Wt. (mg/g)	Total Chlorophyll (A+B) Dry Wt. (mg/g)	Total Chlorophyll (A+B) Total (mg/m^2)
10001	296.40	208.96	104.92	107.04	87.60	1.415	2.007	419.41
10002	308.00	202.56	96.88	108.44	105.60	1.415	2.152	435.82
10003	378.80	284.88	114.44	173.36	94.00	.777	1.033	294.33
10004	491.20	337.88	155.52	186.40	153.20	1.278	1.858	627.75
10005	450.00	320.00	139.48	181.68	130.00	.950	1.336	427.50
10006	436.40	313.24	156.64	160.20	123.20	1.785	2.487	778.97
10007	442.40	320.00	185.04	144.08	122.40	1.756	2.428	776.85
10008	393.60	282.76	132.36	157.08	110.80	1.120	1.559	440.83
10009	404.80	293.60	143.96	151.92	111.20	1.012	1.395	409.66
10010	378.80	271.36	134.28	138.20	107.60	1.655	2.310	626.91
10014	232.00	164.20	89.40	76.00	67.60	1.326	1.874	307.63
10015	188.40	132.72	71.28	62.92	55.60	.354	.503	66.69
10017	174.40	124.44	76.12	52.68	50.00	.600	.841	104.64
10018	155.20	111.12	57.48	56.08	44.00	.571	.798	88.62
10019	124.80	84.96	53.84	35.16	40.00	.425	.624	53.04
10020	124.00	85.48	45.04	43.20	38.40	.800	1.161	99.20
10021	123.60	90.04	60.40	73.28	33.60	.930	1.277	114.95
10022	119.60	76.08	32.80	46.24	43 60	.597	.939	71.40
10023	80.80	49.76	23.24	28.60	31.20	.547	.888	44.20
10024	73.60	45.48	23.52	24.56	28.00	1.355	2.193	99.73
10025	70.80	41.48	17.20	24.92	29.60	.506	.864	35.82
10026	85.60	50.44	17.12	27.96	35.20	.635	1.078	54.36
10027	78.40	44.32	26.12	20.40	34.00	.990	1.751	77.62
10028	138.00	92.00	37.76	56.64	46.00	.580	.870	80.04
10029	133.60	94.28	32.92	58.60	39.20	.414	.587	55.31
10030	124.00	82.88	32.28	51.48	41.20	1.370	2.050	169.88
10031	198.80	122.76	51.60	72.08	76.00	.859	1.391	170.77
10032	183.60	108.80	47.96	58.68	74.80	.670	1.131	123.01
10033	427.60	253.28	152.00	104.96	174.40	1.340	2.262	572.98
10034	437.20	256.32	161.48	139.96	180.80	1.195	2.038	522.45
10035	407.20	227.16	161.48	71.60	180.00	1.250	2.241	509.00
10036	440.80	250.04	167.92	85.44	190.80	1.134	1.999	499.87
10037	178.40	94.52	57.16	37.00	84.00	1.365	2.576	243.52
10038	328.80	176.60	116.08	24.40	152.00	1.235	2.299	406.07

Table 3.--continued

Plot Number	Total Wet Biomass (g/m^2)	Total Dry Biomass (g/m^2)	Dry Green Biomass (g/m^2)	Dry Brown Biomass (g/m^2)	Leaf Water (g/m^2)	Total Chlorophyll (A+B) Wet Wt. (mg/g)	Total Chlorophyll (A+B) Dry Wt. (mg/g)	Total Chlorophyll (A+B) Total (mg/m^2)
10039	248.00	139.88	74.92	47.32	108.00	1.380	2.447	342.24
10040	306.40	174.20	106.48	69.52	132.00	1.024	1.801	313.75
10041	368.00	213.56	126.96	88.64	154.40	1.707	2.941	628.18
10042	360.00	192.20	117.36	80.04	167.60	1.997	3.740	718.92
10043	226.00	129.80	69.24	61.36	96.00	1.037	1.806	234.36
10044	334.40	197.80	104.68	108.24	136.40	2.204	3.726	737.02

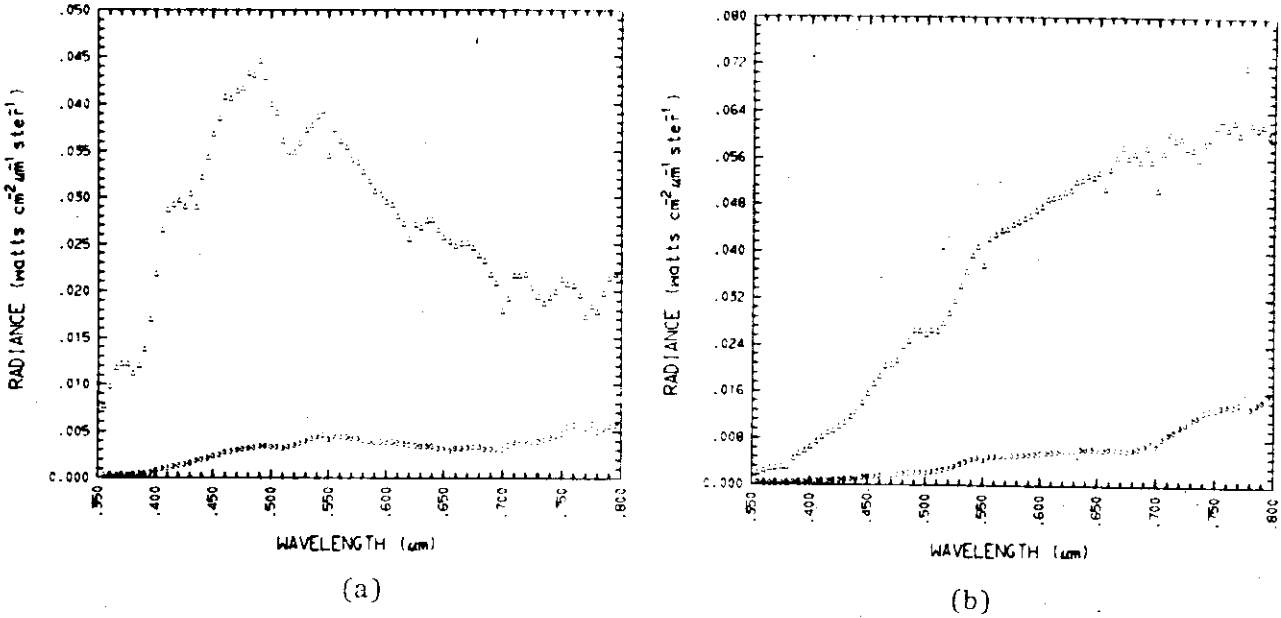

Figure 24. COMPARISON OF SOLAR (a) AND ARTIFICIAL (b) SPECTRO-IRRADIANCE OF A SAMPLE PLOT FOR ONE OF THE 40 BLUE GRAMA (*B. gracilis*) SAMPLE PLOTS. Note the difference in spectroradiance for the reference white panel (△) and sample plot (⊙) between the two types of illumination.

a function of wavelength from .350 to .720 μm than did the results from artificial spectroirradiance. The proximity of the artificial light ring to the sample plot and the absolute temperature of these lights resulted in high incident energy in the .720 to .800 μm region. The spectrocorrelations determined for the artificial spectroirradiance therefore showed better results in this spectral region than did the spectroreflectances corresponding to solar spectroirradiance.[1] The spectrocorrelation values presented in

[1]The actual spectroirradiance and spectroreflectance curves combined used in this analysis are available for inspection in both a tabular and graphical portrayal (Pearson *et al*, 1973).

this section result from using spectroreflectance curves measured using solar spectroirradiance for the interval .350 to .720 μm and artificial spectroirradiance for the interval .725 to .800 μm. This is justified by the high r^2 values between solar and artificial spectroirradiance for each sample plot and the significant incident energy differences of these two sources on a wavelength basis.

7.2 Biophysical Measurements of the Sample Plots

The *in situ* sample plots of blue grama were spectroradiometrically measured using the field spectrometer laboratory. Plots were immediately hand-clipped after the completion of these optical measurements. Initially, a 5 gram aliquot was extracted for chlorophyll analysis and immediately quick frozen in the field in dry ice (Ross, 1972). The balance of the plot was then clipped and quick frozen in the field in a chest filled with dry ice. Biomass determinations were made on the fresh frozen clipped vegetation and again after they had been dried in forced air ovens, separated mechanically with the *girraf*,[1] (Van Wyk, 1972), and then manually separated into green and brown fractions which were subsequently weighed (Dickinson, 1972). All biomass determinations were made by the IBP's Pawnee Site laboratory. The chlorophyll assays were made by the IBP's analytical laboratory on the Colorado State University campus. The various plot measurements were tabulated (Table 4), expressed as a per unit

[1] An air blower device for separating grass vegetation into green (live when clipped) and brown fractions (dead when clipped) based on a gravity principle.

Table 4. COMPARISON OF THE EFFECT OF SOLAR VERSUS ARTIFICIAL SPECTROIRRADIANCE ON THE SPECTROREFLECTANCE MEASURED FROM THE BLUE GRAMA CANOPY. These statistics show the linear relationship between the spectroreflectance of sample plots measured under solar and artificial spectroirradiance. The statistical characteristics result from a simple linear regression between the two spectroreflectance curves measured at 63 of .005 μm wavelength intervals between .480 and .800 μm for 40 of 1/4 square meter plots of blue grama (B. gracilis). Y = predicted artificially illuminated spectroreflectance and NSR = natural spectroreflectance.

Plot Number	r Value	r^2 Value	Standard Error of Estimate	Degrees of Freedom	F Ratio	Regression Equation Y = b + m (NSR)
10001	.9491	.9009	1.8461	1/61	554.37	Y=-1.8388+1.1267(NSR)
10002	.9628	.9270	1.7076	1/61	775.15	Y=-1.3415+1.2082(NSR)
10003	.9802	.9608	.9511	1/61	1495.29	Y=-3.2838+1.1418(NSR)
10004	.9939	.9878	.6158	1/61	4944.90	Y=-1.5015+1.1281(NSR)
10005	.9972	.9944	.3725	1/61	10787.69	Y=-1.1861+ .9074(NSR)
10006	.9903	.9807	.7948	1/61	3096.56	Y=-1.5374+1.1301(NSR)
10007	.9881	.9763	.8568	1/61	2509.03	Y=-1.4281+1.0893(NSR)
10008	.9682	.9374	1.9694	1/61	913.39	Y=-7.6151+1.7069(NSR)
10009	.9850	.9703	1.0086	1/61	1991.02	Y=-1.0012+1.1147(NSR)
10010	.9812	.9627	1.1658	1/61	1574.76	Y=- .5438+1.1469(NSR)
10014	.9823	.9649	1.1161	1/61	1677.68	Y=-3.0017+1.3066(NSR)
10015	.9824	.9651	1.1549	1/61	1687.99	Y=-4.8622+1.3809(NSR)
10017	.9582	.9181	1.4705	1/61	683.46	Y=-2.6120+1.1658(NSR)
10018	.9594	.9205	1.5147	1/61	706.31	Y=-3.4458+1.3751(NSR)
10019	.9699	.9408	1.0953	1/61	969.43	Y=-1.4769+1.1296(NSR)
10020	.9695	.9399	1.3483	1/61	954.12	Y=-1.8890+1.3201(NSR)
10021	.9923	.9847	.5278	1/61	3924.98	Y=- .4329+1.0733(NSR)
10022	.9898	.9797	.6628	1/61	2944.75	Y=-2.2733+1.4102(NSR)
10023	.9753	.9513	.8921	1/61	1191.32	Y=-4.6508+1.2522(NSR)
10024	.9779	.9563	.7661	1/61	1335.21	Y=-3.8165+1.4052(NSR)
10025	.9749	.9505	.7627	1/61	1171.71	Y=-2.6459+1.2948(NSR)
10026	.9871	.9744	.5151	1/61	2318.66	Y=-1.3734+1.0838(NSR)
10027	.9809	.9623	.6392	1/61	1554.91	Y=-2.4435+1.3227(NSR)
10028	.9639	.9291	.9469	1/61	799.01	Y=- .5646+1.1600(NSR)
10029	.9790	.9584	.7872	1/61	1405.57	Y=- .7721+1.0621(NSR)
10030	.9634	.9281	1.0876	1/61	786.99	Y=-3.9014+1.3980(NSR)
10031	.9663	.9337	1.0494	1/61	859.36	Y=-4.8476+1.1751(NSR)
10032	.9902	.9806	.6193	1/61	3075.42	Y=- .9337+1.2564(NSR)
10033	.9911	.9823	1.0053	1/61	3394.58	Y=-4.4711+1.2238(NSR)
10034	.9910	.9820	1.0240	1/61	3335.67	Y=-4.1871+1.1612(NSR)
10035	.9903	.9806	1.0005	1/61	3087.84	Y=-3.7396+1.2507(NSR)
10036	.9666	.9344	2.3121	1/61	868.63	Y=-2.1514+1.2821(NSR)
10037	.9917	.9834	.7940	1/61	3617.24	Y=-1.8878+1.2230(NSR)
10038	.9957	.9915	.7092	1/61	7113.25	Y=-1.4770+1.1154(NSR)

Table 4.--continued

Plot Number	r Value	r^2 Value	Standard Error of Estimate	Degrees of Freedom	F Ratio	Regression Equation Y = b + m(NSR)
10039	.9945	.9891	.7667	1/61	5537.88	Y=-2.6317+1.3420(NSR)
10040	.9932	.9864	.7073	1/61	4423.86	Y=-1.4260+1.1081(NSR)
10041	.9929	.9859	.9026	1/61	4252.81	Y=-2.2261+1.2932(NSR)
10042	.9930	.9860	.8303	1/61	4290.98	Y=-2.3642+1.2675(NSR)
10043	.9890	.9782	.9743	1/61	2734.81	Y=-2.3876+1.4579(NSR)
10044	.8882	.7889	2.8162	1/61	227.95	Y= 1.4918+ .8074(NSR)

value, and stored on punched cards for later analysis. Statistical measures of central tendency were calculated for this same data subset (Table 5).

Table 5. STATISTICAL SUMMARY OF THE BIOPHYSICAL CHARACTERISTICS OF THE SAMPLE PLOTS. A statistical description of the vegetative canopy characteristics of the 40 of 1/4 m^2 sample plots of blue grama (*B. gracilis*) sampled in early September, 1971 and used in constructing Figure 25 through Figure 38.

Sample	Range	Mean	Std. Deviation	Coef. of Variation	Std. Error of the Mean
wet total biomass (g/m^2)	70.83-491.22	261.31	154.40	51.44	21.25
dry total biomass (g/m^2)	41.50-337.84	168.55	90.81	53.88	14.36
dry green biomass (g/m^2)	17.12-185.04	89.38	50.15	56.11	7.93
dry brown biomass (g/m^2)	20.40-186.42	82.41	48.54	58.90	7.68
leaf water (g/m^2)	28.03-190.80	92.75	50.93	54.91	8.05
chlorophyll (mg/m^2)	53.02-778.97	319.58	238.73	74.70	37.75

7.3 Preparation of the Spectroreflectance Data

The spectral curves were converted from punched paper tape to magnetic tape for analysis on the Colorado State University's Control Data Corporation (CDC) 6400 computer. Conversion was accomplished using the University Computer Center's off line data

preparation facility using the paper tape to magnetic tape capability. This process read the paper tape with a 500 character per second paper tape reader under control of a REDCOR mini-computer. The data read from paper tape was written as a 'stranger' formatted magnetic tape[1] with eighty character records (corresponding to card images) under the control of a conversion program. The 'stranger' formatted magnetic tapes were processed by a FORTRAN program which buffers in the information from the 'stranger' tape, creates an internal CDC Scope 3.3 formatted disk file, and inputs this disk file into the CDC UPDATE system library routine which produces a fully packed binary magnetic tape for processing using UPDATE control language (Control Data Corp., 1972). The UPDATE data tapes are software screened by an editing program and carefully reviewed value by value by visual inspection. Data of suspect nature was checked and corrected where logical and necessary. A final UPDATE binary tape was then produced. The efficient packing of the final UPDATE binary tapes resulted in the storage of numerous blocks of 1600 spectral curves in a multi-file manner on two magnetic tapes. The permanent data tapes were duplicated,[2] red-labeled for security,[3] and placed in the magnetic tape library of the computer center for analysis.

---

[1] A 'stranger' formatted magnetic tape is a tape which was not created on the computer center's CDC on-line tape decks.

[2] The duplicated final data tape is stored in a separate locked vault away from the computer center.

[3] A red-labeled tape can only be read and may not be written upon.

7.4 Summary of the Computational Method

A computer program entitled ST38RMF (Appendix C) associated the spectroreflectance curve of a sample plot with the biophysical characteristics of that plot, merged the spectroreflectance measured curves of all plots to be analyzed by wavelength and computed the linear or multiple stepwise least-squares regression at each of 91 of .005 μm wavelength intervals between .350 and .800 μm. The reflectances at a given wavelength were regressed against the biophysical characteristic of the plot. This approach was used to compute simple linear regressions. The results of these regressions and the data point scatter at each .005 μm wavelength interval are displayed in a tabular fashion (Table 6) and as a microfilm plot

Table 6. TABULAR RESULTS OF THE LINEAR REGRESSION BETWEEN GREEN BIOMASS AND CANOPY REFLECTANCE. Tabular results for the simple linear regression between reflectance at .775 μm and the dry green biomass clipped from 40 1/4 m^2 *in situ* sample plots of blue grama (*B. gracilis*).

Wavelength = .775 μm:

Correlation coefficient (r)	=	.8493
Coefficient of determination (r^2)	=	.7213
Standard error of the estimate	=	1.6657

Regression equation: Estimated reflectance (%) = 16.5695 + .0527 (Green Biomass--G/m^2)

Analysis of Variance Table

Source	df	Sum of Squares	Mean Squares	F Ratio	P(F>Comp F)
Regression	1	272.8683	272.8683	98.3517	0.0000
Residual	38	105.4277	2.7744		
Total	39	378.2959			

(Figures 25 and 26). At the conclusion of computation, each of the

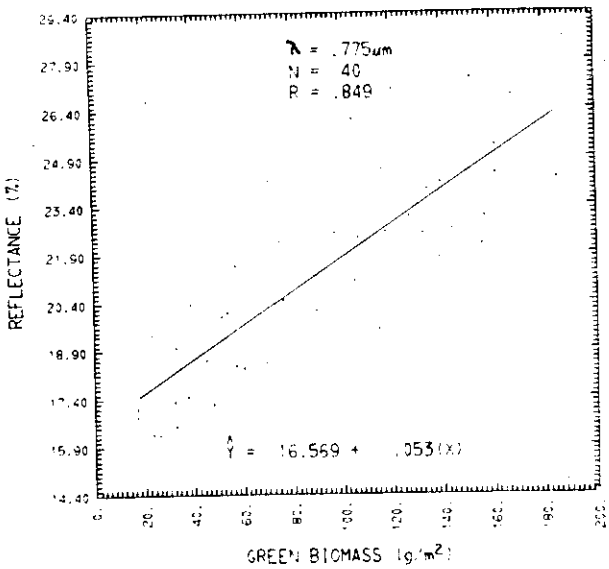

Figure 25. LINEAR REGRESSION BETWEEN GREEN BIOMASS AND CANOPY REFLECTANCE. Simple linear regression of the reflectance at .775 μm (.005 μm spectral bandwidth) against the dry green biomass clipped from 40 1/4 m^2 *in situ* sample plots of blue grama (*B. gracilis*). A summary of the coefficients of this regression occurs in Table D-3 in the appendix.

ninety-one individual linear spectral relations, the simple linear correlation values (r), the simple linear coefficient of determination (r^2), the F ratios for the analysis of variance regression model, the Y-intercepts, and the X-coefficients (slope) were plotted on microfilm as a function of wavelength. The plot of the correlation values (r values) versus wavelengths are hereafter referred to as spectrocorrelation curves (Fig. 27). The coefficient of determinance (r^2) versus wavelength hereafter will be referred to as the spectral coefficient of determinance curve (Fig. 28).

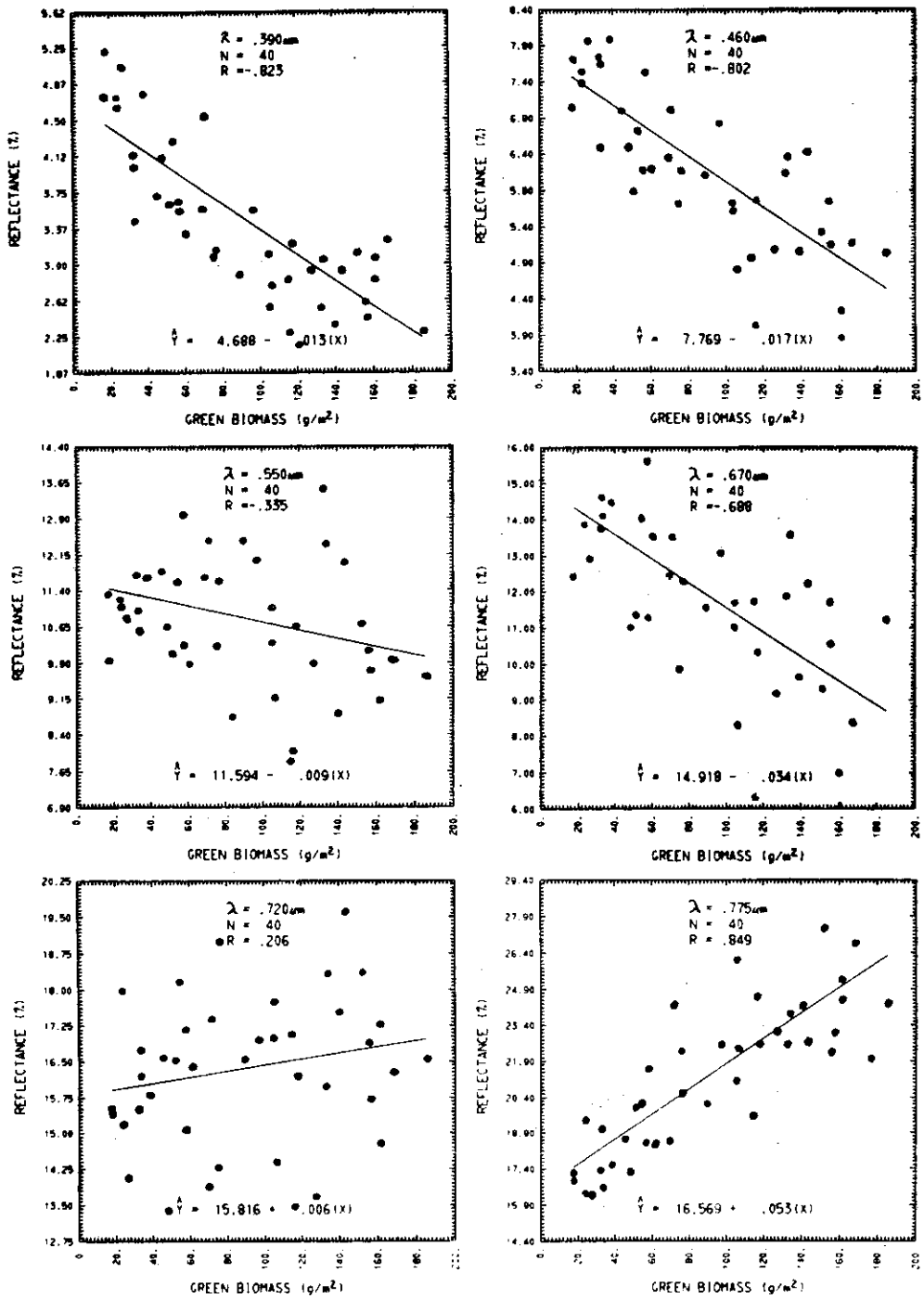

Figure 26. LINEAR REGRESSIONS AT SIX SELECTED WAVELENGTHS. Simple linear regressions of dry green biomass against 6 of the 91 available reflectances of .005 μm spectral bandwidth measured between .350 and .800 μm for 40 of 1/4 m^2 *in situ* sampling plots of blue grama (*B. gracilis*).

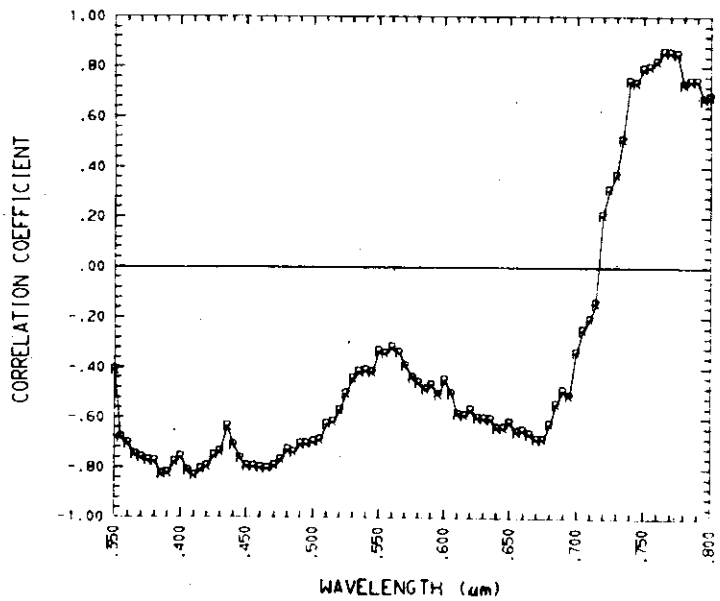

Figure 27. SPECTROCORRELATION CURVE. Simple linear spectrocorrelation curve for dry green biomass constructed by plotting the correlation coefficients (r values) between reflectance and dry green biomass for each of the 91 wavelength intervals. Note: These are the same r values illustrated in Figures 25 and 26.

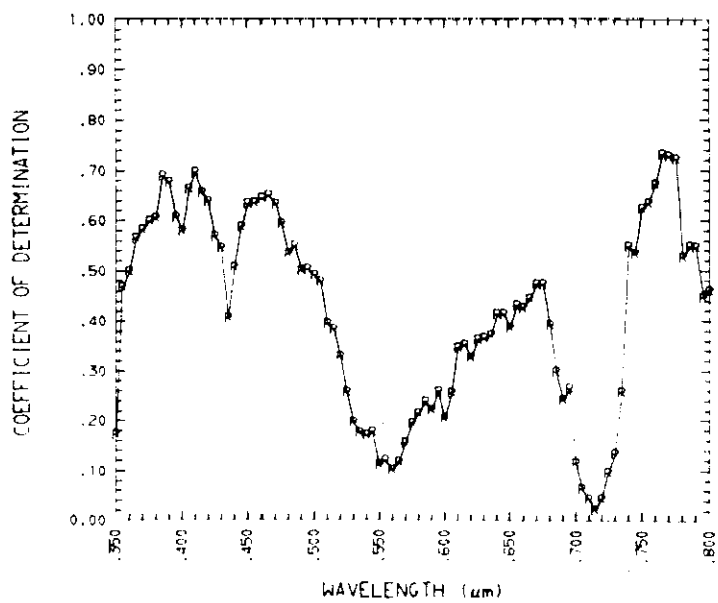

Figure 28. SPECTRAL COEFFICIENT OF DETERMINATION CURVE. Simple linear coefficient of determination curve for dry green biomass constructed by plotting the coefficients of determination (r^2 values) between reflectance and dry green biomass for each of the 91 wavelength intervals. Note: These are the squares of the r values in Figure 27.

These two graphical portrayals show the linear sensitivity of the spectroreflectance to each of the hand sampled biophysical characteristics of the sample plot, in this case the dry green biomass of the canopy (Fig. 27 and 28). The spectral F curve, that is the plot of the F value against wavelength, shows the relative significance of the regression fit resulting from this linear regression (Fig. 29). The probability of significance can be quickly determined by consulting a statistical reference for the level of significance desired.

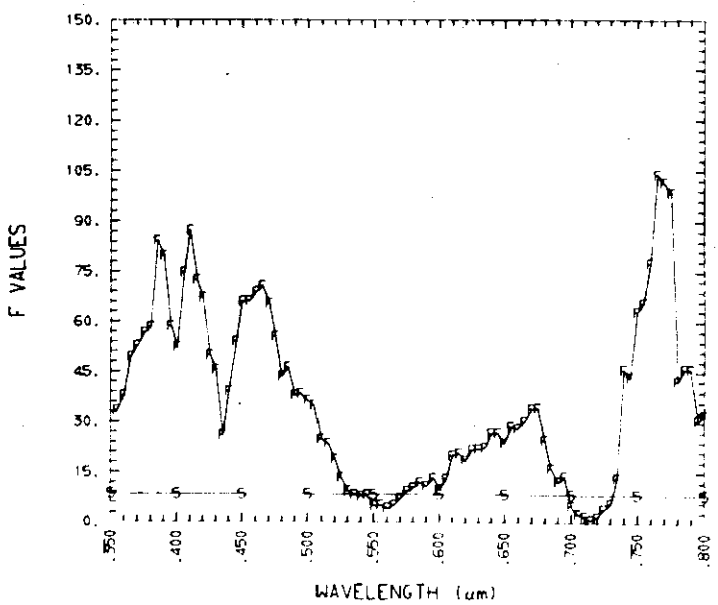

Figure 29. SPECTRAL F CURVE. F value curve resulting from the simple linear regression model analysis of variance for the regression between reflectance and dry green biomass for each of the 91 wavelength intervals. The horizontal (-5-) line represents the .5% level of significance for 1/38 degrees of freedom.

The Y-intercept plotted against wavelength, that is the Y-intercept spectral plot, was an accurate prediction of the

spectroreflectance of the soil surface underlying the canopy (Fig. 30).[1] When the plot parameter in question is taken to zero, the

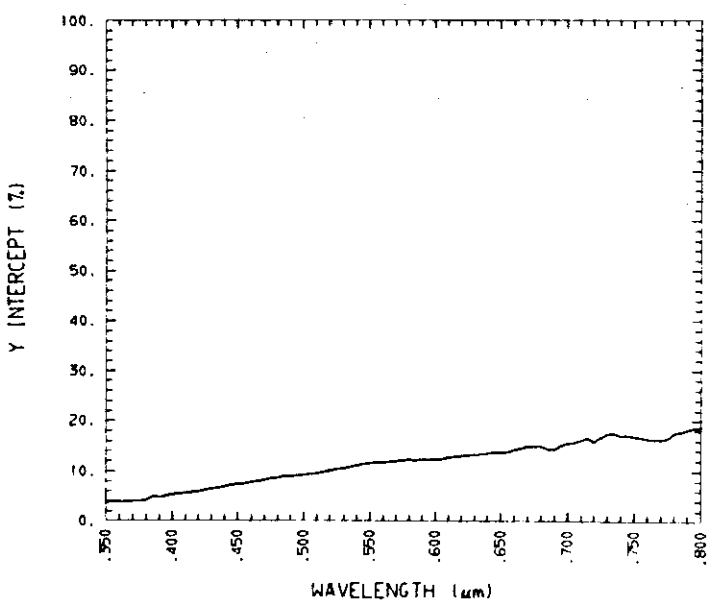

Figure 30. Y-INTERCEPTS PLOTTED AS A FUNCTION OF WAVELENGTH. Computed by the 91 simple linear regressions between reflectance and dry green biomass for the 40 *in situ* blue grama plots. This spectral plot closely approximates the underlying soil-mulch spectra.

Y intercept for the linear equation derived from this computer intercept reflectance was the reflectance of the underlying soil surface at that wavelength. The plots of each of the intercepts was derived as a function of wavelength. This yielded the spectroreflectance of the soil surface and provided a method for extracting the surface spectroreflectance of the surface underlying a vegetative canopy.

---

[1] The litter on the soil surface also contributed to this spectral curve to a lesser extent.

The dependent variable coefficients resulting from the simple linear spectroregression equations represented the weighting coefficients or the degree of deviation from the underlying soil spectroreflectance caused by the canopy when plotted as a wavelength function (Fig. 31). Regions of minimum and maximum values

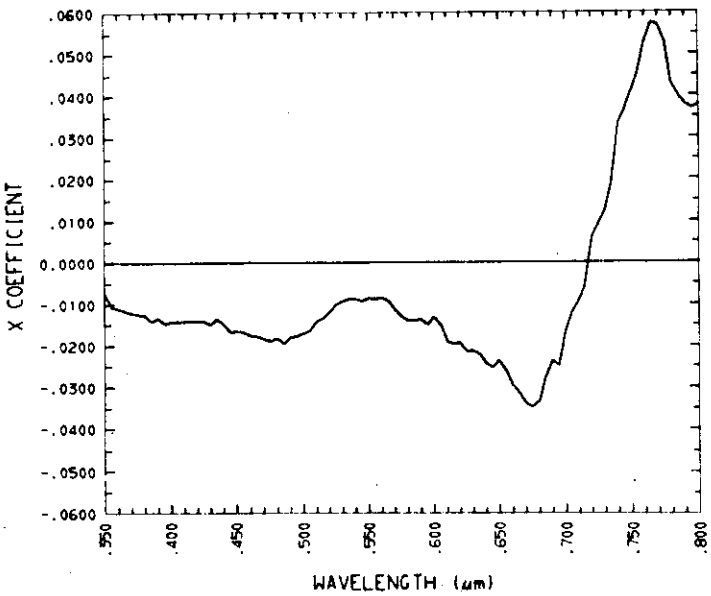

Figure 31. DEPENDENT VARIABLE COEFFICIENTS PLOTTED AS A FUNCTION OF WAVELENGTH. Computed by the 91 simple linear regressions between reflectance and dry green biomass for the 40 *in situ* blue grama plots. Areas of maximum and minimum values represent spectral regions of sensitivity to the spectral estimation of the dependent variable.

represented spectral regions of maximum sensitivity between the dependent biophysical plot characteristics and spectral measurements of this biophysical characteristic (Fig. 31).

The linear spectroregression analysis method yielded five highly significant curves:

1. The spectrocorrelation curve (r values versus wavelength) (Fig. 27).
2. The spectral coefficient of determinance curve (r^2 values versus wavelength) (Fig. 28).
3. The spectral F curve (F values versus wavelength) (Fig. 29).
4. The computed soil spectroreflectance (Y intercept versus wavelength) (Fig. 30).
5. The spectral canopy dependent variable coefficient curve (X coefficient versus wavelength) (Fig. 31).

The five relationships (Figs. 27 through 31) were formed for each of the six measured biophysical characteristics of the blue grama canopy of the sample plots and each was displayed graphically and tabularly (Appendix D). Interpretation of a set of these forty curves added measurably to the understanding of the codes placed upon the outgoing spectroradiance reflected from the plant canopy by the biophysical characteristics of the canopy. The understanding of these processes in at least one earlier case has allowed the development of a simple means for estimating canopy biomass from the solar irradiance reflected from the canopy at selected wavelengths (Pearson and Miller, 1973). It is proposed that similar estimation of chlorophyll, leaf water, soil surface reflectance, and other characteristics of the plant canopy may now be contemplated. The balance of this report will be devoted to a discussion of these relationships.

7.5 Results of the Spectroregression Analysis

7.5.1 Total Wet Biomass

A strong negative correlation occurred between spectroreflectance and total wet biomass (green + brown vegetation) in the two pigment absorption bands of the visible spectrum (.35 to .50 μm and .60 to .69 μm) (Fig. 32). A significant positive correlation

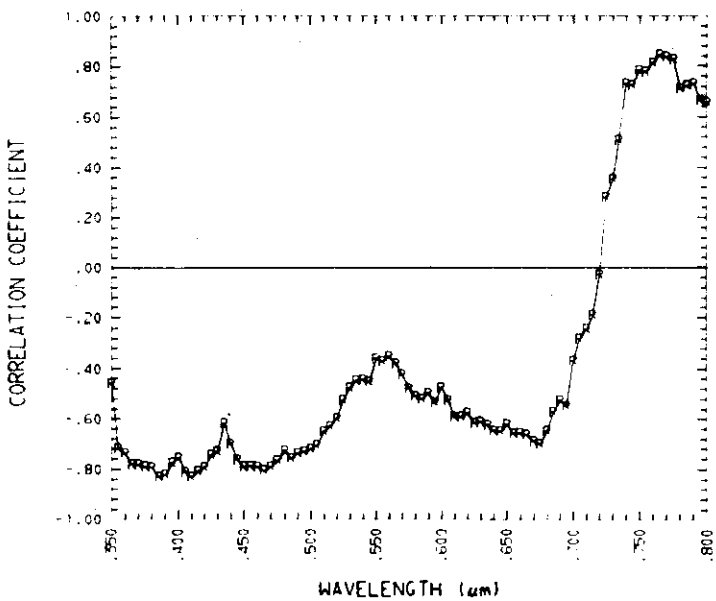

Figure 32. SPECTROCORRELATION FOR TOTAL WET BIOMASS. Simple linear spectrocorrelation curve for total wet biomass constructed by plotting the correlation coefficients (r values) between reflectance and total wet biomass for each of the 91 of .005 μm wavelength intervals.

occurred in the near infrared spectral region (.74 to .80 μm) (Fig. 32). These spectrocorrelation results for total wet biomass were based upon the pigments present (mainly the chlorophylls), the structure of the functioning green leaves, and the geometrical

arrangement of the plant canopy which displays the pigments and green leaf structure.[1]

7.5.2 Total Dry Biomass

The spectrocorrelation curve for total dry biomass (Fig. 33) was very similar to that for total wet biomass (Fig. 32). A close

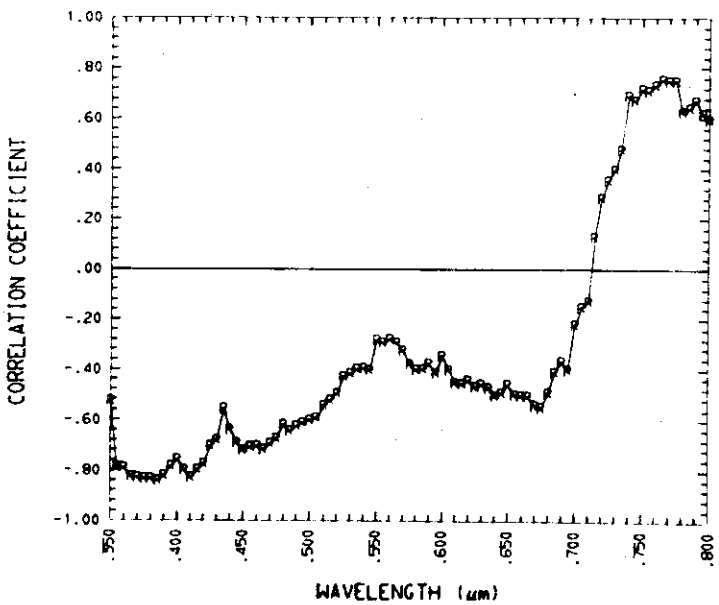

Figure 33. SPECTROCORRELATION FOR TOTAL DRY BIOMASS. Simple linear spectrocorrelation curve for total dry biomass constructed by plotting the correlation coefficients (r values) between reflectance and total dry biomass for each of the 91 of .005 μm wavelength intervals.

comparison of these two curves shows that there is little difference in the regression results between reflectance and the two methods for expressing biomass. Approximately the same rate of conversion

[1]Graphical and tabular representations for each of the 5 spectroregression curves for total wet biomass occur in Appendix D.

from green-functioning biomass to standing dead biomass throughout the growing season for blue grama has been reported (Uresk, 1971). At the time of fall sampling, the ratio of brown biomass to green biomass was roughly equal in the forty plots sampled. The relative leaf water content was approximately constant among plots and accounted for the differences among the values of total wet and dry biomass (Appendix D).

7.5.3 Dry Brown Biomass

Considerable information is available in the literature about the spectroreflectance of green vegetation but little information is available on the leaf characteristics which control the spectroreflectance of dead or senescent vegetation. Thus, sensitivity of the spectroreflectance of the dry brown fraction of the total biomass in the near ultraviolet spectral region was not anticipated (Fig. 34). This high negative correlation of the spectroreflectance in the near ultraviolet wavelengths to standing brown biomass occurred between .355 and .375 μm. The correlation value at .350 μm was degraded due to a biasing error resulting from occasional missetting of the wavelength grating to .355 μm at the start of the scan (i.e. value at .350 μm = 0). An inspection of the simple linear regression (Fig. 35) between reflectance and dry brown biomass at .365 μm where the negative correlation was most significant indicated that there was some biophysical basis for this relationship.[1]

---

[1]Graphical and tabular representations for each of the 5 spectroregression curves for total dry biomass occur in Appendix D.

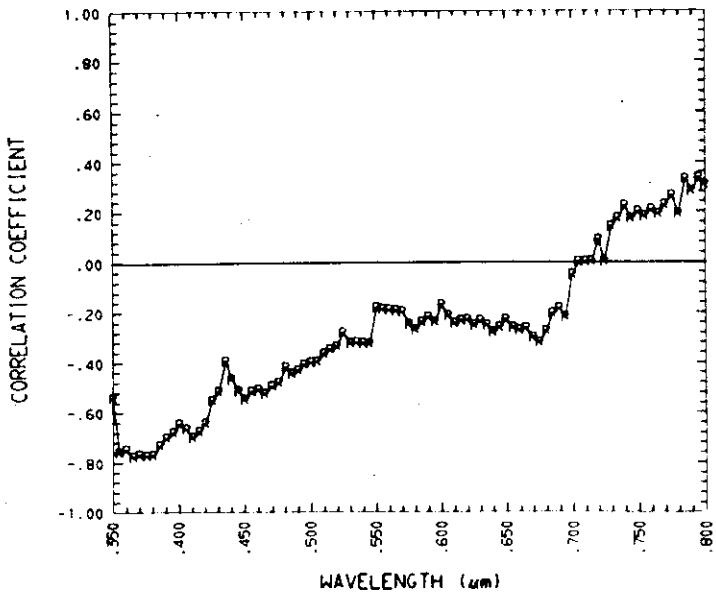

Figure 34. SPECTROCORRELATION FOR DRY BROWN BIOMASS. Simple linear spectrocorrelation curve for dry brown biomass constructed by plotting the correlation coefficients (r values) between reflectance and dry brown biomass for each of the 91 wavelength intervals. Note the significant correlation in the near ultraviolet region of spectrum.

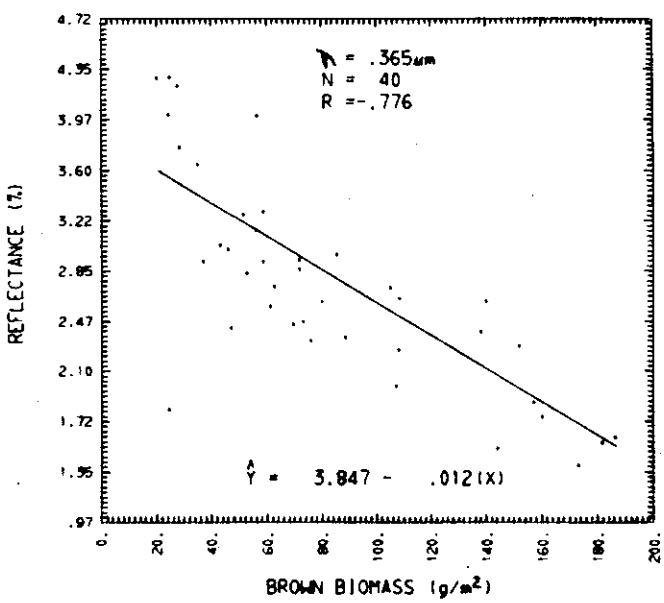

Figure 35. SIMPLE LINEAR REGRESSION BETWEEN REFLECTANCE AND DRY BROWN BIOMASS AT .365 μm. Note the sensitivity of reflectance to dry brown biomass at this wavelength.

7.5.4 Dry Green Biomass

The spectrocorrelation between reflectance and dry green biomass (Fig. 36) closely resembled the results for total wet biomass

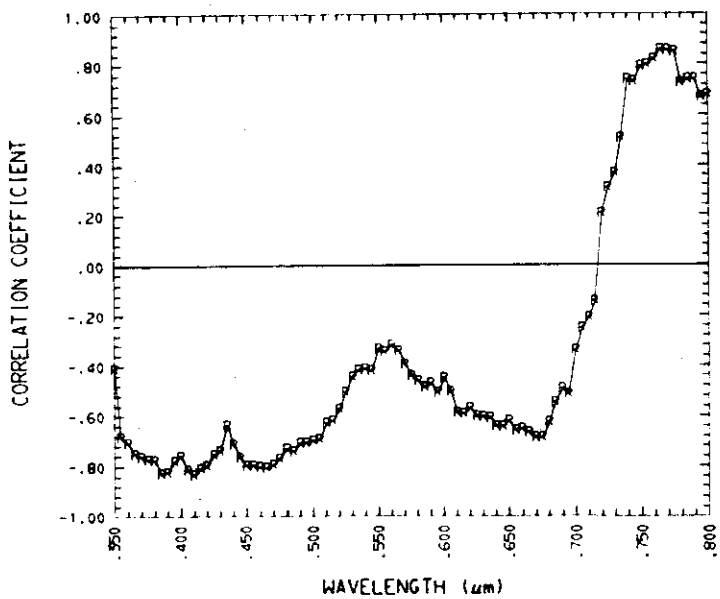

Figure 36. SPECTROCORRELATION OF DRY GREEN BIOMASS. Simple linear spectrocorrelations for dry green biomass was constructed by plotting the correlation coefficients (r values) between reflectance and dry green biomass for each of the 91 wavelength intervals.

and total dry biomass (Figures 32 and 33). Somewhat more significant spectrocorrelations between reflectance and dry green biomass occurred than the corresponding spectrocorrelations between the same reflectances and total wet biomass and total dry biomass. Significant negative correlations occurred in the two spectral regions of pigment absorption (.35 to .50 μm and .60 to .69 μm) and significant positive correlation occurs in the near infrared region of the spectrum. This was in complete agreement with the factors input

into the stochastic model described earlier. The model illustrated the complex interactions acting upon incident spectroirradiance in individual green leaves in the spectral regions of pigment absorption and in the region of near infrared intercellular effects.[1]

7.5.5 Chlorophyll

The stochastic model of the spectroreflectance of a leaf reported earlier was shown to be quite sensitive to the chlorophyll and carotenoid content of leaves modeled. The concentration of chlorophyll directly controls absorption of incidental radiation in the blue and red-orange wavelengths. The spectrocorrelation curve for spectroreflectance and total chlorophyll content (Fig. 37) thus approximated the spectrocorrelation curve between reflectance and dry green biomass (Fig. 36). Chlorophyll was probably largely responsible for establishing the spectroreflectance (green color) of the green biomass by its selective absorption of more blue and red-orange radiation. Laboratory determinations of total chlorophyll were made for the 40 of 1/4 square meter plots sampled in September, 1971 (Ross, 1972). Only one analysis per sample was performed. The results were obtained in terms of mg/g wet weight. Multiplications of the aliquot weight concentration of chlorophyll times the respective total wet weight of the plot biomass expressed the total chlorophyll as a unit area concentration. The chlorophyll values for each plot in mg/m^2 were then regressed against reflectance for the 91 wavelength intervals to yield the chlorophyll

[1] Graphical and tabular representations for each of the five spectroregression curves for dry green biomass occur in Appendix D.

spectrocorrelation curve (Fig. 37). It is interesting to note that the resulting spectrocorrelation curve was very similar to that obtained for dry green biomass even though these two biophysical characteristics were measured by two completely independent methods.[1]

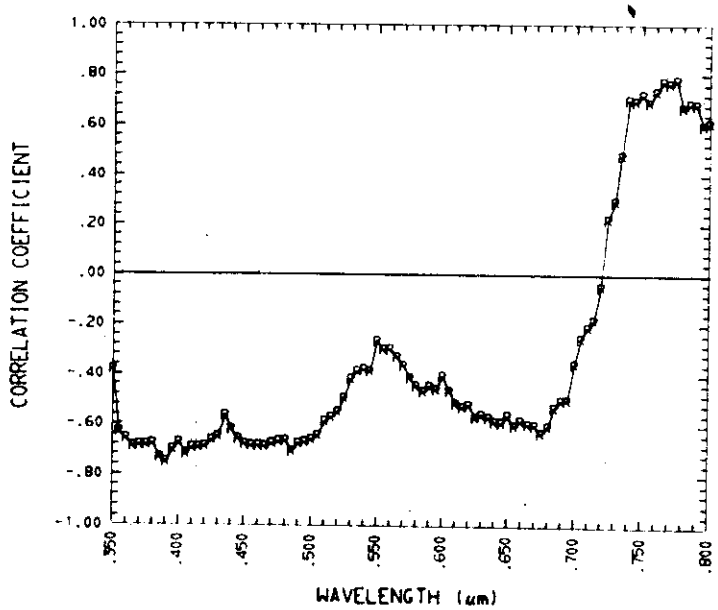

Figure 37. SPECTROCORRELATION OF THE CHLOROPHYLL PRESENT. Simple linear spectrocorrelation curve for total chlorophyll constructed by plotting the correlation coefficients (r values) between reflectance and total chlorophyll for each of the 91 wavelength intervals. Note the similarity between this figure and Figure 36.

7.5.6 Leaf Water

The leaf modeling effort demonstrated that leaf spectroreflectance between 1.30 to 2.50 μm was regulated by the amount of leaf water present which controlled the interaction of these

---

[1] Graphical and tabular representations for each of the 5 spectroregression curves for chlorophyll occur in Appendix D.

wavelengths of electromagnetic energy in leaves by selective absorption. The model also showed that leaf water had no direct effect upon radiation attenuation in the visible and photographic infrared regions of the spectrum although there was indirect coupling of leaf water with the physiological status of vegetation. That is, when leaf water became limiting, green healthy vegetation dried out and changed into brown vegetation. This coupling of leaf water with green biomass in functioning leaves was demonstrated by the spectrocorrelation results between reflectance and leaf water for the 40 sampled plots of blue grama (Fig. 38).

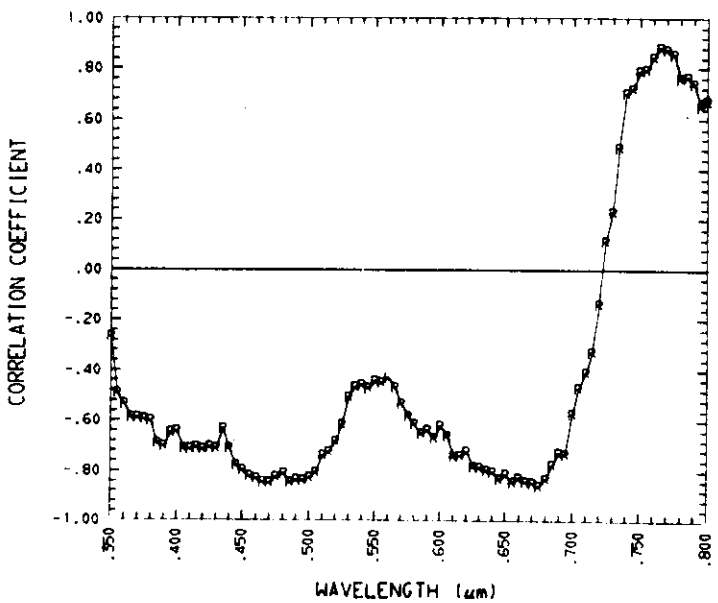

Figure 38. SPECTROCORRELATION OF LEAF WATER. Simple linear spectrocorrelation curve for leaf water constructed by plotting the correlation coefficients (r values) between reflectance and leaf water for each of the 91 wavelength intervals. Note the similarity between this figure and Figures 36 and 37.

The striking similarity between the leaf water, total chlorophyll, and dry green biomass spectrocorrelation curves indicated that these parameters were biologically coupled in the canopy.[1] The relationship between leaf water, chlorophyll and dry green biomass also indirectly controlled the spectrocorrelation curves of total wet biomass and total dry biomass. The spectrocorrelation curve of dry brown biomass, however, was very dissimilar to any of the other five curves.

[1]Graphical and tabular representation for each of the five spectroregression curves for leaf water occur in Appendix D.

8.0 COMPARATIVE INTERPRETATION OF SPECTROCORRELATION CURVES

8.1 Green Biomass, Chlorophyll, Leaf Water

The spectrocorrelation curves for the leaf water, chlorophyll, and green biomass measured for the sample plots were slightly different in magnitude but were similar in character (Figure 39).

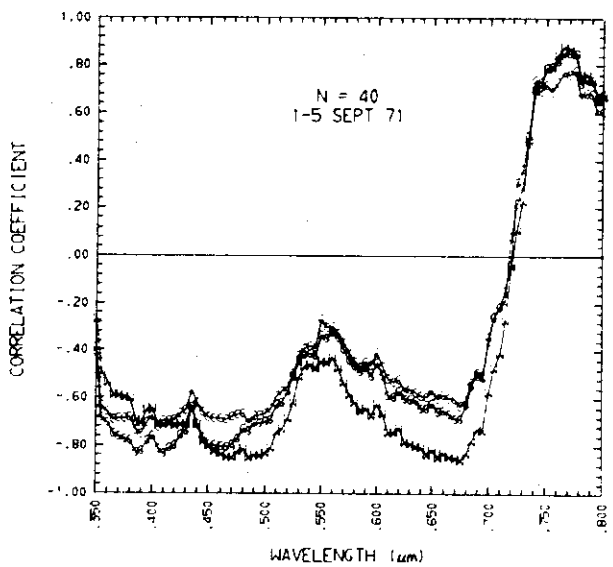

Figure 39. SPECTROCORRELATION COMPARISON FOR DRY GREEN BIOMASS, CHLOROPHYLL, AND LEAF WATER. Simple linear spectrocorrelation curves for the dry green biomass (G), chlorophyll content (C), and leaf water (W) for the same 40 *in situ* plots of 1/4 m^2 of blue grama (*B. gracilis*). Note the similarity in the three curves and that the leaf water correlation was generally most significant.

This indicated that these characteristics of the vegetation canopy sampled were highly interrelated and represented measurements of

the amount of the functioning green biomass on the plot. Significant correlations among these three measured characteristics were calculated and supported the spectrocorrelation similarities obtained (Table 7). The absence of near perfect correlation among

Table 7. CORRELATIONS BETWEEN PLOT CHARACTERISTICS. Correlation matrix of the hand sampled characteristics of the 40 sample plots described in Table 4. Note the high correlations among dry green biomass, chlorophyll, and leaf water.

	total wet biomass	total dry biomass	dry green biomass	dry brown biomass	leaf water	chlorophyll
wet total biomass	1.000	.972	.975	.836	.907	.893
dry total biomass		1.000	.946	.924	.781	.884
dry green biomass			1.000	.780	.885	.880
dry brown biomass				1.000	.559	.698
leaf water					1.000	.850
chlorophyll						1.000

the hand sampled values of dry green biomass, chlorophyll, and leaf water was probably caused by the variability associated in measuring these individual characteristics. Chlorophyll determinations were the most variable because of sampling error, dilutions, blendings, and extractions necessary for this laboratory measurement. Dry biomass measurements used machine sorting on a gravity basis with hand finishing to separate the dried vegetation into green and brown fractions. This process was very time consuming and errors were likely caused by technician fatigue. Leaf water measurements only required that the dry weight of the grass clipped from the plot be

subtracted from the wet weight measured for that sample in the field. The leaf water determination was thus least likely to include measurement error and thus showed the most significant spectrocorrelations of the three measures for functioning green biomass (Fig. 39).

The coefficients of variation for the plot parameters (Table 5) show the variability introduced by the various determinations. Leaf water had the smallest coefficient of variation. The coefficient of variation for dry green biomass was slightly larger. The chlorophyll coefficient of variation of 75 per cent was much larger than either the coefficient of variation for dry green biomass or leaf water indicating the additional variability introduced by this complex laboratory determination.

Functioning green vegetation maintains proportional amounts of green biomass, chlorophyll, and leaf water in an interrelated fashion. Therefore, the interrelationship between green biomass, chlorophyll, and leaf water was a direct relationship. Approximately 70 per cent of the wet weight of green vegetation was tissue water. The water content exerted a direct biological control upon chlorophyll concentrations by preventing enzymatic and photo-oxidative breakdown of the chlorophyll molecules.

Under non-limiting leaf water conditions, photosynthetically absorbed energy is passed along the pigment system without modifying the chlorophyll molecules. However, when leaf water decreases the pigment system is apparently no longer capable of transporting all of the captured electrons and enzymatic and photo-oxidative

degradation of chlorophyll occurs depending on the leaf water concentration (Ross, 1973).

8.2 Total Wet Biomass, Total Dry Biomass, and Dry Green Biomass

Spectrocorrelation results for total wet biomass, total dry biomass, and dry green biomass were compared to graphically measure the impact of the green biomass (the functioning green biomass) upon the spectrocorrelation curves for total wet and total dry biomass (Fig. 40). The interrelationship among amounts of total wet biomass,

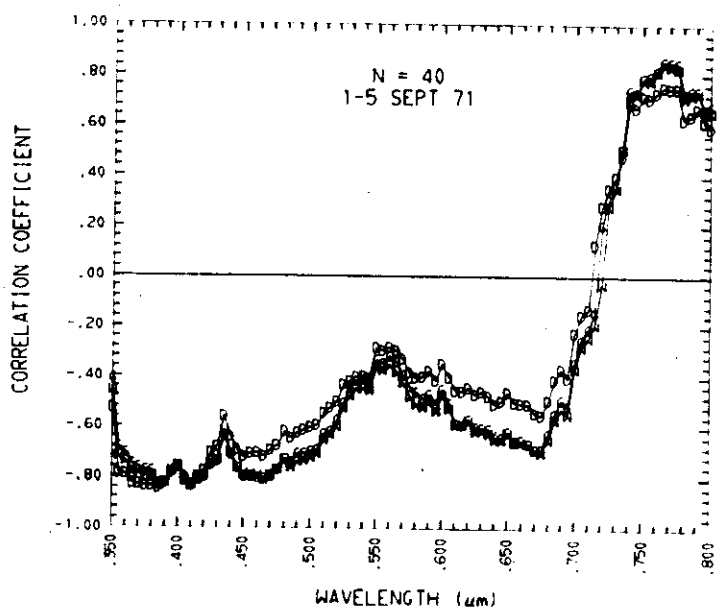

Figure 40. SPECTROCORRELATION COMPARISON FOR TOTAL WET BIOMASS, TOTAL DRY BIOMASS, AND DRY GREEN BIOMASS. Simple linear correlation curves for the total wet biomass (W), total dry biomass (D), and dry green biomass (G) for the same 40 *in situ* plots of 1/4 square meter blue grama (*B. gracilis*). Again note the similarity among these three measures of the total amount of vegetation present on the plot.

total dry biomass, and dry green biomass for this set of forty samples is clearly demonstrated by the similarity of these spectrocorrelation curves. Inspection of the intercorrelation among these three plot characteristics further substantiates this (Table 7). An earlier study at the Pawnee Site reported upon the seasonal dynamics of blue grama and stated that the conversion or transfer of green vegetation to brown vegetation could be modeled utilizing temperature and precipitation (Uresk, 1971). The temperature and precipitation variation among the forty sample plots would be a minimum because of the close proximity among plots. Thus the percentage of standing dead or brown vegetation would be relatively constant from plot to plot. This interrelationship demonstrated the marked sensitivity of the total wet biomass and total dry biomass spectrocorrelations to the green biomass present and the apparent insensitivity to the dry brown biomass present on the plots. The relatively constant conversion of green functioning vegetation to brown or standing dead biomass (Uresk, 1971) resulted in approximately the same ratio of dry green to dry brown biomass for the forty sample plots of blue grama.[1] The similarity of the three spectrocorrelation curves for biomass simply reflected this compositional characteristic of blue grama dynamics. Therefore the estimation of total wet biomass or total dry biomass was possible because of predictable interrelationship to the green functioning biomass at any point in

---

[1]Uresk (1971) states that this conversion is approximately .210 per cent per day of the green biomass present during the growing season for blue grama.

time during the growing season (Pearson and Miller, 1973). Comparisons among sampling dates during the growing season, however, are complicated due to temperature and precipitation variation.

8.3 Dry Brown Biomass, Dry Green Biomass, Chlorophyll and Leaf Water

The spectrocorrelation curve between reflectance and dry brown biomass showed a heretofore unreported effect (Fig. 41). A great

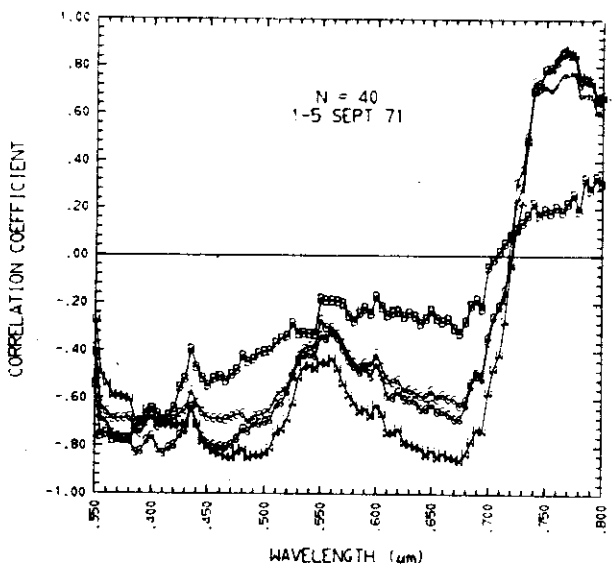

Figure 41. SPECTROCORRELATION COMPARISON FOR DRY GREEN BIOMASS, DRY BROWN BIOMASS, LEAF WATER, AND CHLOROPHYLL. Simple linear spectrocorrelation curves for the dry brown biomass (B), dry green biomass (G), chlorophyll (C), and leaf water (W) for the 40 *in situ* plots of 1/4 square meter blue grama (*B. gracilis*). Note that the similarity exists only in the ultraviolet region of the spectrum among dry brown biomass and the three related measures of the functioning green biomass.

deal of similarity existed among spectrocorrelations of dry brown biomass, dry green biomass, leaf water, and chlorophyll for the

ultraviolet region of the spectrum studied. It is not known whether this effect was caused by sampling at a favorable time or was indicative of a fundamental spectroreflectance property of standing dead vegetation. The absence of good spectrocorrelations for the three measures of the functioning green biomass in the area of strong negative spectrocorrelation between reflectance and dry brown biomass suggested that a method of ultraviolet mapping of standing dead prairie vegetation might be devised (Fig. 41).

8.4 Computation of the Spectroreflectance of the Underlying Soil Surface

An important aspect of the spectroregression analysis developed was that it could be used to extract the spectroreflectance of the soil surface underlying the sample plots. The linear equation obtained by regression at each wavelength interval is of the form

$$\text{Canopy Reflectance} = \text{Intercept} + \text{Slope (Plot Characteristic)}$$

Once this linear relationship at each wavelength was established the plot characteristic could be taken to zero and the intercept equaled the soil reflectance at that wavelength. The linear expression at each wavelength is

$$\text{Canopy Reflectance} = \text{Soil Reflectance} + \text{Coefficient (Plot Characteristic}^{1}\text{)}$$

or

---

[1] Where the plot characteristic was a measured biophysical characteristic of the plot such as green biomass, leaf water, or chlorophyll concentration.

Soil Reflectance = Canopy Reflectance + Coefficient
(Plot Characteristic)

The above regression model was an accurate approximation of the physical situation. The plotted spectrointercept curves utilizing each of the six different available biophysical measures of the vegetation canopy characteristics were very similar, as in all cases as the underlying soil surface was in fact the same and should have the same spectroreflectance (Fig. 42). This was considered to be

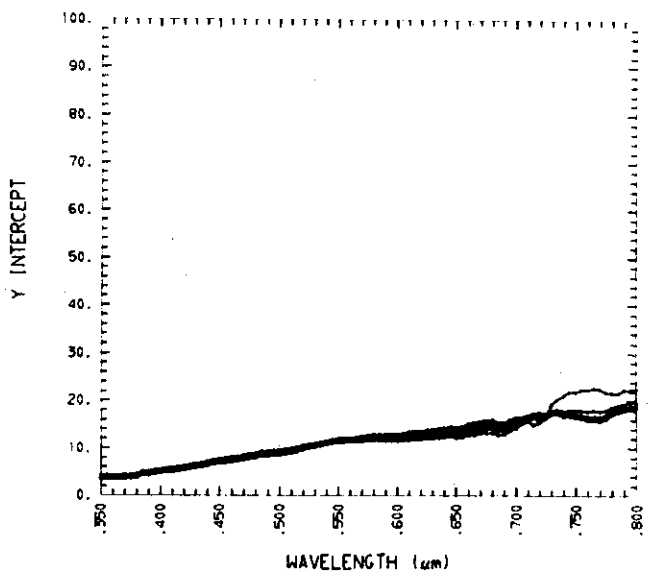

Figure 42. COMPARISON BETWEEN THE SPECTRAL INTERCEPT CURVES FOR THE SIX INDEPENDENTLY SAMPLED BIOPHYSICAL CHARACTERISTICS OF THE OVERLYING PLANT CANOPY. Note the very close similarity between the intercepts for the six different biophysical plot parameters defining the canopy for the same 40 *in situ* plots of 1/4 square meter blue grama (*B. gracilis*).

quite significant as the measurement method used to obtain the green biomass characteristics of the canopy was independent of that method used for chlorophyll assay but yielded an almost identical computed soil spectroreflectance.

Regardless of the biophysical measure of the canopy used, the regression intercepts closely resembled those of the other five intercept curves. All six of these curves in turn closely resembled the independently measured spectroreflectance of bare soil measured in the same area (Fig. 43). The six plot parameters were themselves interrelated as shown earlier (Table 7) by the correlation matrix for these measured biophysical characteristics. The soil reflectance at any wavelength could be estimated in this fashion from the canopy reflectance which was a combination of soil and vegetation reflectance. This estimate could be made for any sample plot at any wavelength for which the following conditions exist:

1. Linear relationship exists between canopy reflectance and a biophysical measure of the vegetation on the plot--i.e., a slope or coefficient is available.
2. The canopy reflectance is measured.
3. The biophysical characteristic of the canopy can be measured or estimated.

All three of these conditions could be met for the blue grama canopy studied:

1. Linear relationships were established with six different characteristics of the blue grama canopy by the spectro-regression analysis method described and the degree of linearity at each wavelength was indicated by the spectro-correlation curves presented.
2. The canopy reflectance could be measured at any wavelength or wavelength interval on the ground, remotely

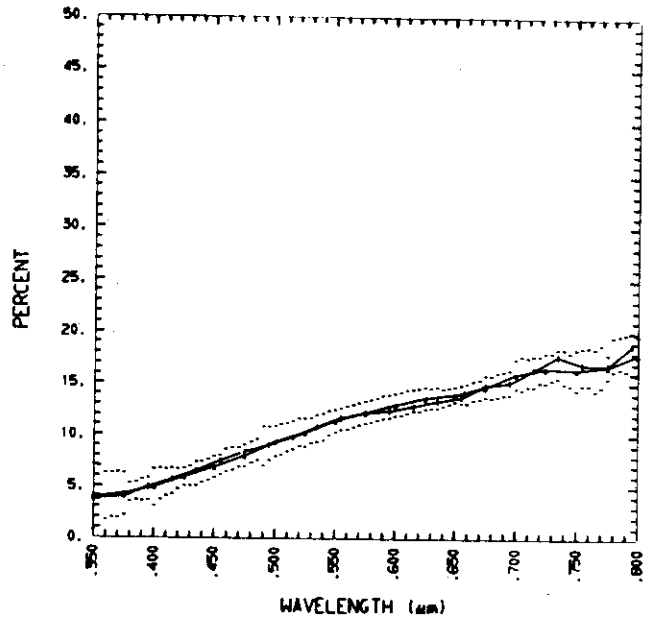

Figure 43. COMPARISON AMONG THE MEAN OF SIX COMPUTED SOIL SPECTRC-REFLECTANCES AND THE MEAN OF SOIL SPECTROREFLECTANCE MEASURED IN THE SAME AREA. -s- represents the mean spectroreflectance of 25 soil curves. - represents plus and minus one standard deviation of the mean. -i- represents the mean of the six regression intercept values. Note the close similarity between the two mean curves from .350 to .800 μm. The soil mean was formed by averaging 25 soil spectroreflectance curves for 5 bare soil plots with 5 repetitive curves per plot. The mean intercept curve was formed from the individual intercept curves resulting (Figure 42) from the simple linear regression between reflectance and the plot parameters for the 40 *in situ* plots of 1/4 square meter blue grama (*B. gracilis*).

from the air and potentially from satellite.

3. The needed biophysical characteristics could be estimated for plots from other remotely measured characteristics of the canopy (Pearson and Miller, 1973).

The consistency of the regression intercept values for different biophysical characteristics at each wavelength compared with

known soil spectroreflectance demonstrated the validity of the regression model and the accuracy or precision of the results of this approach. These results could be used to quantify the contribution of the soil to the canopy spectroradiance or spectroreflectance and hence better estimate the biophysical characteristics of the canopy itself. Application of this concept from aircraft or satellite platforms should be undertaken to evaluate its usefulness in the concurrent mapping of the functioning biomass and the underlying soil spectroreflectance by remote sensing methods. The computation of an accurate soil surface spectroreflectance from canopy reflectance also holds promise for the mapping of soil types from soil surface spectroreflectance in grassland areas. This automated soil typing has only been attempted heretofore for areas with relatively bare soil such as plowed fields.

8.5 Comparison Between Sampling Dates for Dry Green Biomass

The analysis of the forty plots sampled in early September and used throughout the preceeding examples have been compared with a similar analysis of twenty-four plots sampled eight weeks earlier in July. At both sampling times, approximately equal total dry biomass means, standard deviations, coefficients of variations, and standard errors of the mean were evident (Table 8). The data set analyzed and discussed in great detail earlier from the early part of September represented the more complex vegetational situation containing significant amounts of both dry and green biomass

Table 8. COMPARISON OF THE BIOPHYSICAL CHARACTERISTICS OF THE BLUE GRAMA CANOPY FOR TWO SAMPLING PERIODS. A statistical comparison of the vegetative characteristics of plots of blue grama (*B. gracilis*) sampled 8 weeks apart in July and September and used in constructing Figure 44. Note the consistency of the total dry biomass between the two sampling periods but that dry green biomass was transformed to dry brown biomass.

Total dry biomass (g/m^2)	July	September
number of sample plots	24	40
range	69.32 to 352.40	41.50 to 337.84
mean	171.36	168.55
standard deviation	82.36	90.81
coefficient of variation	48.06	53.88
standard error of the mean	16.81	14.36
Dry brown biomass (g/m^2)	**July**	**September**
number of sample plots	24	40
range	17.84 to 91.48	20.40 to 186.42
mean	48.53	82.41
standard deviation	21.81	48.54
coefficient of variation	44.95	58.90
standard error of the mean	4.45	7.68
Dry green biomass (g/m^2)	**July**	**September**
number of sample plots	24	40
range	38.72 to 260.92	17.12 to 185.04
mean	122.83	89.38
standard deviation	71.44	50.15
coefficient of variation	58.16	56.11
standard error of the mean	14.58	7.93

fractions (Table 5). A comparison of these biophysical characteristics for the two dates illustrated that a compositional change from green to brown biomass occurred in the eight weeks, although the mean amount of total dry biomass remained relatively constant (Table 8). The experimental plots contained a dry green to dry brown biomass

ratio of approximately 3:1 in July during the active growing season. In September this ratio had become approximately 1:1. Spectrocorrelation curves for dry green biomass values from the two sampling dates also reflected the change in composition in the vegetation canopy (Figure 44). The two spectral regions of strong pigment

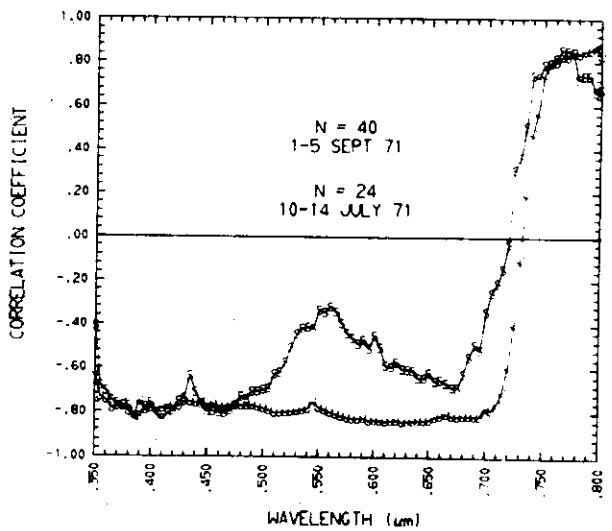

Figure 44. SPECTROCORRELATION COMPARISON FOR TWO SAMPLING PERIODS. Simple linear spectrocorrelation curves for dry green biomass taken at two different times in the growing season. S represents September and J represents July. Note the consistency in the high negative correlations in the two chlorophyll absorption bands in the blue-violet and red-orange and the high positive correlations in the photo infrared spectral region.

absorption had high spectrocorrelations with dry green biomass on both dates as did the photo infrared spectral region where the water in the green biomass controlled the spectroreflectance. The remainder of the September spectrocorrelation curve was degraded because of the presence of large amounts of dry brown biomass in

the plant canopy. The more significant spectrocorrelations existed earlier in the growing season when the ratio of dry green to dry brown biomass was much higher. The September results represented sampling at a less advantageous time in the growing season, although certain spectral intervals continued to be equally sensitive to the functioning green biomass regardless of the presence and amount of standing dead vegetation.

9.0 CONCLUSIONS

9.1 Summary of Results

1. A stochastic leaf model based upon leaf structure, pigment composition and concentration, and leaf water content has been developed using the Markov chain approach and simulated by computer techniques.
2. The predicted values for spectroreflectance, spectrotransmissance, and spectroabsorptance closely agree with measured values in the .70 μm to 2.50 μm region of the spectrum.
3. Model predictions from .35 to .70 μm agree in character with measured values but magnitude differences indicated that major differences existed between the extinction coefficients for plant pigments in organic solvents and the actual *in leaf* situation.
4. Results from the leaf model theoretically support the measurement of canopy biomass, chlorophyll, and leaf water because of their contribution to canopy spectroradiance and spectroreflectance.
5. Green biomass, chlorophyll, and leaf water are measurements of the amount of functioning green biomass and are highly interrelated in blue grama (*B. gracilis*) plots of the shortgrass prairie.
6. Simple linear spectrocorrelation curves for dry green biomass, chlorophyll, and leaf water were very similar. Differences

were probably caused by sampling errors associated with each type of determination.

7. Regions of high negative spectrocorrelation for these plot characteristics occurred in two chlorophyll absorption bands of the visible spectrum. These remained relatively constant for functioning green vegetation and were unaffected by increasing amounts of standing dead vegetation on the plot.
8. The near infrared region of the spectrum showed a high positive spectrocorrelation to the three sample characteristics and was also unaffected by increasing amounts of standing dead vegetation.
9. Spectrocorrelation results for total wet biomass and total dry biomass were similar to the spectrocorrelation results for dry green biomass, chlorophyll, and leaf water. This strong similarity was caused by the contribution of the functioning green biomass to canopy spectroradiance and spectroreflectance and the relative consistency between the sampled plots of the dry green to dry brown biomass ratio.
10. Spectral plots of the regression intercept yielded the spectroreflectance of the underlying soil or soil-mulch surface. This provided a method for extracting the effect of this spectra from the composite spectroradiance or spectroreflectance of the canopy.

9.2 Interpretations of Results

Spectrocorrelation results for total wet biomass, total dry biomass, dry green biomass, leaf water, and total chlorophyll were slightly different in magnitude but were very similar in character. This common similarity was probably based upon the contribution of the functioning green biomass to the grass canopy spectroreflectance. The dry green biomass, leaf water, and chlorophyll were shown to be intercorrelated and are actually measurements of that same biological characteristic--the amount of functioning green biomass present in the blue grama plant canopy.

The spectrocorrelation curve for brown biomass indicated a possible near-ultraviolet sensitivity between this plot characteristic and canopy spectroreflectance. The physical basis for this is not understood and additional investigation is suggested.

Spectrocorrelation comparisons between sampling dates have identified regions of the spectrum which were unaffected by the presence of standing dead vegetation and continued to show strong correlations with the amount of functioning green biomass regardless of the date during the growing season. Other regions of the spectrum were in turn sensitive to the amount of standing dead vegetation on the plot.

Spectral plots of the regression intercept yielded the spectroreflectance of the underlying soil-mulch spectra and provided a method whereby the soil or soil-mulch spectra could be extracted from the composite canopy spectroreflectance.

The various results from the spectrocorrelation-regression analysis defined the spectral sensitivity between spectroradiance and the vegetative parameters and quantified the contribution of the soil or soil-mulch spectra to the canopy spectroradiance or spectroreflectance. These combined results could be used to select spectral intervals or channels for remote aircraft or satellite sensing of grasslands and to extract information from the results of remotely sensed images.

9.3 Current and Future Efforts

Analysis currently underway includes polynomial and multiple regression spectrocorrelations. These approaches are being used to evaluate multiple combinations of all possible wavelengths and sample plot characteristics. Preliminary results have been obtained but are not sufficiently understood to allow presentation. Results generated by a plant canopy bidirectional spectroreflectance model are being used to calculate the projected biomass and projected soil area in the direction of the sun and of a sensor (Smith and Oliver, 1972). Using these more complex analyses methods it is hoped that more of a variation can be accounted for than is explained from the simple linear regressions of the plot characteristics and that the second order variation resulting from solar angle at the time of measurement will be compensated for. Additional research is also underway to more clearly identify and model the contribution of standing dead vegetation or dry brown biomass to canopy spectroreflectance. Multiple and polynomial regressions of the available biophysical measurements

of the plant canopy will be compared with the bidirectional spectroreflectance model predictions to determine the significance of the individual canopy characteristics, including the dry brown biomass.

Detailed investigations have been initiated into the methodology used to compute the spectroreflectance of the soil or soil-mulch surface underlying the plant canopy. The results of future understanding of this approach could lead to automated image processing approaches to extract and map the soil surface type from aircraft or satellite for images of grasslands in concert with the production of biomass maps of the same areas.

LITERATURE CITED

Allen, M. B. 1964. Absorption spectra, spectrophotometry, and action spectra. Photophysiology (1). Academic Press, New York. p. 83-110.

Allen, W. A., H. W. Gausman, and A. J. Richardson. 1970. Mean effective optical constants of cotton leaves. J. Optical Soc. of Amer. 60:542-547.

Allen, W. A., H. W. Guasman, A. J. Richardson, and J. R. Thomas. 1969. Interaction of isotropic light with a compact leaf. J. Optical Soc. of Amer. 59:1376-1379.

Allen, W. A., H. W. Gausman, A. J. Richardson and C. L. Wiegand. 1970b. Mean effective optical constants of thirteen kinds of plant leaves. Appl. Opt. 9:2573-2577.

Allen, W. A. and A. J. Richardson. 1968. Interaction of light with a plant canopy. J. Optical Soc. of Amer. 58:1023-1028.

Allen, W. A. and A. J. Richardson. 1971. A leaf cross section treated as an optical system. Spectral survey of irrigated crops and soils, 1971 annual report. ARS, USDA, Weslaco, Texas. V. 18 - V. 27.

Anderson, M. C. 1967. Photon flux, chlorophyll content and photosynthesis under natural conditions. Ecol. 48:1050-1053.

Arveson, J. C., J. P. Millard, and C. E. Weaver. 1971. Remote sensing of chlorophyll and temperature in marine and fresh waters. NASA, Ames Research Center, Moffit Field, Calif. 42 p.

Bement, R. P. 1968. Herbage growth rate and forage quality on shortgrass range. Ph.D. Dissertation. Colorado State Univ., Ft. Collins. 53 p.

Benedict, H. M. and P. Swidler. 1961. Non-destructive method of measuring chlorophyll content of leaves. Sci.:2015-2016.

Bennett, H. E., and J. O. Porteus. 1961. Relation between surface roughness and specular reflectance at normal incidence. J. Optical Soc. of Amer. 51(2):123-127.

Bray, J. R. 1960. The chlorophyll content of some native and managed plant communities in central Minnesota. Canadian J. of Bot. 38:313-333.

Bray, J. R. 1966. The visible albedo of surfaces in central Minnesota. Ecol. 47:524-531.

Brougham, R. W. 1960. The relationship between critical leaf area, total chlorophyll content, and maximum growth rate of some pasture and crop plants. Ann. of Bot. N. S. 24:463-474.

Cardenas, R. and H. W. Gausman. 1971. Light reflectances, chlorophyll assays and photographic film densities of isogenic barley lines. Spectral survey of irrigated crops and soils annual report. ARS, USDA, Weslaco, Texas. V. I. 36 - V. I. 40.

Carlson, R. E. 1969. Measurement and analysis of the radiation characteristics of plants as a means of evaluating drought. Unpublished M.S. thesis. Iowa State Univ., Ames, Iowa. 92 p.

Carlson, R. E. 1971. Remote detection of moisture stress: Field and laboratory experiments. Ph.D. thesis. Iowa State Univ., Ames, Iowa. 101 p.

Carter, D. L. and V. J. Myers. 1963. Light reflectance and chlorophyll and carotene contents of grapefruit leaves as affected by $NaSO_4$, NaCl, and $CaCl_2$. Proc. Amer. Soc. Hort. Sci. 82:217-221.

Clark, W. 1946. Photography by infrared, 2nd ed. John Wiley and Sons, New York.

Clayton, R. K. 1965. Molecular physics of photosynthesis. Blaisdell Publishing Co., New York. 389 p.

Colwell, R. N. 1969. A summary of the uses and limitations of multispectral remote sensing. First annual IRSI symposium proceedings, Vol. 1. Internat. Remote Sensing Inst., Sacramento, Calif. p. 1-38.

Control Data Corporation. 1970. Scope 3.3 Reference Manual--6000 series computer systems. Control Data Corporation, Sunnyvale, Calif. p. 10.1 - 10.31.

Curcio, J. A. and C. C. Petty. 1951. The near infrared absorption spectrum of liquid water. J. Optical Soc. of Amer. 41(5)/302-304.

David, W. P. 1969. Remote sensing of crop water deficits and its potential applications. Texas A & M University Technical Report RSC-06.

Devlin, R. M. and A. V. Barker. 1971. Photosynthesis. Van Nostrand Reinhold Company, New York. 304 p.

Dickinson, C. E. 1972. Pawnee Site plant live-dead separation. U.S. IBP Grassland Biome Tech. Rep. No. 140. Colorado State Univ., Fort Collins. 18 p.

Dixon, W. J., Ed. 1971. Biomedical computer programs. Univ. Calif. Publications in Automatic Computation, No. 2. Univ. Calif. Press, Berkeley. p. 233-257.

Duntley, S. Q. 1972. Detection of ocean chlorophyll from Earth Orbit. Fourth Annual Earth Resources Program Review. NASA. Manned Spacecraft Center, Houston, Texas. 25 p.

Dye, A. J. 1972. Carbon dioxide exchange of blue grama swards in the field. Ph.D. dissertation, Colorado State Univ., Ft. Collins. 54 p.

Eastman Kodak Company. 1968. Applied infrared photography. Eastman Kodak Technical Publication M-28.

Eglinton, G. 1962. Hydrocarbon constituents of the wax coatings of plant leaves--a taxonomic survey. Phytochemistry, Pergamon Press. Ltd., London. p. 89-102.

Esau, K. 1965. Plant Anatomy. John Wiley and Sons, New York. 767 p.

Fletcher, J. E. and M. E. Robinson. 1956. A capacitance meter for estimating forage weight. J. Range Manage. 9:96-97.

French, N. R. (Ed.). 1971. Preliminary analysis of structure and function in grasslands. Range Science Department Science Series No. 10, Colorado State Univ., Ft. Collins. 387 p.

Fritz, N. L. 1967. Optimum methods for using infrared-sensitive color films. Photogram. Eng. 33:1128-1138.

Gates, D. M. and W. Tantraporn. 1952. The reflectivity of deciduous trees and herbaceous plants in the infrared to 25 microns. Sci. 115:613-616.

Gates, D. M., H. J. Keegan, J. C. Schleter, and V. R. Weider. 1965. Spectral properties of plants. Appl. Opt. 4, 11-20.

Gates. D. M. 1970. Physical and physiological properties of plants. In Remote Sensing: With special reference to agriculture and forestry. Washington, D. C., National Academy of Sciences. p. 224-252.

Gausman, H. W. 1971. Photomicrographic record of light reflected at 850 nanometers by cellular constituents of *Zebrina pendula* leaf epidermis. Spectral survey of irrigated crops and soils, 1971 annual report. ARS, USDA, Weslaco, Texas. VJ. 46 - VJ. 49.

Gausman, H. W., W. A. Allen, R. Cardenas, and A. J. Richardson. 1970. Relation of light reflectance to histological and physical evaluations of cotton leaf maturity. App. Opt. 9:545-552.

Gausman, H. W., W. A. Allen, R. Cardenas, and A. J. Richardson. 1971. Effects of leaf age for four growth stages of cotton and corn plants on leaf reflectance, structure, thickness, water and chlorophyll concentrations and selection of wavelengths for crop discrimination. Spectral survey of irrigated crops and soils. ARS, USDA, Weslaco, Texas. VJ. 34 and VJ. 35.

Gibson, H. L., W. R. Buckley, and K. E. Whitmore. 1965. New vistas in infrared photography for biological surveys. J. Biol. Photo. Assn. 33:1-33.

Goodall, D. W. 1952. Some considerations in the use of point quadrats for the analysis of vegetation. Aust. J. of Sci. Res. B5-1-41.

Holmes, R. 1966. Purdue field experiments using the Perkins-Elmer SG-4 spectrometer. Purdue Univ., School Elec. Eng., July 31.

Jameson, D. A. (Coordinator). 1969. General description of the Pawnee Site. U.S. IBP Grassland Biome Tech. Rep. No. 1. Colorado State Univ., Ft. Collins, Colo. 32 p.

Knight, D. H. 1970. Some measurements of vegetation structure on the Pawnee Grassland. Colorado State Univ., IBP Grassland Biome Tech. Rep. 72. Ft. Collins, Colo. 43 p.

Knippling, E. B. 1970. Physical and physiological basis for the reflectance of visible and near-infrared radiation from vegetation. Remote Sensing of Environment 1(3):155-159.

Kubelka, P. and F. Munk. 1931. Ein Beitrag zur Optik der Farbanstriche. Z. Techn. Physic 12:593-601.

Latimer, P. 1959. Influence of selective light scattering on measurements of absorption spectra of chlorella. Plant Physiology 34:193-199.

Latimer, P. and E. Rabinowitch. 1956. Selective scattering of light by pigment containing plant cells. J. of Chem. Phy. 24:480.

Levy, E. B., and E. A. Madder. 1933. The point method of pasture analysis. New Zealand J. of Agr. 46:267-279.

Mestre, H. 1935. The absorption of radiation by leaves and algae. Cold Springs Harbor Symposium on Quantative Biology 3:191-209.

Miller, J. B. 1967. A formula for average foliage density. Australian J. of Bot. 15:141-144.

Miller. L. D. 1969. A field light quality laboratory--initial experiment--the measurement of per cent of functioning vegetation in grassland areas. Colorado State Univ., IBP Grassland Biome, Prog. Rep., Oct., 1969 to Jan., 1970. 16 p.

Miller, L. D. and R. L. Pearson. 1971. Aerial mapping program of the IBP Grassland Biome: remote sensing of the productivity of the shortgrass prairie as input into biosystem models. Proceedings of the Seventh International Symposium on Remote Sensing of Environment. Univ. of Michigan, Center for Remote Sensing Information and Analysis, Ann Arbor, Michigan, p. 165-205.

Mitchell, J. E. 1972. An analysis of the beta-attenuation technique for estimating standing crop of prairie range. J. Range Manage. 25:300-304.

Mueller, J. L. 1972. Remote measurement of chlorophyll concentration and secchi-depth using the principle components of the ocean's color spectrum. Fourth Annual Earth Resources Program Review. NASA, Manned Spacecraft Center, Houston, Texas. 13 p.

No Author. 1969. Remote multispectral sensing in agriculture. Laboratory for agricultural remote sensing (LARS), Purdue Univ. Annual Report, Volume 4. Lafayette, Indiana.

Olson, C. E. 1969. Early remote detection of physiologic stress in forest stands. Proceedings of the Second Biennial Workshop on Aerial Color Photography in the Plant Sciences, March 5-7, 1969, Univ. of Florida. Gainesville, Florida, Florida Dept. of Agriculture.

Oster, G. 1948. The scattering of light and its applications to chemistry. Chem. Rev. 43, 319-365.

Orvington, J. D., and D. B. Lawrence. 1967. Comparative chlorophyll and energy studies of prairie, savanna, oakwood, and maize field ecosystems. Ecol. 48:515-524.

Pearson, R. L. and L. D. Miller. 1971. Design of a field spectrometer laboratory. Dept. of Watershed Sciences, Science Series 2, Colorado State Univ., Ft. Collins. 102 p.

Pearson, R. L. and L. D. Miller. 1972a. Remote spectral measurements as a method for determining plant cover. Technical report 167, Grassland Biome, International Biological Program, Colorado State Univ., Ft. Collins, Colorado. 48 p.

Pearson, R. L. and L. D. Miller. 1972b. Remote mapping of standing crop biomass for estimation of the productivity of the shortgrass prairie, Pawnee National Grasslands, Colorado. Proc. Eighth Int. Symp. on Remote Sensing of Envir., Univ. of Michigan, Ann Arbor, Michigan.

Pearson, R. L. and L. D. Miller. 1973. Remote multispectral sensing of biomass. Science Series 10, Dept. of Watershed Science. Colorado State Univ., Ft. Collins. 150 p.

Pearson, R. L., L. D. Miller, and C. J. Tucker. 1973 (in preparation). Field spectrometer experimental data--1971: spectroradiance, spectroreflectance, spectroabsorptance, and spectrotransmissance of shortgrass prairie vegetation. Internal. Biological Prog., Grassland Biome Prog., Tech. Rep., Colorado State Univ., Ft. Collins. 1600 p.

Pechanec, J. F. and G. D. Pickford. 1937. A weight estimation method for the determination of range or pasture production. Am. Soc. Agron. J. 29:894-904.

Philip, J. R. 1965. The distribution of foliage density with foliage angle estimated from inclined point quadrat observations. Aust. J. of Bot. 13:357-366.

Preisendorfer, R. W. 1965. Radiative Transfer on Discrete Spaces. Pergamon Press, New York. 459 p.

Rauzi, F., and A. K. Dobrenz. 1970. Seasonal variation of chlorophyll in western wheatgrass and blue grama. J. of Range Manage, 23:372-373.

Ross. D. 1972. Memo to IBP laboratory concerning techniques for chlorophyll determinations on frozen grass samples. Dept. of Botany and Plant Pathology, Colorado State Univ., Ft. Collins, 10 p.

Ross, C. 1973. Personal communication. Plant physiologist, Dept. of Botany and Plant Pathology, Colorado State Univ., Ft. Collins.

Salisbury, F. B. and C. Ross. 1969. Plant physiology. Wadsworth Publishing Company, Belmont, Calif. 765 p.

Sinclair, T. R. 1968. Pathway of solar radiation through leaves. Unpublished M.S. thesis. Lafayette, Indiana, Library, Purdue Univ. 179 p.

Smith, J. A. 1973. Personal communication. Associate Professor, Dept. of Watershed Science, Colorado University.

Smith, J. A. and R. Oliver. 1972. Plant canopy models for simulating composite scene spectroradiance in the .4 to 1.04 μm region. Proc. Eighth Internat. Symp. on Remote Sensing of the Environment, Univ. Mich., Center for Remote Sensing, Information and Analysis, Ann Arbor. 21 p.

Steiner, D. and T. Gutterman. 1966. Russian data on spectral reflectance of vegetation, soil, and rock types. Final Technical Report, United States Army European Research Office.

Tarkington, R. G. and A. L. Sorem. 1963. Color and false-color films for aerial photography. Photogram. Eng. 29:88-95.

Teare, I. D., G. O. Mott, and J. R. Eaton. 1966. Beta Attenuation--a technique for estimating forage yield *in situ*. Radiation Bot. 6:7-11.

Thomas J. R., Wiegand, C. L., and V. I. Myers. 1967. Reflectance of cotton leaves and its relation to yield. Agron. J. 59:551-554.

Trlica, J. 1973. Personal communication. Assistant Professor, Dept. of Range Science, Colorado State Univ.

Tucker, C. J., L. D. Miller, and R. L. Pearson. 1973 (in preparation). Field spectrometer experimental data--1972: spectroradiance, spectroreflectance, spectroabsorptance, and spectrotransmissance of shortgrass prairie vegetation. Internat. Biological Prog., Grassland Biome Prog., Tech. Rep., Colo. State Univ., Ft. Collins. 2000 p.

Tucker, C. J., L. D. Miller, and R. L. Pearson. 1973. Measurement of the combined effect of biomass, chlorophyll, and leaf water on canopy spectroreflectance of the shortgrass prairie. Proc. of the second annual Remote Sensing of Earth Resources Conference. University of Tennessee Space Institute, Tullahoma. 27 p. (in press).

Uresk, D. M. 1971. Dynamics of blue grama within a shortgrass ecosystem. Ph.D. dissertation, Colo. State Univ., Ft. Collins. 52 p.

Van Dyne, G. M., F. M. Glass, and P. A. Opstrup. 1968. Development and use of capacitance meters to measure standing crop of herbaceous vegetation. Oak Ridge Natl. Lab. ORNL-TM 2247, Oak Ridge, Tenn. 47 p.

Van Wyk, J. J. P. 1972. A preliminary report on new separation techniques for live-dead aboveground grass herbage and roots from dry soil cores. Internat. Biological Prog., Grassland Biome Prog., Tech. Rep. 144, Colo. State Univ., Ft. Collins. 16 p.

Warren Wilson, J. 1959. Analysis of the spatial distribution of foliage by two dimensional point quadrats. New Phytol. 58:92-101.

Warren Wilson, J. 1960. Inclined point quadrats. New Phytol. 59:1-8.

Warren Wilson, J. 1963. Estimation of foliate denseness and foliage angle by inclined point quadrats. Aust. J. Bot. 11:95-105.

Willstätter, A. and K. Stoll. 1913. Untersuchungen über die Assimilation der Kohlensäure, Verlag-Springer, Berlin. p. 122-127.

Winkworth, R. E. 1955. The use of point quadrats for the analysis of heathland. Aust. J. of Bot. 3:68-81.

Wong, C. L. and W. R. Blevin. 1967. Infrared reflectances of plant leaves. Aust. J. Biol. Sci., 20:501-508.

Woolley, J. T. 1971. Reflectance and transmittance of light by leaves. Plant Physiol. 47:656-662.

APPENDIX A

APPENDIX A

LFMOD1 Description

This appendix contains detailed information concerning the operating sequence of LFMOD1 (Figure A-1), a complete listing of the FORTRAN code and subroutines (Exhibits A-1 to A-5), and the tabular model predictions (Table A-1).

LFMOD1 predicts the spectro-optical properties of a single green leaf based upon the histological structure, leaf thickness, pigment composition and concentration, and leaf water content. Model predictions are made for the absorbed, reflected, and transmitted energy at each of 216 of .10 μm intervals between .35 and 2.50 μm based upon the noted input parameters.

LFMOD1 requires $40{,}000_8$ words of central memory to load and took approximately 90 seconds to perform the 216 wavelength interactions between 0.35 and 2.50 μm on a CDC 6400 computer.

The following sections are contained in this appendix:

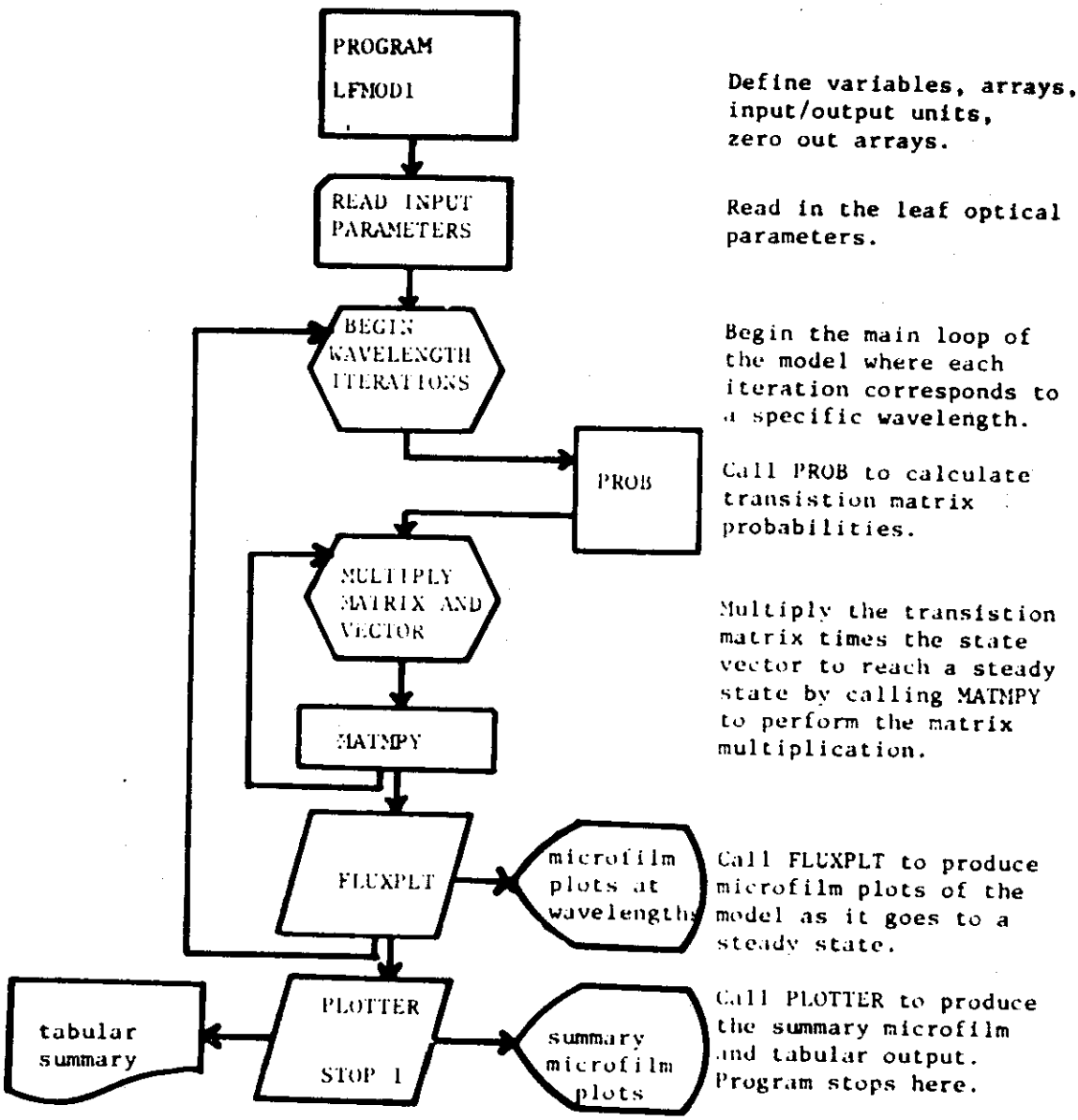

Figure A-1. AN EXECUTION SEQUENCE DIAGRAM FOR THE SIMULATION PROGRAM LFMOD1 WHICH COMPUTES THE SPECTRO-OPTICAL CHARACTERISTICS OF A SINGLE LEAF FROM ITS MORPHOLOGICAL AND PHYSIOLOGICAL PROPERTIES. The spectro-optical characteristics of a single leaf of black maple (*A. negundo*) computed by this program occurs in Table A-1. The complete FORTRAN listing for the main program LFMOD1 and its subroutines MATMPY, PROB, FLUXPLT, and PLOTTER occur as Exhibits A-1 through A-5.

Exhibit A-1. PROGRAM LFMOD1. Input, output, and program control are handled by this main section of LFMOD1. See Figure A-1 for the execution sequence diagram.

```
      PROGRAM LFMOD1
     1 (INPUT=64, OUTPUT=64, FILMPL=128, PUNCH=64, TAPE5=
     1INPUT, TAPE7=64)
      COMMON/11111/TRAN(12, 12), ST1(12), ST2(12), TRAN2(12, 12)
      COMMON/22222/PFL(300), ABS(300), TRN(300), WAVLN(300)
      COMMON/33333/CAROT(300), CHLOROA(300), CHLOROB(300),
     1H2O(300)
      COMMON/44444/ OUT(12,250), M, LEVEL, IS
     1, CONCART, CONCHLA, CONCHLR, EWT
      DIMENSION COMP(12), N(250), ST0(12)
      READ(5, 100)M, LEVEL
      NROWS=LEVEL/10
      READ(5, 101)  (COMP(I), I=1, M)
      READ(5, 102)    (ST0(I), I=1, M)
      DO 1 I=1,250
      N(I)=I-1
    1 CAROT(I)=CHLOROA(I)=CHLOROB(I)=H2O(I)=0.
      READ(5, 105)  CONCART, CONCHLA, CONCHLR, EWT
      READ(5, 304)    (CAROT(I), CHLOROA(I), CHLOROA(I), H2O(I),
     1I=1, 7)
      READ(5, 303)    (CHLOROA(I), CHLOROB(I), I=8, 216)
      READ(5, 305)    A, B
      READ(5, 301)    (CAROT(I), I=8, 216)
      READ(5, 302)    (H2O(I), I=6, 216)
      PUNCH 300,   (CAROT(I), I=1, 216)
      PUNCH 300,   (CHLOROA(I), CHLOROB(I),  I=2, 216)
      PUNCH 300,   (H2O(I), I=1, 216)
      DO5I=1,216
      WL=WAVLN(I)=.340+FLOAT(I)*.01
    5 PRINT 250, I, WL, CAROT(I), CHLOROA(I), CHLOROB(I),
     1H2O(I)
      CALL PLTDATA
      DO 10 I=1, M
      DO 10 J=1, M
   10 TRAN(I, J)=0.0000
      DO76IS=1, 216
      CALL PROB
      WRITE(7, 300) WAVLN(IS)
      WRITE(7, 201) (COMP(I), I=1, M)
      DO 20 I=1, M
```

Exhibit A-1 - cont.

```
20      WRITE(7,202) COMP(I), (TRAN(I,L), L=1,M)
        DO 30 I=1,M
30      ST1(I)=ST0(I)
        DO 40 I=1,M
40      OUT(I,1)=ST1(I)
        DO 50 K=2,LEVEL
        CALL MATMPY
        DO 50 I=1,M
        OUT(I,K)=ST2(I)
50      ST1(I)=ST2(I)
        CALL FLUXPLT
        K=MM=1          $          NN=10
        DO75L=1,NROWS
        WRITE(7,203)N(K),N(K+1),N(K+2),N(K+3),N(K+4),N(K+5),
       1N(K+6),N(K+7),N(K+8),N(K+9)
        K=K+10
        DO 70 I=1,M
70      WRITE(7,204) COMP(I),(OUT(I,J),J=MM,NN)
        MM=MM+10
        IF(MOD(L,5).EQ.0) WRITE(7,210)
75      NN=MM+9
        RFL(IS)=ST2(2)+ST2(6)
        ABS(IS)=ST2(4)+ST2(8)
76      TRN(IS)=ST2(10)
        PRINT 210
        PRINT 207
        IS=IS-1
        DO 80 I=1,IS
80      PRINT 206, WAVLN(I), ABS(I), RFL(I), TRN(I)
        CALL PLOTTER
100     FORMAT(4I5)
101     FORMAT( 8A10)
102     FORMAT(16F5.3)
103     FORMAT(2F6.3)
104     FORMAT(F6.3,3X,3(F6.3,3X))
105     FORMAT(8(F10.0))
107     FORMAT(10X,2(F10.3))
200     FORMAT(//25X*TRANSISTION MATRIX AT WAVELENGTH =
       1*F6.3*MICROMETERS*)
201     FORMAT(1X*TO/FROM*/14X,10(A10,1X)/)
202     FORMAT(1X,A10,2X,10(F8.6,3X))
203     FORMAT(/18X,10(I3,7X))
204     FORMAT(1X,A10,3X,10(F8.6,2X))
205     FORMAT(//50X*WAVELENGTH = *F6.4*MICROMETERS*/)
```

Exhibit A-1 - cont.

```
206     FORMAT(10X,4(F10.3))
207     FORMAT(14X*WAVELEN.  ABSORB.  REFLECT.  TRANS.
       1*//)
210     FORMAT(1H1)
250     FORMAT(5X,I3,5(F10.4))
300     FORMAT(10(F8.3))
301     FORMAT(2(10X,F10.0,20X))
302     FORMAT(4(10X,F10.0))
303     FORMAT(2(10X,2(F10.0)))
304     FORMAT(4(F10.0))
305     FORMAT(A10/A10)
        END
```

Exhibit A-2. SUBROUTINE MATMPY. This subroutine multiplies the Markov transition matrix times the state vector. See Figure A-1 for the execution sequence diagram.

```
      SUBROUTINE MATMPY
      COMMON/11111/TRAN(12, 12), ST1(12), ST2(12), TRAN2(12, 12)
      COMMON/44444/  OUT(12,250), M, LEVEL,  IS
      DO 10 J=1, M
10    ST2(J)=0.
      DO 20 I=1, M
      DO 20 J=1, M
20    ST2(I)=TRAN(I, J)*ST1(J)+ST2(I)
      RETURN
      END
```

Exhibit A-3. SUBROUTINE PROB. PROB is called to calculate the Markov transition matrix probabilities for each wavelength interval. Entry point PLTDATA produces a microfilm plot of all input data values. See Figure A-1 for the execution sequence diagram.

```
      SUBROUTINE PROB
      COMMON/11111/TRAN(12,12),ST1(12),ST2(12),TRAN2(12,12)
      COMMON/22222/RFL(300),ABS(300),TRN(300),WAVLN(300)
      COMMON/33333/CAROT(300),CHLOROA(300),CHLOROB(300),
     1H20(300)
      COMMON/44444/ OUT(12,250),M, LEVEL, IS
     1,CONCART,CONCHLA,CONCHLB,EWT
      ECAT=-.008    $    ECBT=-.003    $    ECRT=-.002
      EWT=-.015
      PP=.55    $    XM=.45
      TRAN(2,2)=TRAN(4,4)=TRAN(6,6)=TRAN(8,8)=TRAN(10,10)=
     11.000
      TRAN(2,1)=.01
      TRAN(3.1)=.99
      A=1.- EXP(CHLOROA(IS)*ECAT)
      B=1.-EXP(CHLOROB(IS)*ECBT)
      C=1.-EXP(CAROT(IS)*ECRT)
      HOH=1.-EXP(H20(IS)*EWT)
      TOTAL=A+B+C+HOH
      IF(TOTAL.GE.1.)TOTAL=1.
      IF(TOTAL.LE.0)TOTAL=0.000
      TRAN(4,3)=TOTAL*PP
      TRAN(4,5)=TRAN(4,3)/2.
      TRAN(8,7)=TOTAL*SM
      TRAN(8,9)=TRAN(8,7)/2.
      TRAN(5,3)=TRAN(7,3)=(1.-TRAN(4,3))/2.
      TRAN(9,7)=1.-TRAN(8,7)
      TRAN(6,5)=TRAN(5,3)*.3
      TRAN(7,5)=TRAN(5,3)*.2
      TRAN(5,5)=1.-TRAN(4,5)-TRAN(6,5)-TRAN(7,5)
      TRAN(10,9)=.08
      TRAN(3,9)=.12
      TRAN(9,9)=1.-TRAN(3,8)-TRAN(10,9)-TRAN(8,9)
      RETURN
      ENTRY PLTDATA
      CALL SET(.15,.9,.18,.85, .350,.800,0.,300.,1)
      CALL LABMOD(7H(F10.3),7H(F10.0),10,10,1,1,0,0,1)
      CALL PERIML(10 5,10,5)
      CALL PWRT(428, 90,19HWAVELENGTH ($L?M$U),19,2,0)
      CALL PWRT(428, 90,19HWAVELENGTH ($L?M$U),19,2,0)
```

Exhibit A-3 - cont.

```
      CALL PWRT(35,343,26HCOEFFICIENT OF ABSORBTANCE,
     126,2,1)
      CALL PWRT(35,343,26HCOEFFICIENT OF ABSORBTANCE,
     126,2,1)
      CALL FRSTPT(WAVLN(2),CAROT(2))
      DO10I=2,17
10    CALL PSYM(WAVLN(I),CAROT(I),1HL,1,0,2)
      CALL FRAME
      CALL SET(.15,.9,.18,.85, .350,.800,0.,300.,1)
      CALL LABMOD(7H(F10.3),7H(F10.0),10,10,1,1,0,0,1)
      CALL PERIML(10,5,10,5)
      CALL PWRT(428, 90,19HWAVELENGTH ($L?M$U),19,2,0)
      CALL PWRT(428, 90,19HWAVELENGTH ($L?M$U),19,2,0)
      CALL PWRT(35,343,26HCOEFFICIENT OF ABSORBTANCE,
     126,2,1)
      CALL PWRT(35,343,26HCOEFFICIENT OF ABSORBTANCE,
     126,2,1)
      CALL FRSTPT(WAVLN(1),CHLOROA(1))
      DO20I=1,30
20    CALL PSYM(WAVLN(I),CHLOROA(I),1HA,1,0,2)
      CALL FRSTPT(WAVLN(1),CHLOROB(1))
      DO30I=1,29
30    CALL PSYM(WAVLN(I),CHLOROB(I),1HB,1,0,2)
      CALL FRAME
      CALL SET(.15,.9,.18,.85, .350,2.50,0.,150.,1)
      CALL LABMOD(7H(F10.3),7H(F10.1),10,10,1,1,0,0,1)
      CALL PERIML(10,5,10,5)
      CALL PWRT(428, 90,19HWAVELENGTH ($L?M$U),19,2,0)
      CALL PWRT(428, 90,19HWAVELENGTH ($L?M$U),19,2,0)
      CALL PWRT(35,343,26HCOEFFICIENT OF ABSORBTANCE,
     126,2,1)
      CALL PWRT(35,343,26HCOEFFICIENT OF ABSORBTANCE,
     126,2,1)
      CALL FRSTPT(WAVLN(36),H20(36))
      DO40I=36,211,2
40    CALL PSYM(WAVLN(I),H20(I),1HW,0,0,2)
      CALL FRAME
      RETURN
      END
```

Exhibit A-4. SUBROUTINE FLUXPLT. This subroutine produces a microfilm plot of the interleaf radiative flux at each wavelength. See Figure A-1 for the execution sequence diagram.

```
      SUBROUTINE FLUXPLT
      COMMON/22222/RFL(300), ABS(300), TRN(300), WAVLN(300)
      COMMON/44444/ OUT(12,250), M, LEVEL, IS
      DIMENSION ICHAR(10), ISIZE(10), TITLE(5)
      DATA ICHAR/1H(, 1H, , 1HP, 1HA, 1HS, 1H', 1HM, 1H9, 1H", 1HT
     1/ISIZE/2*1, 5*0, 2*1, 0 /
      OUT(11, 1)=0.00
      IWL=IS*10+340
      ENCODE(36, 100, TITLE) IWL
      CALL SET(.15, .9, .18, .90, 0., 39., 0., 60., 1)
      CALL LABMOD(7H(F10.2), 7H(F10.2), 10, 10, 1, 1, 0, 0, 1)
      CALL PERIMI(10,5,10,5)
      CALL PWRT(440, 40, 11HSTEP NUMBER, 11, 2, 0)
      CALL PWRT(440, 40, 11HSTEP NUMBER, 11, 2, 0)
      CALL PWRT(40, 470, 7HPERCENT, 7, 2, 1)
      CALL PWRT(40, 470, 7HPERCENT, 7, 2, 1)
      CALL PWRT( 80, 950, TITLE, 36, 3, 0)
      CALL PWRT( 80, 950, TITLE, 36, 3, 0)
      CALL FRSTPT(0., OUT(4, 1))
      DO20I=4, M
      DO10J=1, LEVEL
      ALEVEL=J-1
      IF(    I    .EQ.   7    )  GOTO10
      IF (OUT(I, J)  .LT.  .005)  GOTO10
      OUTS=OUT(I, J)*100.
      CALL PSYM(ALEVEL, OUTS, ICHAR(I), 1, ISIZE(I), 2)
10    CONTINUE
20    CALL FRSTPT(0., OUT(I+1, 1))
      CALL FRAME
100   FORMAT(28HINTERLEAF RADIATIVE FLUX AT I5, 3H NM)
      RETURN
      END
```

Exhibit A-5. SUBROUTINE PLOTTER. The final model predictions are plotted on microfilm by this subroutine. Refer to Figure A-1 for the execution sequence diagram.

```
      SUBROUTINE PLOTTER
      COMMON/22222/RFL(300,ABS(300),TRN(300),WAVLN(300)
      COMMON/44444/OUT(12,250),M,LEVEL,IS
      DO 10 I=1,IS
      ABS(I)=1.-RFL(I)
10    CONTINUE
      CALL SET(.15,.9,.18,.80,.350,2.50,0.,1.,1)
      CALL LABMOD(7H(F10.3),7H(F10.2),10,10,1,1,0,0,1)
      CALL PERIML(10,5,10,5)
      CALL PWRT(428, 90,19WAVELENGTH ($L?M$U),19,2,0)
      CALL PWRT(428, 90,19WAVELENGTH ($L?M$U),19,2,0)
      CALL PWRT(30,485,7HPERCENT,7,2,1)
      CALL PWRT(30,485,7HPERCENT,7,2,1)
      ICHAR=1H*
      CALL FRSTPT(WAVLN(1),TRN(1))
      DO 20 I=1,IS
20    CALL PSYM(WAVLN(I),TRN(I),ICHAR,1,0,2)
      CALL FRSTPT(WAVLN(1),ABS(1))
      DO 30 I=1,IS
30    CALL PSYM(WAVLN(I),ABS(I),ICHAR,1,0,2)
      CALL FRAME
      STOP 1
      END
```

Table A.1. THE MODELED SPECTRO-OPTICAL CHARACTERISTICS OF A SINGLE LEAF. The values for spectro reflectance (RFLCTD), spectro transmissance (TRANSMTTD), and spectro absorbance (ABSRBD) were computed at .01 μm by the program LFMOD1. The input data were the leaf thickness and structure, pigment composition and water content of a single leaf of black maple.

WAVE-LENGTH (μm)	RFLCTD (%)	TRNSMTTD (%)	ABSRBD (%)	WAVE-LENGTH (μm)	RFLCTD (%)	TRNSMTTD (%)	ABSRBD (%)
.350	22.25	16.27	61.47	.650	33.28	27.04	39.67
.360	20.22	14.44	65.34	.660	26.69	20.45	52.87
.370	18.56	12.97	68.47	.670	20.33	14.53	65.14
.380	17.30	11.90	70.80	.680	14.09	9.24	76.67
.390	15.60	10.47	73.92	.690	22.99	16.95	60.07
.400	14.21	9.34	76.45	.700	46.98	41.84	11.06
.410	13.32	8.63	78.05	.710	50.79	46.15	2.86
.420	9.61	5.82	84.56	.720	52.06	47.61	.08
.430	7.67	4.44	87.88	.730	52.05	47.60	.11
.440	5.21	2.79	92.00	.740	52.04	47.59	.12
.450	5.04	2.68	92.28	.750	52.03	47.57	.15
.460	7.77	4.52	87.71	.760	52.04	47.58	.14
.470	9.17	5.50	85.33	.770	52.04	47.58	.13
.480	7.80	4.53	87.67	.780	52.04	47.59	.12
.490	14.33	9.44	76.23	.790	52.05	47.59	.12
.500	29.64	23.35	47.00	.800	52.50	47.59	.11
.510	34.89	28.71	36.38	.810	52.04	47.58	.13
.520	35.89	29.76	34.32	.820	52.03	47.57	.16
.530	37.87	31.85	30.25	.830	52.02	47.56	.18
.540	38.11	32.11	29.75	.840	52.01	47.55	.20
.550	38.33	32.35	29.29	.850	52.00	47.53	.22
.560	38.53	32.56	28.87	.860	51.98	47.52	.26
.570	39.95	34.09	25.92	.870	51.97	47.50	.29
.580	38.90	32.96	28.11	.880	51.95	47.48	.33
.590	38.71	32.75	28.51	.890	51.94	47.46	.36
.600	38.16	32.16	29.65	.900	51.92	47.45	.39
.610	36.95	30.88	32.15	.910	51.72	47.22	.83
.620	36.55	30.45	32.98	.920	51.52	46.99	1.26
.630	35.27	29.10	35.61	.930	51.33	46.76	1.68
.640	34.69	28.51	36.79	.940	51.13	46.54	2.11

Table A.1. Cont.

WAVE-LENGTH (μm)	RFLCTD (%)	TRNSMTTD (%)	ABSRBD (%)
.950	50.94	46.32	2.53
.960	50.99	46.38	2.42
.970	51.04	46.43	2.31
.980	51.09	46.49	2.20
.990	51.14	46.55	2.10
1.000	51.19	46.60	1.99
1.010	51.30	46.74	1.74
1.020	51.42	46.87	1.49
1.030	51.53	47.00	1.23
1.040	51.65	47.13	.98
1.050	51.77	47.27	.73
1.060	51.74	47.23	.79
1.070	51.71	47.20	.86
1.080	51.68	47.16	.93
1.090	51.65	47.13	.99
1.100	51.61	47.09	1.06
1.110	51.31	46.74	1.73
1.120	51.00	46.39	2.39
1.130	50.70	46.05	3.04
1.140	50.40	45.71	3.68
1.150	50.11	45.38	4.32
1.160	50.01	45.27	4.53
1.170	49.92	45.16	4.73
1.180	49.82	45.05	4.94
1.190	49.73	44.94	5.14
1.200	49.63	44.84	5.35
1.210	49.68	44.89	5.24
1.220	49.73	44.94	5.14
1.230	49.78	45.00	5.04
1.240	49.82	45.05	4.94
1.250	49.87	45.11	4.84
1.260	49.80	45.02	4.99
1.270	49.73	44.94	5.14
1.280	49.66	44.86	5.30
1.290	49.59	44.78	5.45

WAVE-LENGTH (μm)	RFLCTD (%)	TRNSMTTD (%)	ABSRBD (%)
1.300	49.52	44.70	5.60
1.310	48.62	43.69	7.53
1.320	47.75	42.71	9.39
1.330	46.92	41.77	11.19
1.340	46.11	40.86	12.92
1.350	45.33	39.99	14.58
1.360	42.03	36.35	21.56
1.370	39.16	33.24	27.56
1.380	36.65	30.56	32.76
1.390	34.44	28.24	37.31
1.400	32.46	26.20	41.33
1.410	29.78	23.49	46.72
1.420	27.49	21.23	51.27
1.430	25.51	19.32	55.17
1.440	23.79	17.69	58.53
1.450	22.26	16.28	61.45
1.460	23.11	17.06	59.83
1.470	24.02	17.91	58.07
1.480	25.00	18.83	56.17
1.490	26.05	19.84	54.11
1.500	27.19	20.94	51.87
1.510	28.43	22.15	49.41
1.520	29.78	23.49	46.72
1.530	31.26	24.98	43.76
1.540	32.88	26.63	40.48
1.550	34.67	28.48	36.83
1.560	35.54	29.39	35.06
1.570	36.45	30.34	33.19
1.580	37.40	31.36	31.22
1.590	38.41	32.43	29.13
1.600	39.46	33.56	26.93
1.610	39.89	34.02	26.04
1.620	40.33	34.50	25.13
1.630	40.77	34.98	24.20
1.640	41.22	35.47	23.25

Table A.1. Cont.

WAVE-LENGTH (μm)	RFLCTD (%)	TRNSMTTD (%)	ABSRBD (%)
1.650	41.69	35.98	22.27
1.660	41.62	35.91	22.41
1.670	41.56	35.83	22.55
1.680	41.49	35.76	22.69
1.690	41.42	35.69	22.83
1.700	41.36	35.62	22.97
1.710	40.96	35.19	23.80
1.720	40.58	34.77	24.60
1.730	40.20	34.36	25.40
1.740	39.83	33.96	26.17
1.750	39.46	33.56	26.93
1.760	38.99	33.05	27.93
1.770	38.52	32.55	28.90
1.780	38.07	32.06	29.84
1.790	37.19	31.13	31.66
1.800	34.67	28.48	36.83
1.810	32.46	26.20	41.33
1.820	31.45	25.17	43.37
1.830	29.61	23.32	47.07
1.840	27.96	21.68	50.36
1.850	25.78	19.57	54.64
1.860	23.56	17.47	58.97
1.870	17.50	12.07	70.43
1.880	13.87	9.07	77.07
1.890	11.50	7.22	81.28
1.900	9.87	6.07	84.11
1.910	9.33	5.62	85.04
1.920	8.87	5.29	85.85
1.930	8.46	5.00	86.55
1.940	8.10	4.74	87.16
1.950	7.78	4.52	87.69
1.960	8.24	4.84	86.92
1.970	8.78	5.22	86.00
1.980	9.44	5.70	84.87
1.990	10.23	6.28	83.49

WAVE-LENGTH (μm)	RFLCTD (%)	TRNSMTTD (%)	ABSRBD (%)
2.000	11.22	7.01	81.77
2.010	11.94	7.56	80.50
2.020	12.78	8.21	79.02
2.030	13.74	8.97	77.28
2.040	14.88	9.88	75.24
2.050	16.21	10.98	72.81
2.060	17.22	11.82	70.96
2.070	28.35	12.79	68.86
2.080	19.63	13.92	66.45
2.090	21.10	15.22	63.68
2.100	22.79	16.76	60.45
2.110	23.56	17.47	58.97
2.120	24.38	18.24	57.38
2.130	25.25	19.07	55.67
2.140	26.19	19.97	53.84
2.150	27.19	20.94	51.87
2.160	27.49	21.23	51.27
2.170	27.80	21.53	50.67
2.180	28.11	21.84	50.05
2.190	28.43	22.15	49.41
2.200	28.76	22.47	48.76
2.210	28.43	22.15	49.41
2.220	28.11	21.84	50.05
2.230	27.80	21.53	50.67
2.240	27.49	21.23	51.27
2.250	27.19	20.94	51.87
2.260	26.61	20.37	53.01
2.270	26.05	19.84	54.11
2.280	25.51	19.32	55.17
2.290	25.00	18.83	56.17
2.300	24.50	18.36	57.14
2.310	23.33	17.27	59.40
2.320	22.26	16.28	61.45
2.330	21.29	15.39	63.32
2.340	20.38	14.58	65.03

Table A.1. Cont.

WAVE-LENGTH (μm)	RFLCTD (%)	TRNSMTTD (%)	ABSRBD (%)
2.350	19.55	13.84	66.60
2.360	18.71	13.11	68.18
2.370	17.93	12.44	69.63
2.380	17.22	11.82	70.96
2.390	16.55	11.26	72.19
2.400	15.93	10.75	73.32
2.410	15.07	10.04	74.90
2.420	14.29	9.40	76.31
2.430	13.59	8.84	77.57
2.440	12.95	8.34	78.70
2.450	12.38	7.90	79.73
2.460	11.71	7.38	80.91
2.470	11.11	6.93	81.95
2.480	10.58	6.54	82.88
2.490	10.11	6.19	83.70
2.500	9.68	5.88	84.44

APPENDIX B

APPENDIX B

The Selection of a Species for Field Validation Measurements

Description of Study Area

The measurements made in the field and used in this thesis were obtained from the shortgrass prairie at the International Biological Program's (IBP) Grassland Biome Pawnee Intensive Site located on the Central Plains Experiment Station of the Pawnee National Grasslands. The Pawnee Intensive Site is approximately 30 miles northeast of Ft. Collins, Colorado, near the town of Nunn on sections 21 and 27, Township 10N, Range 66W in Weld County (Jameson, 1969). The soil underlying the sample plots is as an Ascalon sandy loam, aridic arguistall, fine-loamy mixed, and mesic (Dye, 1972). The 29-year (1939-1967) average annual precipitation of the area is about 31 cm per year with approximately 80 per cent of the precipitation falling as rain during the growing season from May 1 to September 30. Annual precipitation has varied from a low of 11 cm to a high of 58 cm (Bement, 1968). Wind velocity averages 10.3 kilometers per hour and the mean high and low temperatures during the growing season were 25.6°C and 8.3°C respectively. The average frost period was 135 days.

Selection of Species

The shortgrass prairie which was used as the field site is dominated by various species of grasses (Table B-1). One species, blue grama (*Bouteloua gracilis*) (H.B.K. Lag. ex. steud.) is the major forage species in the shortgrass ecosystem, comprises about 43 per cent of the weight of the graminous vegetation at the Pawnee Intensive Site, and is one of the important grass species on well over 200 million acres in the Great Plains of the United States (Uresk, 1971). The development of remote methods to estimate and map the biomass and physiological status of blue grama will enable researchers to estimate the nutrient cycling and energy flow through this important species to other trophic levels of the shortgrass prairie. Therefore, blue grama was selected for the field experimentation.

Selection of Sample Plots

The selection of blue grama plots was made in the Ecosystem Stress Area (ESA) located to the west of the headquarters building at the Pawnee Intensite Site. The ESA contains two repetitions of 4 types of treatments: control, irrigated, nitrogen fertilized, and irrigated and fertilized. These treated areas were selected for use as they allow a much wider biomass sampling range and the vegetation does not dry out so rapidly in the irrigated areas. The field portions of this research were conducted at the boundary between an irrigated treatment and an irrigated and nitrogen fertilized treatment and used plots of 1/4 m^2 in area.

Table B-1. NATIVE RANGE PLANTS OF THE SHORTGRASS PRAIRIE (extracted from Uresk, 1971).

VEGETATION TYPE		Percent of Total Aboveground Biomass by Dry Weight
GRASSES:		57%
Blue grama	(*Bouteloua gracilis*)	43
Red threeawn	(*Aristida longiseta*)	8
Sunsedge	(*Carex heliophila*)	3
Buffalo grass	(*Buchloe dactyloides*)	2
Sand dropseed	(*Sporobulus cryptandrus*)	1
PRICKLY PEAR	(*Opuntia polyacantha*)	26%
SHRUBS:*		7%
Fringed sagewort	(*Artemisia frigida*)	
Rubber rabbitbrush	(*Chrysothamnus nauseosus*)	
Broom snakeweed	(*Gutieirizia sorothrae*)	
FORBS:*		6%
Plains bahia	(*Bahia oppositifolia*)	
Scarlet globemallow	(*Sphaerolcec coccinea*)	
Evening primrose	(*Oenothera* spp.)	
MISC.		4%
	TOTAL	100%

*The individual contribution of these vegetation types was not given.

APPENDIX C

APPENDIX C

ST38RMF Statistical Program Description

ST38RMF is a modified version of the Colorado State University Statistical Laboratory's stepwise multiple regression FORTRAN program STAT38R, which is, in turn, adapted from a BMD02R program originally developed at UCLA under sponsorship of the National Institute of Health (Dixon, 1971). The Colorado State University Statistical Laboratory modified the program for use on the University's CDC 6400 central computer and makes the STAT38R version available on permanent file for anyone wishing to use it. A card deck version of STAT38R was obtained from the Statistical Laboratory and modified to accept a series of spectral data as gathered by the IBP field spectrometer laboratory. No modifications of any sort were made to the statistical logic of the original program and the control card setup for ST38RMF is identical to that of STAT38R. The modifications made to the program included reducing the size of all input/output buffers, reducing the total number of input/output units to eight, and adding a microfilm plotting subroutine to plot the simple linear regressions and the summary spectrocorrelation plots. Both STAT38R and ST38RMF are documented and any interested parties should address their inquiries to the CSU Statistical Laboratory or to C. J. Tucker for further information or a copy of the program(s).

A brief summary of the features and options of ST38RMF follows to acquaint the reader with the utility of this software package.

ST38RMF computes a sequence of multiple linear regression equations in a stepwise manner. The program will handle a simple linear regression of two variables to an eighty variable multiple regression. The user has the option of forcing variables into the equation and specifying a regression intercept if desired. Output at every step of the program includes simple or multiple correlation coefficients, standard error of estimate, analysis of variance table, the F value to remove and the standard error of the regression coefficient(s), and the partial correlation coefficient of variables not in the equation and their F value to enter. Optional output includes:

1. Tables of the means, standard deviations, coefficients of variation, and standard errors of the mean.
2. Correlation matrix.
3. Covariance matrix.
4. Variable plot residual list.
5. List of the unit normal deviate form of the residuals.
6. Plots of the unit normal deviate forms of the residual against the variables.
7. Full normal plot of the unit normal deviate form of the residuals.
8. A microfilm plot of a two-variable regression, including the point scatter, r value, sample size, regression line, and regression equation.

At the conclusion of each computer run, ST38RMF outputs a punched card, tabular, and microfilm summary of the r, r^2, F, slope

and intercept values for every case. In addition, a complete analysis of variance table of the regression model is printed and punched onto cards for storage (see Appendix D for an example of the tabular output of this analysis). Limitations include a minimum of two original variables and a maximum of eighty, a maximum of seventy-eight transgenerated variables, a total number of eighty variables, and a total number of data values not to exceed 9999. Operating time in central processor (CP) seconds on a CDC 6400 computer is approximately equal to the sample size divided by 18 for each wavelength interval operated upon. This is a total CP time of approximately 200 seconds for the ninety-one wavelength intervals between .350 and .800 μm with all optional output generated.

APPENDIX D

APPENDIX D

Statistical Results of Spectrocorrelation Analysis

Detailed statistical results of the spectrocorrelation analyses are presented in this appendix as plotted on microfilm and in tabular format for all ninety-one .005 μm wavelength intervals.

All of the results presented in this appendix were generated by the ST38RMF statistical program (see Appendix B) and output by that program in the tabular form and also in a punched card deck for subsequent display on microfilm. All figures presented in this appendix were generated on the CDC 280 microfilm plot package of the CSU computer center. The resulting microfilm was then printed photographically and the high contrast prints included directly into the thesis and this appendix. No retouching of any data points has been done in either the microfilm prints or in the statistical tables. A complete summary of the input plot data parameters was given in Table 4 in the text (Pearson *et al*, 1973). The complete suite of spectral curves utilized are given in both tabular and plotted format.

The tabular graphical and tabular output which follows is broken into the following subsections:

Total wet biomass

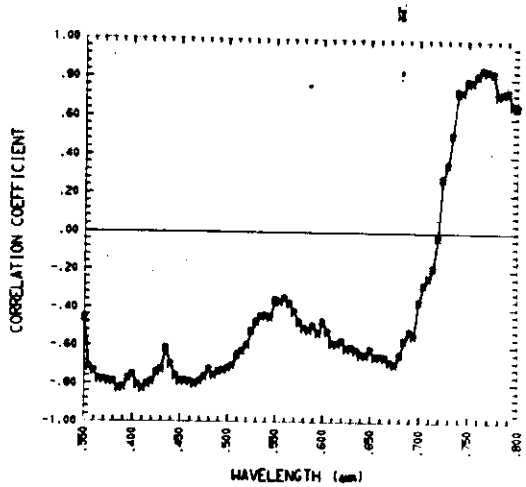

(a) Spectrocorrelation curve

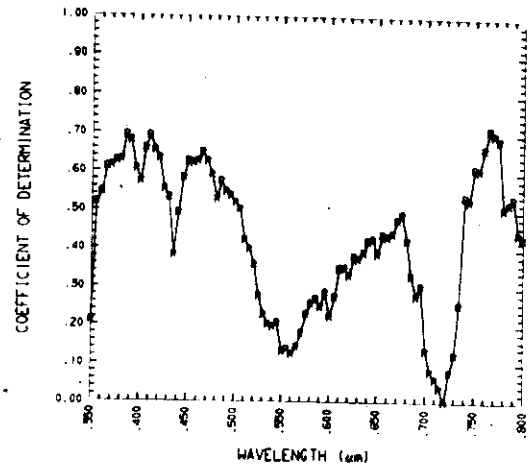

(b) r^2 versus wavelength

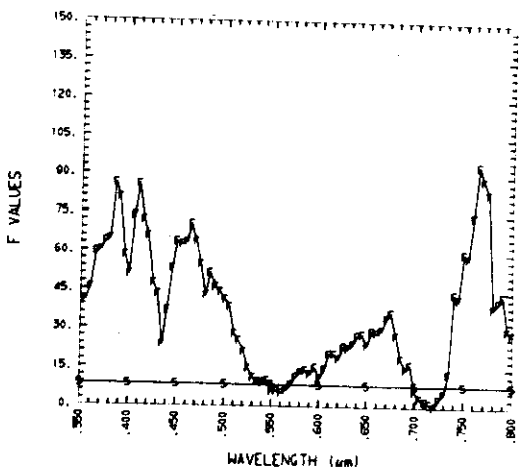

(c) F value versus wavelength

Figure D-1. STATISTICAL COEFFICIENTS OF THE SIMPLE LINEAR REGRESSION FOR TOTAL WET BIOMASS (TWB) VERSUS REFLECTANCE AT EACH WAVELENGTH. The linear regressions were formed for the total wet biomass present on 40 of 1/4 meter squared plots of blue grama (*B. gracilis*) and the reflectance of the plot at 91 wavelengths between .350 and .800 μm. The tabular values of these coefficients can be found in Table D-1. (a) The correlation coefficient (r) versus wavelength or the spectrocorrelation curve. (b) The coefficient of determination (r^2) versus wavelength. (c) The F value versus wavelength where the horizontal line shown by -5- represents the .5% level of significance for 1/38 degrees of freedom.

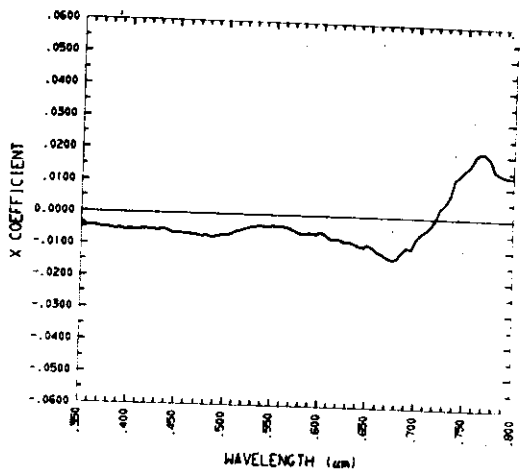

(a) Slope versus wavelength

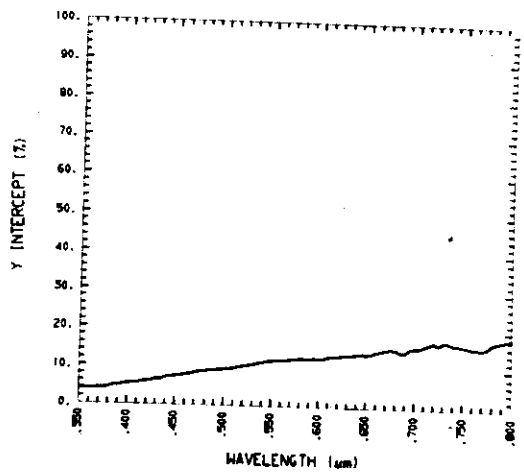

(b) Intercept versus wavelength (soil spectroreflectance)

Figure D-2. THE SLOPE AND THE INTERCEPT OF THE SIMPLE LINEAR REGRESSION FOR TOTAL WET BIOMASS (TWB) VERSUS REFLECTANCE AT EACH WAVELENGTH. The linear regressions were formed for the total wet biomass present on 40 of 1/4 meter squared plots of blue grama (*B. gracilis*) and the reflectance between .350 and .800 μm. Each regression equation at each wavelength yields a slope and intercept value which occur in Table D-1. (a) The plot of the slope at each wavelength. (b) The plot of the "y" intercept of the straight line which represents the reflectance of the plot when the total wet biomass value is zero. Plotted against wavelength it represents the spectroreflectance of the underlying, unexposed soil surface.

Table D-1. SIMPLE LINEAR REGRESSION BETWEEN CANOPY REFLECTANCE AND TOTAL WET BIOMASS (TWB). The coefficients and equation resulting from these computations are shown for each available wavelength. The sample set in each case consisted of 40 of 1/4 square meter plots of blue grama (B. gracilis). Plots of r, r^2, F, Y, and m values versus wavelength occur in Figures D-1 and D-2.

Wave-Length (μm)	r Value	r^2 Value	Standard Error of Estimate	Degrees of Freedom	F Ratio	Regression Equation (y = b + mx)
.350	-.4595	.2112	.8417	1/38	10.1718	Y= 3.7951-.0032(TWB)
.355	-.7197	.5179	.5455	1/38	40.8235	Y= 4.0252-.0042(TWB)
.360	-.7385	.5454	.5396	1/38	45.5950	Y= 3.9758-.0043(TWB)
.365	-.7816	.6108	.4911	1/38	59.6432	Y= 4.0034-.0045(TWB)
.370	-.7834	.6137	.5077	1/38	60.3638	Y= 4.0755-.0047(TWB)
.375	-.7914	.6263	.5023	1/38	63.6901	Y= 4.1508-.0048(TWB)
.380	-.7935	.6296	.5069	1/38	64.5936	Y= 4.2493-.0049(TWB)
.385	-.8329	.6937	.4834	1/38	86.0811	Y= 4.9326-.0053(TWB)
.390	-.8242	.6793	.4645	1/38	80.4997	Y= 4.7979-.0050(TWB)
.395	-.7783	.6057	.6055	1/38	58.3810	Y= 5.1374-.0055(TWB)
.400	-.7568	.5727	.6211	1/38	50.9338	Y= 5.3566-.0053(TWB)
.405	-.8117	.6589	.5226	1/38	73.4025	Y= 5.5292-.0053(TWB)
.410	-.8324	.6928	.4809	1/38	85.7126	Y= 5.6525-.0053(TWB)
.415	-.8091	.6547	.5181	1/38	72.0531	Y= 5.8477-.0052(TWB)
.420	-.7960	.6336	.5405	1/38	65.7158	Y= 6.0136-.0052(TWB)
.425	-.7445	.5542	.6349	1/38	47.2431	Y= 6.2448-.0052(TWB)
.430	-.7295	.5322	.7069	1/38	43.2241	Y= 6.5804-.0055(TWB)
.435	-.6180	.3819	.8562	1/38	23.4751	Y= 6.6678-.0049(TWB)
.440	-.7021	.4929	.7490	1/38	36.9392	Y= 7.0213-.0054(TWB)
.445	-.7638	.5833	.7135	1/38	53.1963	Y= 7.3960-.0063(TWB)
.450	-.7916	.6266	.6436	1/38	63.7692	Y= 7.5171-.0061(TWB)
.455	-.7889	.6223	.6547	1/38	62.6059	Y= 7.6704-.0062(TWB)
.460	-.7912	.6260	.6775	1/38	63.6053	Y= 7.8870-.0064(TWB)
.465	-.8061	.6498	.6613	1/38	70.5081	Y= 8.1039-.0066(TWB)
.470	-.7914	.6263	.7164	1/38	63.6780	Y= 8.3224-.0068(TWB)
.475	-.7686	.5908	.8033	1/38	54.8548	Y= 8.6088-.0071(TWB)
.480	-.7276	.5294	.8744	1/38	42.7510	Y= 8.7463-.0068(TWB)
.485	-.7587	.5756	.7803	1/38	51.5345	Y= 9.1150-.0074(TWB)
.490	-.7403	.5480	.8630	1/38	46.0654	Y= 9.1413-.0070(TWB)
.495	-.7331	.5375	.8634	1/38	44.1591	Y= 9.2437-.0068(TWB)

Table D-1 - cont.

Wave-Length (μm)	r Value	r^2 Value	Standard Error of Estimate	Degrees of Freedom	F Ratio	Regression Equation (y = b + mx)
.500	-.7212	.5202	.8607	1/38	41.1936	Y= 9.3875-.0066(TWB)
.505	-.7084	.5018	.8600	1/38	38.2819	Y= 9.5719-.0063(TWB)
.510	-.6503	.4229	.8791	1/38	27.8456	Y= 9.6965-.0055(TWB)
.515	-.6320	.3994	.8596	1/38	25.2736	Y= 9.9432-.0051(TWB)
.520	-.5980	.3576	.8483	1/38	21.1571	Y=10.2475-.0046(TWB)
.525	-.5263	.2770	.8733	1/38	14.5562	Y=10.4614-.0040(TWB)
.530	-.4754	.2260	.9479	1/38	11.0937	Y=10.7238-.0038(TWB)
.535	-.4485	.2012	.9561	1/38	9.5690	Y=10.9824-.0035(TWB)
.540	-.4435	.1967	.9728	1/38	9.3059	Y=11.2477-.0035(TWB)
.545	-.4546	.2067	1.0068	1/38	9.8986	Y=11.5394-.0038(TWB)
.550	-.3604	.1299	1.2115	1/38	5.6731	Y=11.7272-.0034(TWB)
.555	-.3710	.1376	1.1926	1/38	6.0652	Y=11.8322-.0035(TWB)
.560	-.3526	.1243	1.2554	1/38	5.3962	Y=11.9280-.0035(TWB)
.565	-.3792	.1438	1.2890	1/38	6.3837	Y=12.0332-.0039(TWB)
.570	-.4239	.1797	1.3202	1/38	8.3258	Y=12.1915-.0045(TWB)
.575	-.4799	.2303	1.3165	1/38	11.3685	Y=12.3732-.0053(TWB)
.580	-.5075	.2576	1.3349	1/38	13.1824	Y=12.4841-.0058(TWB)
.585	-.5192	.2695	1.2465	1/38	14.0213	Y=12.4234-.0056(TWB)
.590	-.4982	.2482	1.2956	1/38	12.5454	Y=12.4689-.0055(TWB)
.595	-.5349	.2861	1.2640	1/38	15.2296	Y=12.5512-.0059(TWB)
.600	-.4727	.2234	1.3148	1/38	10.9330	Y=12.4770-.0052(TWB)
.605	-.5249	.2755	1.2876	1/38	14.4506	Y=12.6656-.0058(TWB)
.610	-.5910	.3492	1.3270	1/38	20.3930	Y=12.9804-.0071(TWB)
.615	-.5913	.3497	1.3516	1/38	20.4331	Y=13.0725-.0073(TWB)
.620	-.5750	.3307	1.4158	1/38	18.7718	Y=13.1482-.0073(TWB)
.625	-.6156	.3789	1.4209	1/38	23.1847	Y=13.4051-.0081(TWB)
.630	-.6105	.3727	1.4112	1/38	22.5792	Y=13.4166-.0080(TWB)
.635	-.6248	.3903	1.4369	1/38	24.3293	Y=13.5991-.0084(TWB)
.640	-.6491	.4214	1.4621	1/38	27.6749	Y=13.7670-.0092(TWB)
.645	-.6516	.4246	1.5086	1/38	28.0367	Y=14.0338-.0095(TWB)

Table D-1 - cont.

Wave-Length (μm)	r Value	r^2 Value	Standard Error of Estimate	Degrees of Freedom	F Ratio	Regression Equation (y = b + mx)
.650	-.6220	.3869	1.5102	1/38	23.9782	Y=13.7631-.0088(TWB)
.655	-.6609	.4368	1.5043	1/38	29.4709	Y=14.0374-.0097(TWB)
.660	-.6561	.4305	1.7223	1/38	28.7216	Y=14.5034-.0110(TWB)
.665	-.6631	.4397	1.7789	1/38	29.8185	Y=14.7383-.0116(TWB)
.670	-.6897	.4757	1.8086	1/38	34.4717	Y=15.2024-.0126(TWB)
.675	-.7002	.4902	1.8351	1/38	36.5440	Y=15.3091-.0132(TWB)
.680	-.6495	.4219	2.0604	1/38	27.7294	Y=15.2758-.0129(TWB)
.685	-.5742	.3298	2.0975	1/38	18.6953	Y=14.6722-.0108(TWB)
.690	-.5250	.2756	2.0660	1/38	14.4559	Y=14.6305-.0094(TWB)
.695	-.5507	.3033	2.0362	1/38	16.5426	Y=15.4744-.0099(TWB)
.700	-.3675	.1351	2.2861	1/38	5.9336	Y=15.7971-.0066(TWB)
.705	-.2820	.0795	2.2727	1/38	3.2832	Y=15.8641-.0049(TWB)
.710	-.2425	.0588	2.1273	1/38	2.3750	Y=16.3235-.0039(TWB)
.715	-.1897	.0360	1.8390	1/38	1.4190	Y=16.8226-.0026(TWB)
.720	-.0316	.0010	1.7449	1/38	.0380	Y=17.3031-.0004(TWB)
.725	.2798	.0783	1.4459	1/38	3.2275	Y=16.6579+.0031(TWB)
.730	.3533	.1248	1.6474	1/38	5.4190	Y=17.3558+.0046(TWB)
.735	.5056	.2556	1.6316	1/38	13.0475	Y=17.4782+.0070(TWB)
.740	.7326	.5368	1.5721	1/38	44.0328	Y=16.7683+.0124(TWB)
.745	.7248	.5253	1.7604	1/38	42.0456	Y=16.8337+.0136(TWB)
.750	.7826	.6124	1.6547	1/38	60.0477	Y=16.5894+.0153(TWB)
.755	.7780	.6053	1.8227	1/38	58.2794	Y=16.3563+.0166(TWB)
.760	.8138	.6623	1.9082	1/38	74.5184	Y=15.9349+.0196(TWB)
.765	.8442	.7126	1.8240	1/38	94.2423	Y=15.9123+.0211(TWB)
.770	.8362	.6993	1.8566	1/38	88.3554	Y=15.8646+.0208(TWB)
.775	.8285	.6864	1.7669	1/38	83.1797	Y=16.2678+.0192(TWB)
.780	.7106	.5049	2.0979	1/38	38.7579	Y=17.3323+.0156(TWB)
.785	.7216	.5206	1.8854	1/38	41.2727	Y=17.6789+.0144(TWB)
.790	.7312	.5347	1.7828	1/38	43.6663	Y=18.0484+.0140(TWB)
.795	.6640	.4409	2.0889	1/38	29.9673	Y=18.3578+.0136(TWB)
.800	.6562	.4306	2.1336	1/38	28.7401	Y=18.5500+.0136(TWB)

Total dry biomass

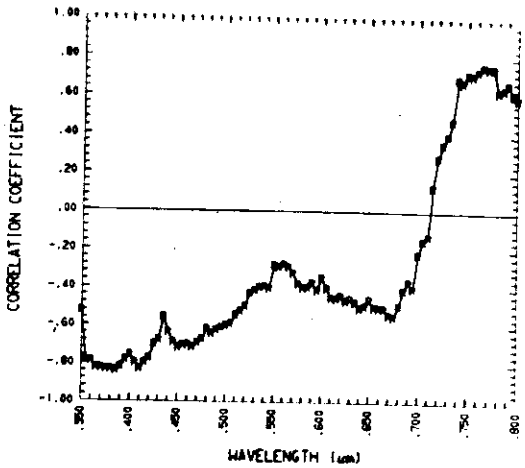

(a) Spectrocorrelation curve

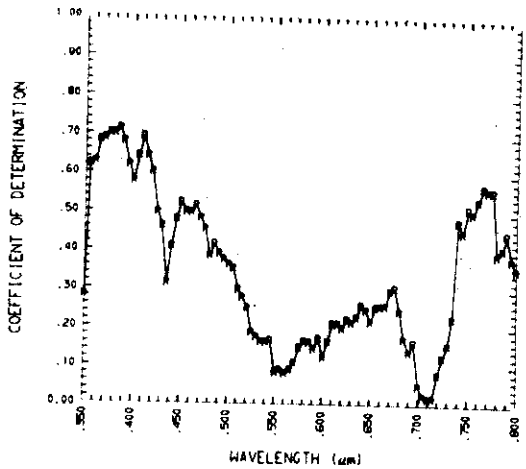

(b) r^2 versus wavelength

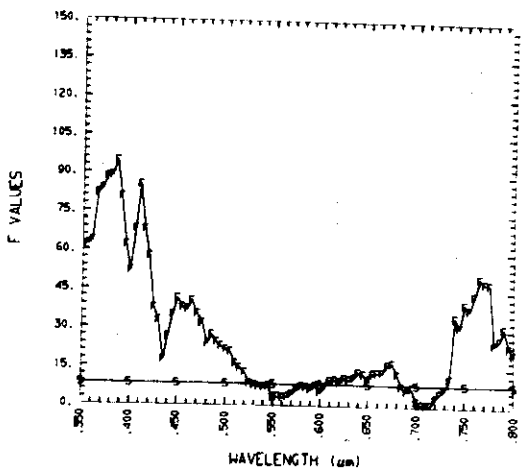

(c) F value versus wavelength

Figure D-3. STATISTICAL COEFFICIENTS OF THE SIMPLE LINEAR REGRESSION FOR TOTAL DRY BIOMASS (TDB) VERSUS REFLECTANCE AT EACH WAVELENGTH. The linear regressions were formed for the total dry biomass present on 40 of 1/4 meter squared plots of blue grama (*B. gracilis*) and the reflectance of the plot at 90 wavelengths between .350 and .800 μm. The tabular values of these coefficients can be found in Table D-2. (a) The correlation coefficient (r) versus wavelength or the spectrocorrelation curve. (b) The coefficient of determination (r^2) versus wavelength. (c) The F value versus wavelength where the horizontal line shown by -5- represents the .5% level of significance for 1/38 degrees of freedom.

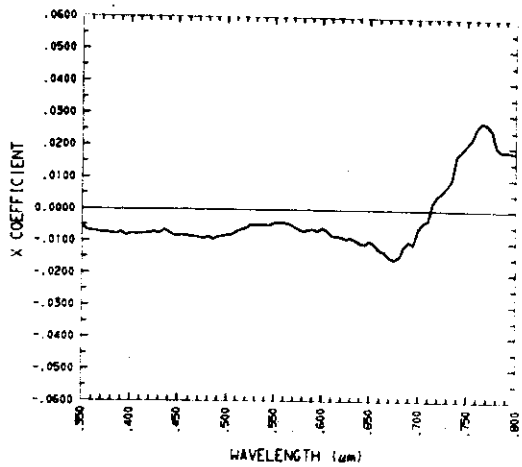

(a) Slope versus wavelength

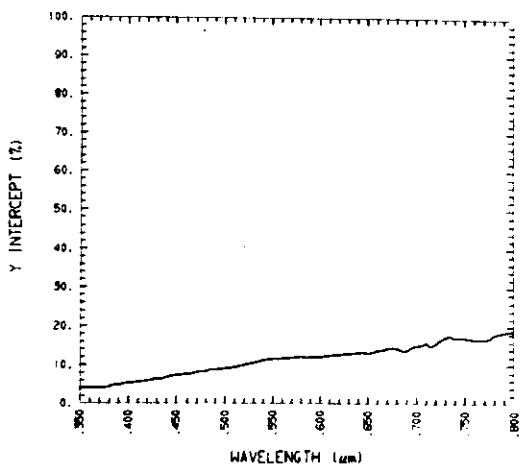

(b) Intercept versus wavelength (soil spectroreflectance)

Figure D-4. THE SLOPE AND THE INTERCEPT OF THE SIMPLE LINEAR REGRESSION FOR TOTAL DRY BIOMASS (TDB) VERSUS REFLECTANCE AT EACH WAVELENGTH. The linear regressions were formed for the total dry biomass present on 40 of 1/4 meter squared plots of blue grama (*B. gracilis*) and the reflectance between .350 and .800 µm. Each regression equation at each wavelength yields a slope and intercept value which occur in Table D-2. (a) The plot of the slope at each wavelength which represents the rate of change in the reflectance of the plot with wavelength. (b) The plot of the "y" intercept of the straight line which represents the reflectance of the plot when the total dry biomass value is zero. Plotted against wavelength it represents the spectroreflectance of the underlying, unexposed soil surface.

Table D-2. SIMPLE LINEAR REGRESSION BETWEEN CANOPY REFLECTANCE AND TOTAL DRY BIOMASS (TDB). The coefficients and equation resulting from these computations are shown for each available wavelength. The sample set in each case consisted of 40 of 1/4 square meter plots of blue grama (B. gracilis). Plots of r, r^2, F, Y, and m values versus wavelength occur in Figures D-3 and D-4.

Wave-Length (μm)	r Value	r^2 Value	Standard Error of Estimate	Degrees of Freedom	F Ratio	Regression Equation (y = b + mx)
.350	-.5291	.2800	.8041	1/38	14.7748	Y= 3.8780-.0054(TDB)
.355	-.7875	.6202	.4842	1/38	62.0513	Y= 4.0737-.0067(TDB)
.360	-.7911	.6258	.4895	1/38	63.5506	Y= 4.0015-.0069(TDB)
.365	-.8260	.6823	.4438	1/38	81.6113	Y= 4.0141-.0071(TDB)
.370	-.8288	.6869	.4570	1/38	83.3554	Y= 4.0878-.0074(TDB)
.375	-.8362	.6993	.4506	1/38	88.3756	Y= 4.1618-.0075(TDB)
.380	-.8367	.7000	.4561	1/38	88.6810	Y= 4.2577-.0076(TDB)
.385	-.8443	.7129	.4680	1/38	94.3587	Y= 4.8876-.0080(TDB)
.390	-.8241	.6791	.4646	1/38	80.4346	Y= 4.7390-.0073(TDB)
.395	-.7873	.6198	.5946	1/38	61.9455	Y= 5.0881-.0083(TDB)
.400	-.7597	.5771	.6179	1/38	51.8549	Y= 5.2991-.0078(TDB)
.405	-.8018	.6428	.5348	1/38	68.3875	Y= 5.4498-.0078(TDB)
.410	-.8317	.6918	.4817	1/38	85.2984	Y= 5.5888-.0078(TDB)
.415	-.8011	.6418	.5277	1/38	68.0883	Y= 5.7728-.0077(TDB)
.420	-.7761	.6023	.5631	1/38	57.5588	Y= 5 9193-.0075(TDB)
.425	-.7047	.4966	.6747	1/38	37.4883	Y= 6.1141-.0073(TDB)
.430	-.6799	.4622	.7579	1/38	32.6615	Y= 6.4209-.0076(TDB)
.435	-.5590	.3124	.9030	1/38	17.2681	Y= 6.4917-.0066(TDB)
.440	-.6395	.4089	.8087	1/38	26.2874	Y= 6.8364-.0073(TDB)
.445	-.6919	.4787	.7980	1/38	34.8999	Y= 7.1772-.0083(TDB)
.450	-.7217	.5209	.7290	1/38	41.3144	Y= 7.3098-.0083(TDB)
.455	-.7058	.4981	.7546	1/38	37.7171	Y= 7.4353-.0082(TDB)
.460	-.7031	.4944	.7878	1/38	37.1544	Y= 7.6320-.0085(TDB)
.465	-.7174	.5147	.7784	1/38	40.3064	Y= 7.8441-.0087(TDB)
.470	-.6941	.4818	.8435	1/38	35.3286	Y= 8.0330-.0088(TDB)
.475	-.6742	.4545	.9274	1/38	31.6626	Y= 8.3077-.0092(TDB)
.480	-.6207	.3853	.9993	1/38	23.8196	Y= 8.4161-.0086(TDB)
.485	-.6458	.4170	1.0200	1/38	27.1837	Y= 8.7506-.0094(TDB)
.490	-.6244	.3898	1.0027	1/38	24.2768	Y= 8.7862-.0087(TDB)
.495	-.6127	.3754	1.0034	1/38	22.8350	Y= 8.8826-.0085(TDB)

Table D-2 - cont.

Wave-length (μm)	r Value	r^2 Value	Standard Error of Estimate	Degrees of Freedom	F Ratio	Regression Equation (y = b + mx)
.500	-.6015	.3617	.9926	1/38	21.5375	Y= 9.0370-.0081(TDB)
.505	-.5938	.3526	.9865	1/38	20.6935	Y= 9.2409-.0079(TDB)
.510	-.5454	.2975	.9699	1/38	16.0931	Y= 9.4088-.0069(TDB)
.515	-.5262	.2769	.9432	1/38	14.5534	Y= 9.6673-.0063(TDB)
.520	-.4999	.2499	.9166	1/38	12.6633	Y=10.0024-.0058(TDB)
.525	-.4318	.1864	.9264	1/38	8.7077	Y=10.2366-.0048(TDB)
.530	-.4175	.1743	.9190	1/38	8.0218	Y=10.5650-.0049(TDB)
.535	-.4011	.1609	.9799	1/38	7.2573	Y=10.8478-.0047(TDB)
.540	-.3986	.1589	.9955	1/38	7.1789	Y=11.1166-.0047(TDB)
.545	-.4064	.1651	1.0328	1/38	7.5171	Y=11.3950-.0050(TDB)
.550	-.2845	.0809	1.2451	1/38	3.3455	Y=11.5058-.0040(TDB)
.555	-.2956	.0874	1.2268	1/38	3.6384	Y=11.6134-.0041(TDB)
.560	-.2807	.0788	1.2877	1/38	3.2494	Y=11.7101-.0041(TDB)
.565	-.2968	.0881	1.3303	1/38	3.6701	Y=11.7769-.0045(TDB)
.570	-.3269	.1069	1.3775	1/38	4.5479	Y=11.8788-.0052(TDB)
.575	-.3820	.1459	1.3867	1/38	6.4938	Y=12.0417-.0062(TDB)
.580	-.4047	.1638	1.4167	1/38	7.4436	Y=12.1241-.0068(TDB)
.585	-.4007	.1606	1.3365	1/38	7.2679	Y=12.0410-.0064(TDB)
.590	-.3782	.1431	1.3832	1/38	6.3443	Y=12.0759-.0061(TDB)
.595	-.4140	.1714	1.3618	1/38	7.8588	Y=12.1502-.0067(TDB)
.600	-.3495	.1221	1.3980	1/38	5.2861	Y=12.0789-.0057(TDB)
.605	-.4040	.1632	1.3838	1/38	7.4113	Y=12.2615-.0066(TDB)
.610	-.4569	.2087	1.4633	1/38	10.0240	Y=12.4918-.0082(TDB)
.615	-.4579	.2097	1.4900	1/38	10.0811	Y=12.5766-.0083(TDB)
.620	-.4441	.1973	1.5505	1/38	9.3373	Y=12.6467-.0084(TDB)
.625	-.4702	.2211	1.5912	1/38	10.7878	Y=12.8286-.0092(TDB)
.630	-.4605	.2121	1.5816	1/38	10.2298	Y=12.8326-.0089(TDB)
.635	-.4753	.2260	1.6190	1/38	11.0926	Y=12.9954-.0095(TDB)
.640	-.5082	.2583	1.6554	1/38	13.2345	Y=13.1624-.0106(TDB)
.645	-.4958	.2458	1.7271	1/38	12.3872	Y=13.3537-.0107(TDB)

Table D-2 - cont.

Wave-length (μm)	r Value	r^2 Value	Standard Error of Estimate	Degrees of Freedom	F Ratio	Regression Equation (y = b + mx)
.650	-.4634	.2148	1.7090	1/38	10.3923	Y=13.0985-.0097(TDB)
.655	-.5026	.2526	1.7329	1/38	12.8437	Y=13.3410-.0109(TDB)
.660	-.5057	.2557	1.9689	1/38	13.0547	Y=13.7443-.0125(TDB)
.665	-.5077	.2578	2.0474	1/38	13.1974	Y=13.9249-.0131(TDB)
.670	-.5445	.2965	2.0950	1/38	16.0134	Y=14.3884-.0148(TDB)
.675	-.5527	.3055	2.1420	1/38	16.7136	Y=14.4583-.0154(TDB)
.680	-.4948	.2449	2.3548	1/38	12.3224	Y=14.3550-.0146(TDB)
.685	-.4129	.1705	2.3134	1/38	7.8109	Y=13.7872-.0115(TDB)
.690	-.3684	.1357	2.2566	1/38	5.9680	Y=13.8237-.0097(TDB)
.695	-.4029	.1623	2.2327	1/38	7.3618	Y=14.6968-.0107(TDB)
.700	-.2218	.0492	2.3969	1/38	1.9667	Y=15.0626-.0059(TDB)
.705	-.1524	.0232	2.3412	1/38	.9032	Y=15.2435-.0039(TDB)
.710	-.1283	.0165	2.1746	1/38	.6364	Y=15.8185-.0031(TDB)
.715	.1277	.0163	1.5833	1/38	.6295	Y=14.9192+.0022(TDB)
.720	.2817	.0794	1.4847	1/38	3.2764	Y=15.5779+.0047(TDB)
.725	.3512	.1233	1.4101	1/38	5.3466	Y=16.4975+.0057(TDB)
.730	.3948	.1558	1.6179	1/38	7.0146	Y=17.2761+.0076(TDB)
.735	.4757	.2263	1.6634	1/38	11.1142	Y=17.6648+.0098(TDB)
.740	.6920	.4788	1.6675	1/38	34.9146	Y=17.0875+.0174(TDB)
.745	.6708	.4500	1.8948	1/38	31.0908	Y=17.2471+.0186(TDB)
.750	.7164	.5133	1.8544	1/38	40.0699	Y=17.0923+.0207(TDB)
.755	.7073	.5002	2.0510	1/38	38.0347	Y=16.9286+.0223(TDB)
.760	.7312	.5346	2.2399	1/38	43.6560	Y=16.6641+.0261(TDB)
.765	.7551	.5702	2.2308	1/38	50.4171	Y=16.7172+.0279(TDB)
.770	.7483	.5600	2.2458	1/38	48.3617	Y=16.6558+.0275(TDB)
.775	.7475	.5587	2.0960	1/38	48.1073	Y=16.9635+.0256(TDB)
.780	.6267	.3928	2.3234	1/38	24.5824	Y=17.9745+.0203(TDB)
.785	.6399	.4094	2.0927	1/38	26.3444	Y=18.2572+.0189(TDB)
.790	.6695	.4482	1.9414	1/38	30.8717	Y=18.5100+.0190(TDB)
.795	.6176	.3815	2.1971	1/38	23.4369	Y=18.7563+.0188(TDB)
.800	.5954	.3545	2.2718	1/38	20.8699	Y=19.0263+.0183(TDB)

Dry green biomass

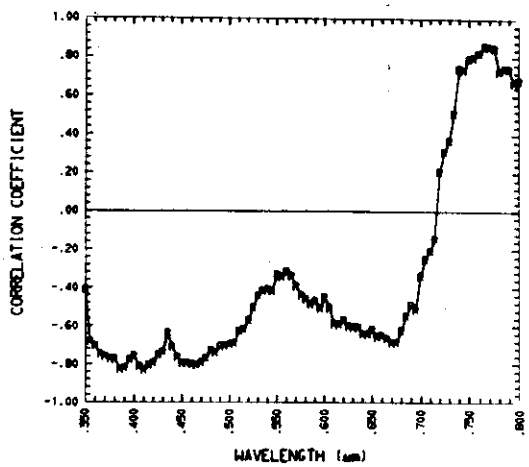

(a) Spectrocorrelation curve

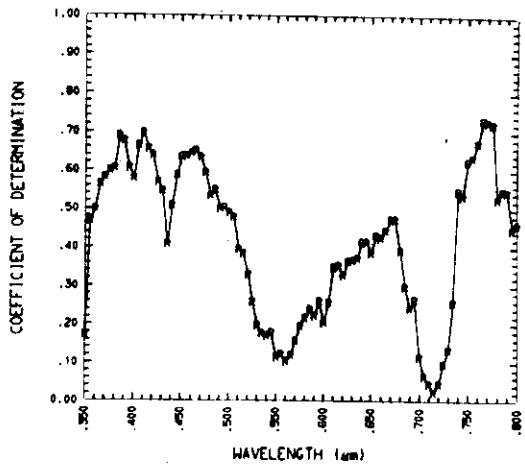

(b) r^2 versus wavelength

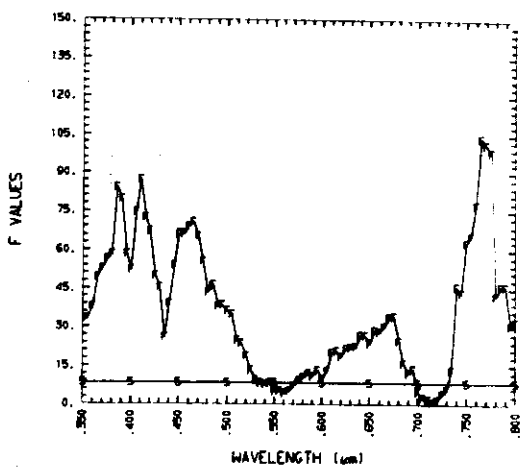

(c) F value versus wavelength

Figure D-5. STATISTICAL COEFFICIENTS OF THE SIMPLE LINEAR REGRESSION FOR DRY GREEN BIOMASS (DGB) VERSUS REFLECTANCE AT EACH WAVELENGTH. The linear regressions were formed for the dry green biomass present on 40 of 1/4 meter squared plots of blue grama (*B. gracilis*) and the reflectance of the plot at 91 wavelengths between .350 and .800 µm. The tabular values of these coefficients can be found in Table D-3. (a) The correlation coefficient (r) versus wavelength or the spectrocorrelation curve. (b) The coefficient of determination (r^2) versus wavelength. (c) The F value versus wavelength where the horizontal line shown by -5- represents the .5% level of significance for 1/38 degrees of freedom.

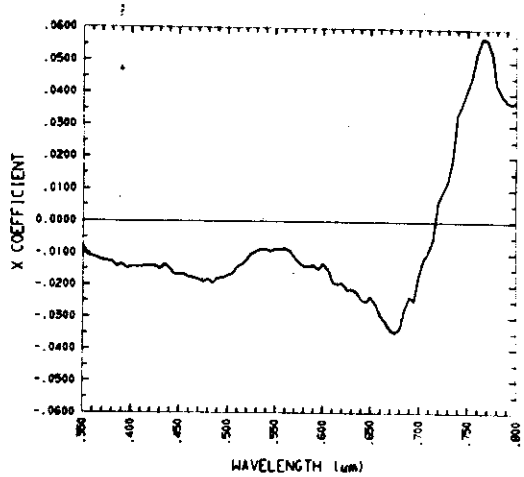

(a) Slope versus wavelength

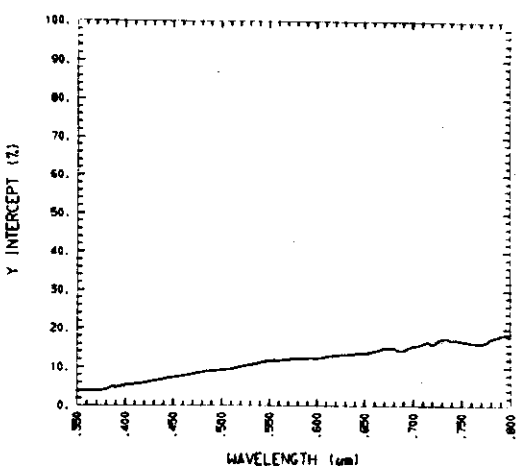

(b) Intercept versus wavelength (soil spectroreflectance)

Figure D-6. THE SLOPE AND THE INTERCEPT OF THE SIMPLE LINEAR REGRESSION FOR DRY GREEN BIOMASS (DGB) VERSUS REFLECTANCE AT EACH WAVELENGTH. The linear regressions were formed for the dry green biomass present on 40 of 1/4 meter squared plots of blue grama (*B. gracilis*) and the reflectance between .350 and .800 µm. Each regression equation at each wavelength yields a slope and intercept value which occur in Table D-3. (a) The plot of the slope at each wavelength which represents the rate of change in the reflectance of the plot with wavelengths. (b) The plot of the "y" intercept of the straight line which represents the reflectance of the plot when the dry green biomass value is zero. Plotted against wavelength it represents the spectroreflectance of the underlying, unexposed soil surface.

Table D-3. SIMPLE LINEAR REGRESSION BETWEEN CANOPY REFLECTANCE AND DRY GREEN BIOMASS (DGB). The coefficients and equation resulting from these computations are shown for each available wavelength. The sample set in each case consisted of 40 of 1/4 square meter plots of blue grama (B. gracilis). Plots of r, r^2, F, Y, and m values versus wavelength occur in Figures D-5 and D-6.

Wave-Length (μm)	r Value	r^2 Value	Standard Error of Estimate	Degrees of Freedom	F Ratio	Regression Equation (y = b + mx)
.350	-.4130	.1706	.8631	1. 38	7.8149	Y= 3.6481-.0077(DGB)
.355	-.6831	.4667	.5738	1. 38	33.2525	Y= 3.8845-.0106(DGB)
.360	-.7057	.4981	.5670	1. 38	37.7091	Y= 3.8354-.0111(DGB)
.365	-.7512	.5643	.5196	1. 38	49.2245	Y= 3.8632-.0116(DGB)
.370	-.7619	.5805	.5290	1. 38	52.5735	Y= 3.9425-.0122(DGB)
.375	-.7734	.5981	.5209	1. 38	56.5605	Y= 4.0211-.0125(DGB)
.380	-.7778	.6050	.5234	1. 38	58.2017	Y= 4.1209-.0127(DGB)
.385	-.8300	.6889	.4872	1. 38	84.1609	Y= 4.8120-.0143(DGB)
.390	-.8226	.6767	.4664	1. 38	79.5239	Y= 4.6877-.0133(DGB)
.395	-.7789	.6067	.6048	1. 38	58.6175	Y= 5.0187-.0148(DGB)
.400	-.7608	.5789	.6166	1. 38	52.2374	Y= 5.2487-.0142(DGB)
.405	-.8139	.6624	.5199	1. 38	74.5640	Y= 5.4167-.0143(DGB)
.410	-.8345	.6963	.4781	1. 38	87.1386	Y= 5.5405-.0143(DGB)
.415	-.8097	.6556	.5175	1. 38	72.3245	Y= 5.7347-.0141(DGB)
.420	-.7989	.6383	.5370	1. 38	67.0465	Y= 5.9047-.0140(DGB)
.425	-.7533	.5675	.6253	1. 38	49.8650	Y= 6.1467-.0141(DGB)
.430	-.7380	.5446	.6974	1. 38	45.4505	Y= 6.4755-.0150(DGB)
.435	-.6367	.4054	.8398	1. 38	25.9080	Y= 6.5964-.0136(DGB)
.440	-.7123	.5073	.7383	1. 38	39.1298	Y= 6.9223-.0147(DGB)
.445	-.7658	.5864	.7108	1. 38	53.8872	Y= 7.2653-.0167(DGB)
.450	-.7965	.6344	.6368	1. 38	65.9473	Y= 7.3932-.0165(DGB)
.455	-.7971	.6353	.6433	1. 38	66.1950	Y= 7.5517-.0167(DGB)
.460	-.8024	.6439	.6611	1. 38	68.7184	Y= 7.7690-.0175(DGB)
.465	-.8062	.6499	.6611	1. 38	70.5534	Y= 7.9604-.0177(DGB)
.470	-.7952	.6323	.7106	1. 38	65.3447	Y= 8.1823-.0183(DGB)
.475	-.7703	.5934	.8006	1/ 38	55.4635	Y= 8.4587-.0190(DGB)
.480	-.7304	.5335	.8706	1/ 38	43.4533	Y= 8.6046-.0183(DGB)
.485	-.7412	.5493	.8968	1/ 38	46.3179	Y= 8.9121-.0195(DGB)
.490	-.7071	.5000	.9077	1/ 38	37.9995	Y= 8.9149-.0179(DGB)
.495	-.7085	.5019	.8960	1/ 38	38.2911	Y= 9.0401-.0177(DGB)

Table D-3 - cont.

Wave-Length (μm)	r Value	r^2 Value	Standard Error of Estimate	Degrees of Freedom	F Ratio	Regression Equation (y = b + mx)
.500	-.6993	.4890	.8882	1/38	36.3626	Y= 9.1965-.0171(DGB)
.505	-.6916	.4782	.8802	1/38	34.8306	Y= 9.3980-.0166(DGB)
.510	-.6278	.3941	.9007	1/38	24.7185	Y= 9.5306-.0143(DCB)
.515	-.6182	.3822	.8719	1/38	23.5082	Y= 9.8044-.0135(DGB)
.520	-.5731	.3284	.8674	1/38	18.5818	Y=10.1001-.0119(DGB)
.525	-.5066	.2566	.8955	1/38	13.1186	Y=10.3396-.0102(DGB)
.530	-.4435	.1967	.9657	1/38	9.3057	Y=10.5817-.0094(DCB)
.535	-.4186	.1752	.9715	1/38	8.0734	Y=10.8495-.0088(DGB)
.540	-.4127	.1703	.9887	1/38	7.7998	Y=11.1120-.0088(DGB)
.545	-.4211	.1773	1.0252	1/38	8.1897	Y=11.3908-.0094(DGB)
.550	-.3346	.1120	1.2239	1/38	4.7919	Y=11.5936-.0086(DGB)
.555	-.3462	.1199	1.2048	1/38	5.1763	Y=11.7003-.0088(DGB)
.560	-.3192	.1019	1.2715	1/38	4.3097	Y=11.7735-.0084(DGB)
.565	-.3434	.1179	1.3084	1/38	5.0793	Y=11.8610-.0094(DGB)
.570	-.3939	.1552	1.3398	1/38	6.9797	Y=12.0159-.0113(DCB)
.575	-.4409	.1944	1.3468	1/38	9.1707	Y=12.1555-.0130(DGB)
.580	-.4629	.2143	1.3733	1/38	10.3616	Y=12.2371-.0141(DCB)
.585	-.4877	.2379	1.2734	1/38	11.8613	Y=12.2219-.0140(DGB)
.590	-.4704	.2213	1.3186	1/38	10.7977	Y=12.2771-.0138(DGB)
.595	-.5083	.2584	1.2883	1/38	13.2398	Y=12.3535-.0150(DGB)
.600	-.4501	.2026	1.3324	1/38	9.6537	Y=12.3052-.0132(DGB)
.605	-.5059	.2559	1.3049	1/38	13.0698	Y=12.4883-.0151(DGB)
.610	-.5881	.3459	1.3304	1/38	20.0963	Y=12.8171-.0190(DGB)
.615	-.5939	.3527	1.3485	1/38	20.7019	Y=12.9218-.0196(DGB)
.620	-.5709	.3259	1.4208	1/38	18.3742	Y=12.9768-.0194(DCB)
.625	-.6024	.3629	1.4391	1/38	21.6487	Y=13.1864-.0214(DGB)
.630	-.6043	.3652	1.4197	1/38	21.8620	Y=13.2237-.0212(DCB)
.635	-.6090	.3709	1.4596	1/38	22.4031	Y=13.3646-.0221(DGB)
.640	-.6430	.4135	1.4721	1/38	26.7891	Y=13.5472-.0243(DGB)
.645	-.6425	.4128	1.5239	1/38	26.7168	Y=13.7953-.0252(DGB)

Table D-3 - cont.

Wave-Length (μm)	r Value	r^2 Value	Standard Error of Estimate	Degrees of Freedom	F Ratio	Regression Equation (y = b + mx)
.650	-.6205	.3850	1.5124	1/38	23.7901	Y=13.5666-.0236(DGB)
.655	-.6568	.4314	1.5114	1/38	28.8325	Y=13.8117-.0259(DGB)
.660	-.6523	.4255	1.7298	1/38	28.1442	Y=14.2492-.0293(DGB)
.665	-.6662	.4438	1.7724	1/38	30.3171	Y=14.4997-.0312(DGB)
.670	-.6875	.4727	1.8138	1/38	34.0594	Y=14.9180-.0338(DGB)
.675	-.6880	.4734	1.8652	1/38	34.1571	Y=14.9671-.0348(DGB)
.680	-.6261	.3920	2.1130	1/38	24.4983	Y=14.8833-.0334(DGB)
.685	-.5457	.2977	2.1470	1/38	16.1108	Y=14.3087-.0275(DGB)
.690	-.4913	.2414	2.1142	1/38	12.0891	Y=14.2834-.0235(DGB)
.695	-.5138	.2640	2.0928	1/38	13.6328	Y=15.1017-.0247(DGB)
.700	-.3388	.1148	2.3127	1/38	4.9272	Y=15.5288-.0164(DGB)
.705	-.2521	.0635	2.2924	1/38	2.5779	Y=15.6327-.0118(DGB)
.710	-.2084	.0434	2.1446	1/38	1.7259	Y=16.1071-.0090(DGB)
.715	-.1442	.0208	1.8535	1/38	.8066	Y=16.6158-.0053(DGB)
.720	.2059	.0424	1.5142	1/38	1.6830	Y=15.8159+.0063(DGB)
.725	.3095	.0958	1.4321	1/38	4.0254	Y=16.6465+.0092(DGB)
.730	.3656	.1337	1.6390	1/38	5.8626	Y=17.4169+.0127(DGB)
.735	.5070	.2571	1.6300	1/38	13.1501	Y=17.6259+.0189(DGB)
.740	.7397	.5472	1.5543	1/38	45.9205	Y=17.0096+.0336(DGB)
.745	.7300	.5329	1.7462	1/38	43.3525	Y=17.1056+.0367(DGB)
.750	.7900	.6241	1.6296	1/38	63.0993	Y=16.8865+.0413(DGB)
.755	.7963	.6340	1.7551	1/38	65.8298	Y=16.6234+.0455(DGB)
.760	.8193	.6713	1.8826	1/38	77.5924	Y=16.3295+.0529(DGB)
.765	.8555	.7319	1.7619	1/38	103.7334	Y=16.3029+.0573(DGB)
.770	.8528	.7273	1.7678	1/38	101.3680	Y=16.2173+.0568(DGB)
.775	.8493	.7213	1.6657	1/38	98.3517	Y=16.5695+.0527(DGB)
.780	.7255	.5264	2.0519	1/38	42.2348	Y=17.5920+.0426(DGB)
.785	.7404	.5483	1.8303	1/38	46.1200	Y=17.9019+.0397(DGB)
.790	.7393	.5466	1.7598	1/38	45.8163	Y=18.3160+.0380(DGB)
.795	.6686	.4470	2.0775	1/38	30.7163	Y=18.6313+.0368(DGB)
.800	.6780	.4596	2.0786	1/38	32.3218	Y=18.7380+.0377(DGB)

Dry brown biomass

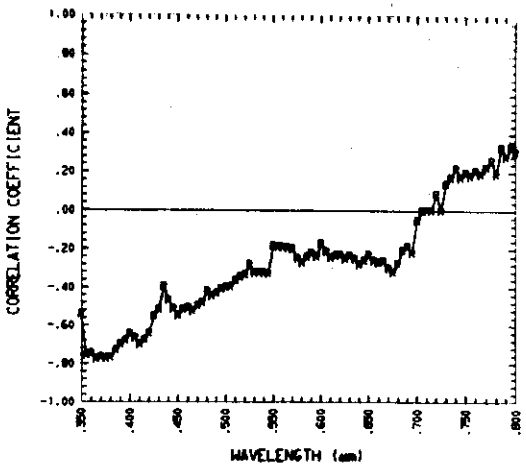

(a) Spectrocorrelation curve

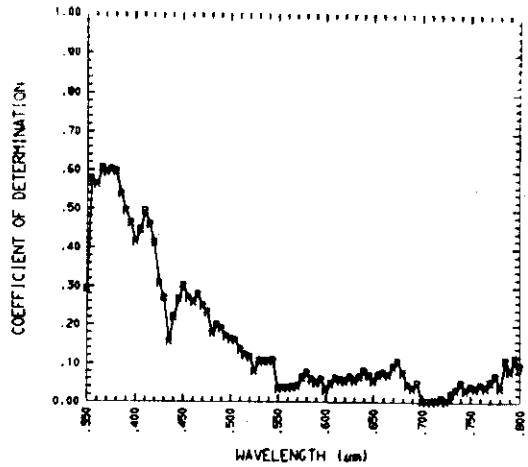

(b) r^2 versus wavelength

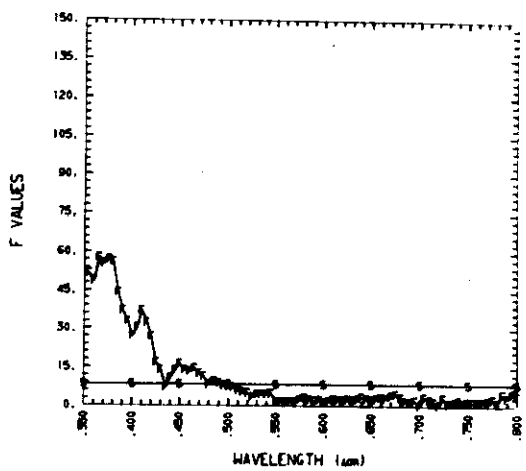

(c) F value versus wavelength

Figure D-7. STATISTICAL COEFFICIENTS OF THE SIMPLE LINEAR REGRESSION FOR DRY BROWN BIOMASS (DBB) VERSUS REFLECTANCE AT EACH WAVELENGTH. The linear regressions were formed for the dry brown biomass present on 40 of 1/4 meter squared plots of blue grama (*B. gracilis*) and the reflectance of the plot at 91 wavelengths between .350 and .800 µm. The tabular values of these coefficients can be found in Table D-4. (a) The correlation coefficient (r) versus wavelength or the spectrocorrelation curve. (b) The coefficient of determination (r^2) versus wavelength. (c) The F value versus wavelength where the horizontal line shown by -5- represents the .5% level of significance for 1/38 degrees of freedom.

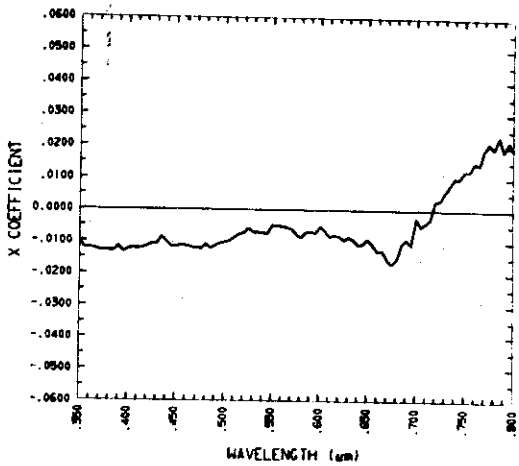

(a) Slope versus wavelength

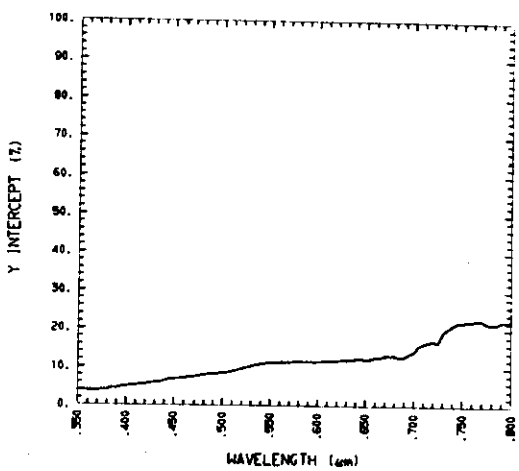

(b) Intercept versus wavelength (soil spectroreflectance)

Figure D-8. THE SLOPE AND THE INTERCEPT OF THE SIMPLE LINEAR REGRESSION FOR DRY BROWN BIOMASS (DBB) VERSUS REFLECTANCE AT EACH WAVELENGTH. The linear regressions were formed for the dry brown biomass present on 40 of 1/4 meter squared plots of blue grama (*B. gracilis*) and the reflectance between .350 and .800 µm. Each regression equation at each wavelength yields a slope and intercept value which occur in Table D-4. (a) The plot of the slope at each wavelength which represents the rate of change in the reflectance of the plot with wavelength. (b) The plot of the "y" intercept of the straight line which represents the reflectance of the plot when the dry brown biomass value is zero. Plotted against wavelength it represents the spectroreflectance of the underlying, unexposed soil surface.

Table D-4. SIMPLE LINEAR REGRESSION BETWEEN CANOPY REFLECTANCE AND DRY BROWN BIOMASS (DBB). The coefficients and equation resulting from these computations are each available wavelength. The sample set in each case consisted of 40 of 1/4 square meter plots of blue grama (B. gracilis). Plots of r, r^2, F, Y, and m values versus wavelength occur in Figures D-7 and D-8.

Wave-Length (μm)	r Value	r^2 Value	Standard Error of Estimate	Degrees of Freedom	F Ratio	Regression Equation (y = b + mx)
.350	-.5403	.2919	.7974	1/38	15.6676	Y= 3.8175-.0104(DBB)
.355	-.7588	.5757	.5118	1/38	51.5617	Y= 3.9393-.0121(DBB)
.360	-.7486	.5604	.5306	1/38	48.4368	Y= 3.8457-.0122(DBB)
.365	-.7765	.6029	.4961	1/38	57.6921	Y= 3.8471-.0124(DBB)
.370	-.7697	.5925	.5214	1/38	55.2453	Y= 3.9013-.0128(DBB)
.375	-.7744	.5997	.5199	1/38	56.9248	Y= 3.9694-.0129(DBB)
.380	-.7723	.5964	.5291	1/38	56.1498	Y= 4.0590-.0131(DBB)
.385	-.7328	.5370	.5944	1/38	44.0735	Y= 4.6092-.0130(DBB)
.390	-.7023	.4932	.5839	1/38	36.9799	Y= 4.4660-.0117(DBB)
.395	.6804	.4630	.7067	1/38	32.7651	Y= 4.7969-.0133(DBB)
.400	-.6447	.4156	.7264	1/38	27.0282	Y= 5.0033-.0125(DBB)
.405	-.6670	.4449	.6667	1/38	30.4547	Y= 5.1357-.0121(DBB)
.410	-.7022	.4931	.6177	1/38	36.9683	Y= 5.2878-.0124(DBB)
.415	-.6771	.4585	.6489	1/38	32.1708	Y= 5.4792-.0121(DBB)
.420	-.6423	.4125	.6844	1/38	26.6857	Y= 5.6108-.0117(DBB)
.425	-.5537	.3066	.7918	1/38	16.8038	Y= 5.7688-.0107(DBB)
.430	-.5181	.2684	.8839	1/38	13.9441	Y= 6.0311-.0190(DBB)
.435	-.3938	.1551	1.0010	1/38	6.9755	Y= 6.0952-.0087(DBB)
.440	-.4692	.2201	.9289	1/38	10.7269	Y= 6.4313-.0100(DBB)
.445	-.5156	.2658	.9470	1/38	13.7597	Y= 6.7312-.0116(DBB)
.450	-.5483	.3006	.8808	1/38	16.3347	Y= 6.8850-.0117(DBB)
.455	-.5183	.2686	.9110	1/38	13.9577	Y= 6.9832-.0112(DBB)
.460	-.5079	.2579	.9544	1/38	13.2093	Y= 7.1479-.0114(DBB)
.465	-.5264	.2771	.9501	1/38	14.5642	Y= 7.3612-.0120(DBB)
.470	-.4982	.2482	1.0160	1/38	12.5453	Y= 7.5213-.0119(DBB)
.475	-.4811	.2315	1.1008	1/38	11.4462	Y= 7.7694-.0123(DBB)
.480	-.4205	.1768	1.1564	1/38	8.1616	Y= 7.8649-.0109(DBB)
.485	-.4464	.1993	1.1954	1/38	9.4579	Y= 8.1696-.0121(DBB)
.490	-.4338	.1882	1.1655	1/38	8.8079	Y= 8.2511-.0113(DBB)
.495	-.4101	.1682	1.1579	1/38	7.6846	Y= 8.3303-.0106(DBB)

Table D-4 - cont.

Wave-Length (μm)	r Value	r^2 Value	Standard Error of Estimate	Degrees of Freedom	F Ratio	Regression Equation (y = b + mx)
.500	-.4019	.1615	1.1377	1/38	7.3197	Y= 8.5048-.0102(DBB)
.505	-.3985	.1588	1.1176	1/38	7.1740	Y= 8.7292-.0099(DBB)
.510	-.3670	.1347	1.0765	1/38	5.9152	Y= 8.9642-.0086(DBB)
.515	-.3473	.1206	1.0402	1/38	5.2119	Y= 9.2435-.0078(DBB)
.520	-.3372	.1137	.9964	1/38	4.8766	Y= 9.6312-.0073(DBB)
.525	-.2810	.0790	.9857	1/38	3.2573	Y= 9.9078-.0059(DBB)
.530	-.3245	.1053	1.0191	1/38	4.4711	Y=10.3268-.0071(DBB)
.535	-.3227	.1042	1.0125	1/38	4.4184	Y=10.6403-.0070(DBB)
.540	-.3244	.1052	1.0267	1/38	4.4693	Y=10.9140-.0072(DBB)
.545	-.3276	.1073	1.0679	1/38	4.5691	Y=11.1740-.0075(DBB)
.550	-.1809	.0327	1.2774	1/38	1.2850	Y=11.2226-.0048(DBB)
.555	-.1889	.0357	1.2611	1/38	1.4063	Y=11.3245-.0049(DBB)
.560	-.1897	.0360	1.3173	1/38	1.4180	Y=11.4467-.0052(DBB)
.565	-.1939	.0376	1.3666	1/38	1.4848	Y=11.4722-.0055(DBB)
.570	-.2002	.0401	1.4281	1/38	1.5872	Y=11.4949-.0059(DBB)
.575	-.2493	.0622	1.4532	1/38	2.5190	Y=11.6185-.0076(DBB)
.580	-.2728	.0744	1.4904	1/38	3.0564	Y=11.6838-.0086(DBB)
.585	-.2399	.0576	1.4161	1/38	2.3214	Y=11.5568-.0071(DBB)
.590	-.2190	.0480	1.4580	1/38	1.9145	Y=11.5889-.0067(DBB)
.595	-.2408	.0580	1.4519	1/38	2.3390	Y=11.6194-.0073(DBB)
.600	-.1715	.0294	1.4699	1/38	1.1514	Y=11.5525-.0052(DBB)
.605	-.2150	.0462	1.4774	1/38	1.8417	Y=11.6870-.0066(DBB)
.610	-.2469	.0610	1.5941	1/38	2.4665	Y=11.7956-.0083(DBB)
.615	-.2354	.0554	1.6289	1/38	2.2295	Y=11.8319-.0080(DBB)
.620	-.2304	.0531	1.6840	1/38	2.1299	Y=11.9068-.0081(DBB)
.625	-.2525	.0638	1.7445	1/38	2.5875	Y=12.0384-.0093(DBB)
.630	-.2349	.0552	1.7320	1/38	2.2185	Y=12.0305-.0085(DBB)
.635	-.2509	.0630	1.7813	1/38	2.5533	Y=12.1668-.0094(DBB)
.640	-.2818	.0794	1.8442	1/38	3.2788	Y=12.2805-.0110(DBB)
.645	-.2613	.0683	1.9197	1/38	2.7844	Y=12.4180-.0106(DBB)

Table D-4 - cont.

Wave-Length (μm)	r Value	r^2 Value	Standard Error of Estimate	Degrees of Freedom	F Ratio	Regression Equation (y = b + mx)
.650	-.2290	.0524	1.8774	1/38	2.1025	Y=12.2013-.0090(DBB)
.655	-.2616	.0684	1.9347	1/38	2.7905	Y=12.3741-.0107(DBB)
.660	-.2727	.0744	2.1957	1/38	3.0538	Y=12.6733-.0127(DBB)
.665	-.2627	.0690	2.2930	1/38	2.8179	Y=12.7609-.0127(DBB)
.670	-.3023	.0914	2.3809	1/38	3.8217	Y=13.1623-.0154(DBB)
.675	-.3226	.1041	2.4328	1/38	4.4138	Y=13.2454-.0169(DBB)
.680	-.2744	.0753	2.6059	1/38	3.0930	Y=13.1443-.0151(DBB)
.685	-.2067	.0427	2.5067	1/38	1.6962	Y=12.7367-.0108(DBB)
.690	-.1841	.0339	2.3859	1/38	1.3324	Y=12.9342-.0091(DBB)
.695	-.2207	.0487	2.3793	1/38	1.9462	Y=13.7988-.0109(DBB)
.700	-.0495	.0025	2.4551	1/38	.0933	Y=14.2676-.0025(DBB)
.705***	F value is less than .010, no regression is possible					
.710***	F value is less than .010, no regression is possible					
.715***	F value is less than .010, no regression is possible					
.720	.0851	.0072	1.7395	1/38	.2774	Y=16.9482+.0030(DBB)
.725***	F value is less than .010, no regression is possible					
.730	.1377	.0190	2.0266	1/38	.7344	Y=19.3744+.0057(DBB)
.735	.1723	.0297	2.1659	1/38	1.1622	Y=20.3795+.0077(DBB)
.740	.2220	.0493	2.1983	1/38	1.9702	Y=21.2712+.0102(DBB)
.745	.1701	.0289	2.8835	1/38	1.1316	Y=21.8962+.0101(DBB)
.750	.1960	.0384	3.1057	1/38	1.5175	Y=21.9887+.0126(DBB)
.755	.1811	.0328	3.2923	1/38	1.2884	Y=22.3716+.0123(DBB)
.760	.2066	.0427	3.5499	1/38	1.6936	Y=22.3697+.0152(DBB)
.765	.1884	.0355	3.6852	1/38	1.3978	Y=22.7041+.0144(DBB)
.770	.2240	.0502	4.1190	1/38	2.0071	Y=22.5819+.0192(DBB)
.775	.2612	.0682	3.8724	1/38	2.7820	Y=21.7474+.0213(DBB)
.780	.1899	.0361	4.9929	1/38	1.4220	Y=21.6220+.0196(DBB)
.785	.3298	.1088	3.2993	1/38	4.6383	Y=21.6641+.0234(DBB)
.790	.2804	.0786	3.1574	1/38	3.2434	Y=22.4095+.0188(DBB)
.795	.3349	.1122	3.0343	1/38	4.8011	Y=22.2954+.0219(DBB)
.800	.3067	.0940	2.9492	1/38	3.9447	Y=22.4669+.0193(DBB)

Leaf water

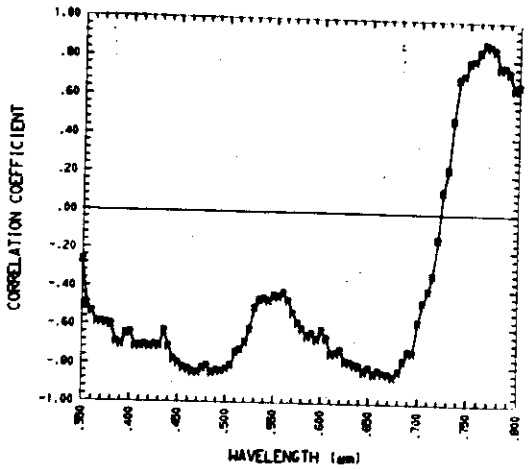

(a) Spectrocorrelation curve

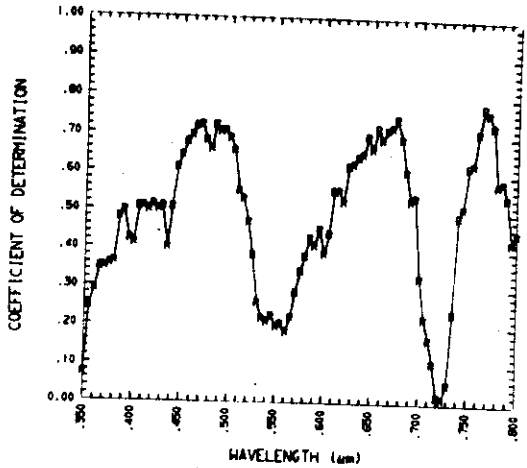

(b) r^2 versus wavelength

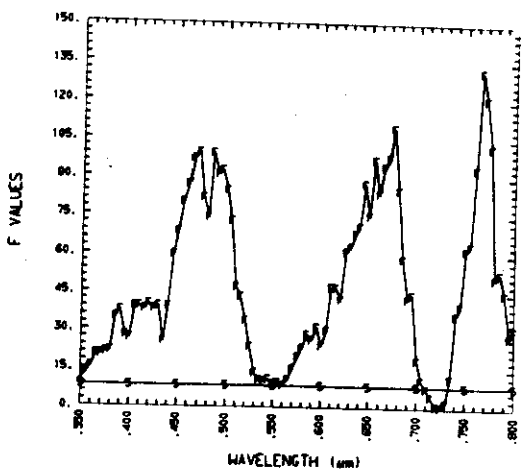

(c) F value versus wavelength

Figure D-9. STATISTICAL COEFFICIENTS OF THE SIMPLE LINEAR REGRESSION FOR LEAF WATER (LW) VERSUS REFLECTANCE AT EACH WAVELENGTH. The linear regressions were formed for the leaf water present on 40 of 1/4 meter squared plots of blue grama (*B. gracilis*) and the reflectance of the plot at 91 wavelengths between .350 and .800 µm. The tabular values of these coefficients can be found in Table D-5. (a) The correlation coefficient (r) versus wavelength or the spectrocorrelation curve. (b) The coefficient of determination (r^2) versus wavelength. (c) The F value versus wavelength where the horizontal line shown by -5- represents the .5% level of significance for 1/38 degrees of freedom.

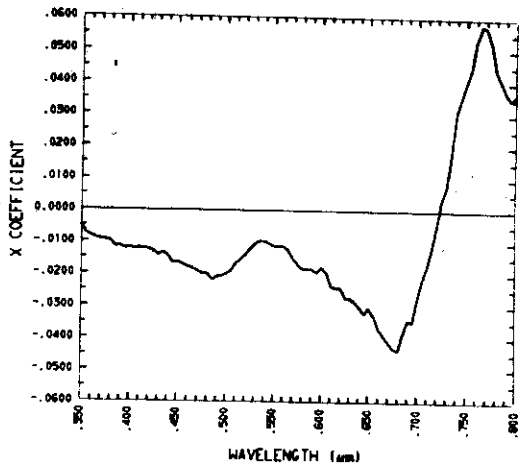

(a) Slope versus wavelength

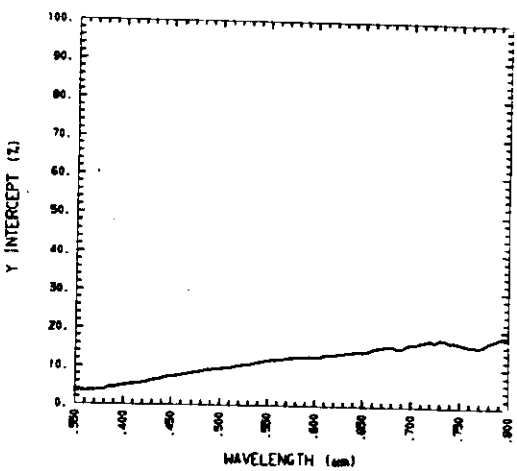

(b) Intercept versus wavelength (soil spectroreflectance)

Figure D-10. THE SLOPE AND THE INTERCEPT OF THE SIMPLE LINEAR REGRESSION FOR LEAF WATER (LW) VERSUS REFLECTANCE AT EACH WAVELENGTH. The linear regressions were formed for the leaf water present on 40 of 1/4 meter squared plots of blue grama (*B. gracilis*) and the reflectance between .350 and .800 µm. Each regression equation at each wavelength yields a slope and intercept value which occur in Table D-5. (a) The plot of the slope at each wavelength which represents the rate of change in the reflectance of the plot with wavelength. (b) The plot of the "y" intercept of the straight line which represents the reflectance of the plot when the leaf water value is zero. Plotted against wavelength it represents the spectroreflectance of the underlying, unexposed soil surface.

Table D-5. SIMPLE LINEAR REGRESSION BETWEEN CANOPY REFLECTANCE AND LEAF WATER (LW). The coefficients and equation resulting from these computations are shown for each available wavelength. The sample set in each case consisted of 40 of 1/4 square meter plots of blue grama (B. gracilis). Plots of r, r^2, F, Y, and m values versus wavelength occur in Figures D-9 and D-10.

Wave-Length (μm)	r Value	r^2 Value	Standard Error of Estimate	Degrees of Freedom	F Ratio	Regression Equation (y = b + mx)
.350	-.2688	.0723	.9128	1/38	2.9598	Y= 3.4174-.0049(LW)
.355	-.4947	.2447	.6828	1/38	12.3142	Y= 3.6390-.0075(LW)
.360	-.5381	.2895	.6746	1/38	15.4841	Y= 3.6158-.0083(LW)
.365	-.5893	.3473	.6361	1/38	20.2163	Y= 3.6567-.0090(LW)
.370	-.5892	.3472	.6599	1/38	20.2084	Y= 3.7128-.0093(LW)
.375	-.5971	.3565	.6592	1/38	21.0548	Y= 3.7850-.0095(LW)
.380	-.6018	.3622	.6651	1/38	21.5765	Y= 3.8822-.0097(LW)
.385	-.6921	.4790	.6305	1/38	34.9382	Y= 4.6233-.0117(LW)
.390	-.7052	.4973	.5815	1/38	37.5923	Y= 4.5404-.0112(LW)
.395	-.6497	.4221	.7331	1/38	27.7554	Y= 4.8235-.0121(LW)
.400	-.6422	.4125	.7283	1/38	26.6791	Y= 5.0738-.0118(LW)
.405	-.7121	.5071	.6282	1/38	39.0931	Y= 5.2809-.0123(LW)
.410	-.7133	.5088	.6081	1/38	39.3588	Y= 5.3793-.0120(LW)
.415	-.7065	.4991	.6240	1/38	37.8663	Y= 5.5985-.0121(LW)
.420	-.7164	.5132	.6230	1/38	40.0644	Y= 5.7996-.0124(LW)
.425	-.7077	.5008	.6719	1/38	38.1195	Y= 6.0961-.0130(LW)
.430	-.7125	.5076	.7252	1/38	39.1794	Y= 6.4574-.0143(LW)
.435	-.6337	-.4016	.8425	1/38	25.4978	Y= 6.6170-.0134(LW)
.440	-.7121	.5071	.7385	1/38	39.0877	Y= 6.9506-.0145(LW)
.445	-.7813	.6104	.6899	1/38	59.5382	Y= 7.3285-.0167(LW)
.450	-.8015	.6424	.6298	1/38	68.2644	Y= 7.4347-.0164(LW)
.455	-.8228	.6770	.6054	1/38	79.6306	Y= 7.6335-.0170(LW)
.460	-.8338	.6952	.6117	1/38	86.6704	Y= 7.8655-.0179(LW)
.465	-.8475	.7182	.5931	1/38	96.8697	Y= 8.0779-.0184(LW)
.470	-.8503	.7230	.6168	1/38	99.1634	Y= 8.3340-.0193(LW)
.475	-.8257	.6818	.7083	1/38	81.4157	Y= 8.6207-.0201(LW)
.480	-.8126	.6603	.7429	1/38	73.8546	Y= 8.8285-.0201(LW)
.485	-.8501	.7227	.7034	1/38	99.0484	Y= 9.2117-.0220(LW)
.490	-.8396	.7049	.6974	1/38	90.7502	Y= 9.2553-.0209(LW)
.495	-.8417	.7084	.6856	1/38	92.3047	Y= 9.3785-.0207(LW)

Table D-5 - cont.

Wave-Length (μm)	r Value	r^2 Value	Standard Error of Estimate	Degrees of Freedom	F Ratio	Regression Equation (y = b + mx)
.500	-.8302	.6893	.6926	1/38	84.3037	Y= 9.5223-.0200(LW)
.505	-.8102	.6564	.7143	1/38	72.5943	Y= 9.6901-.0191(LW)
.510	-.7429	.5519	.7746	1/38	46.8102	Y= 9.7979-.0167(LW)
.515	-.7289	.5313	.7594	1/38	43.0836	Y=10.0514-.0157(LW)
.520	-.6861	.4708	.7700	1/38	33.8020	Y=10.3384-.0141(LW)
.525	-.6183	.3823	.8072	1/38	23.5232	Y=10.5658-.0123(LW)
.530	-.5096	.2596	.9271	1/38	13.3267	Y=10.7279-.0106(LW)
.535	-.4679	.2189	.9454	1/38	10.6495	Y=10.9614-.0097(LW)
.540	-.4592	.2109	.9642	1/38	10.1547	Y=11.2200-.0097(LW)
.545	-.4746	.2252	.9949	1/38	11.0456	Y=11.5177-.0104(LW)
.550	-.4438	.1970	1.1639	1/38	9.3206	Y=11.8652-.0112(LW)
.555	-.4517	.2041	1.1457	1/38	9.7426	Y=11.9608-.0112(LW)
.560	-.4298	.1848	1.2114	1/38	8.6119	Y=12.0569-.0112(LW)
.565	-.4713	.2221	1.2286	1/38	10.8515	Y=12.1997-.0127(LW)
.570	-.5355	.2867	1.2311	1/38	15.2741	Y=12.4087-.0151(LW)
.575	-.5847	.3419	1.2173	1/38	19.7410	Y=12.5687-.0170(LW)
.580	-.6171	.3808	1.2191	1/38	23.3697	Y=12.6940-.0185(LW)
.585	-.6549	.4289	1.1023	1/38	28.5387	Y=12.6875-.0185(LW)
.590	-.6397	.4092	1.1485	1/38	26.3184	Y=12.7587-.0185(LW)
.595	-.6728	.4527	1.1068	1/38	31.4261	Y=12.8250-.0195(LW)
.600	-.6235	.3888	1.1665	1/38	24.1720	Y=12.7961-.0180(LW)
.605	-.6640	.4409	1.1311	1/38	29.9712	Y=12.9477-.0195(LW)
.610	-.7443	.5539	1.0987	1/38	47.1871	Y=13.3158-.0237(LW)
.615	-.7435	.5528	1.1208	1/38	46.9738	Y=13.4108-.0242(LW)
.620	-.7250	.5256	1.1920	1/38	42.0982	Y=13.4940-.0243(LW)
.625	-.7855	.6170	1.1158	1/38	61.2216	Y=13.8213-.0274(LW)
.630	-.7894	.6232	1.0938	1/38	62.8394	Y=13.8577-.0273(LW)
.635	-.8006	.6410	1.1026	1/38	67.8533	Y=14.0414-.0286(LW)
.640	-.8064	.6503	1.1366	1/38	70.6720	Y=14.1591-.0300(LW)
.645	-.8349	.6971	1.0946	1/38	87.4391	Y=14.5320-.0322(LW)

Table D-5 - cont.

Wave-Length (μm)	r Value	r^2 Value	Standard Error of Estimate	Degrees of Freedom	F Ratio	Regression Equation (y = b + mx)
.650	-.8146	.6635	1.1187	1/38	74.9393	Y=14.2853-.0304(LW)
.655	-.8474	.7180	1.0644	1/38	96.7631	Y=14.5486-.0329(LW)
.660	-.8292	.6876	1.2755	1/38	83.6530	Y=15.0321-.0367(LW)
.665	-.8440	.7123	1.2747	1/38	94.0855	Y=15.3200-.0389(LW)
.670	-.8485	.7200	1.3216	1/38	97.7295	Y=15.7068-.0411(LW)
.675	-.8617	.7425	1.3043	1/38	109.5569	Y=15.8371-.0429(LW)
.680	-.8312	.6908	1.5068	1/38	84.9040	Y=15.9472-.0437(LW)
.685	-.7785	.6061	1.6079	1/38	58.4775	Y=15.4348-.0387(LW)
.690	-.7278	.5296	1.6647	1/38	42.7886	Y=15.3609-.0342(LW)
.695	-.7344	.5394	1.6556	1/38	44.4983	Y=16.1170-.0347(LW)
.700	-.5733	.3286	2.0141	1/38	18.6017	Y=16.5968-.0273(LW)
.705	-.4718	.2226	2.0886	1/38	10.8818	Y=16.5914-.0217(LW)
.710	-.4105	.1685	1.9995	1/38	7.7015	Y=16.9211-.0174(LW)
.715	-.3265	.1066	1.7704	1/38	4.5349	Y=17.2401-.0119(LW)
.720	-.1372	.0188	1.7293	1/38	.7294	Y=17.6279-.0046(LW)
.725	.1127	.0127	1.4965	1/38	.4891	Y=17.1613+.0033(LW)
.730	.2287	.0523	1.7142	1/38	2.0979	Y=17.8255+.0078(LW)
.735	.4861	.2363	1.6526	1/38	11.7561	Y=17.6604+.0178(LW)
.740	.6994	.4892	1.6508	1/38	36.3928	Y=17.1114+.0313(LW)
.745	.7163	.5131	1.7828	1/38	40.0392	Y=17.0971+.0355(LW)
.750	.7875	.6202	1.6380	1/38	62.0599	Y=16.8179+.0406(LW)
.755	.7919	.6270	1.7718	1/38	63.8898	Y=16.5578+.0445(LW)
.760	.8436	.7116	1.7632	1/38	93.7762	Y=16.0832+.0537(LW)
.765	.8811	.7763	1.6093	1/38	131.8821	Y=16.0349+.0581(LW)
.770	.8722	.7607	1.6560	1/38	120.8263	Y=15.9889+.0572(LW)
.775	.8535	.7285	1.6440	1/38	101.9702	Y=16.4428+.0522(LW)
.780	.7575	.5738	1.9465	1/38	51.1629	Y=17.3377+.0438(LW)
.785	.7631	.5823	1.7600	1/38	52.9758	Y=17.7138+.0403(LW)
.790	.7359	.5415	1.7697	1/38	44.8818	Y=18.2583+.0373(LW)
.795	.6510	.4238	2.1206	1/38	27.9540	Y=18.6479+.0352(LW)
.800	.6700	.4490	2.0990	1/38	30.9600	Y=18.7048+.0367(LW)

Total chlorophyll

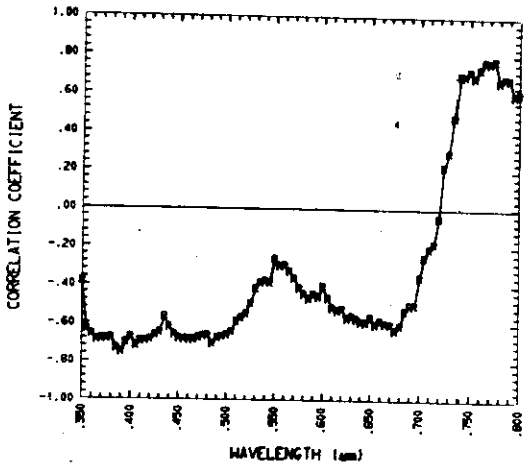

(a) Spectrocorrelation curve

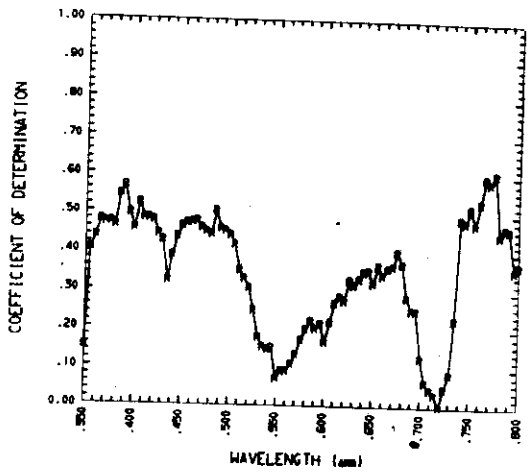

(b) r^2 versus wavelength

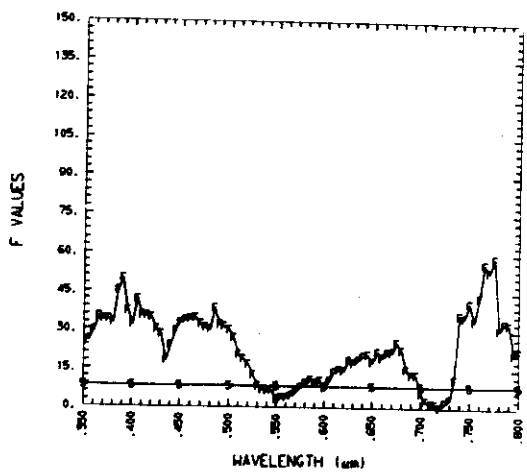

(c) F value versus wavelength

Figure D-11. STATISTICAL COEFFICIENTS OF THE SIMPLE LINEAR REGRESSION FOR TOTAL CHLOROPHYLL (CHL) VERSUS REFLECTANCE AT EACH WAVELENGTH. The linear regressions were formed for the total chlorophyll present on 40 of 1/4 meter squared plots of blue grama (*B. gracilis*) and the reflectance of the plot at 91 wavelengths between .350 and .800 µm. The tabular values of these coefficients can be found in Table D-6. (a) The correlation coefficient (r) versus wavelength or the spectrocorrelation curve. (b) The coefficient of determination (r^2) versus wavelength. (c) The F value versus wavelength where the horizontal line shown by -5- represents the .5% level of significance for 1/38 degrees of freedom.

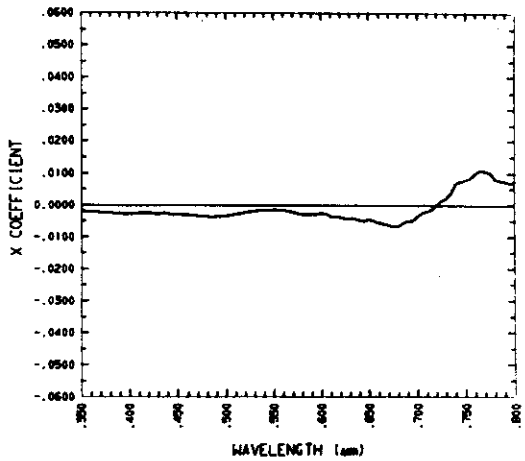

(a) Slope versus wavelength

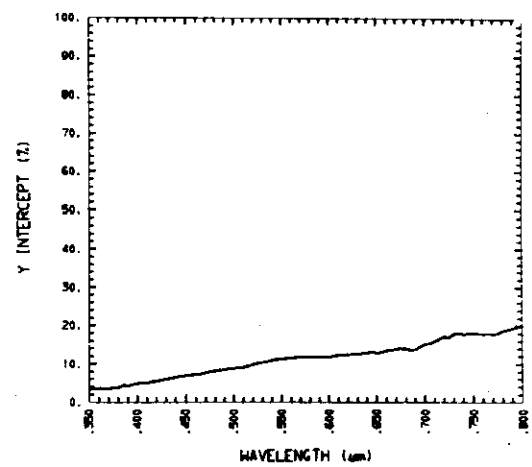

(b) Intercept versus wavelength (soil spectroreflectance)

Figure D-12. THE SLOPE AND THE INTERCEPT OF THE SIMPLE LINEAR REGRESSION FOR TOTAL CHLOROPHYLL (CHL) VERSUS REFLECTANCE AT EACH WAVELENGTH. The linear regressions were formed for the total chlorophyll present on 40 of 1/4 meter squared plots of blue grama (*B. gracilis*) and the reflectance between .350 and .800 µm. Each regression equation at each wavelength yields a slope and intercept value which occur in Table D-6. (a) The plot of the slope at each wavelength which represents the rate of change in the reflectance of the plot with wavelength. (b) The plot of the "y" intercept of the straight line which represents the reflectance of the plot when the total chlorophyll value is zero. Plotted against wavelength it represents the spectroreflectance of the underlying, unexposed soil surface.

Table D-6. SIMPLE LINEAR REGRESSION BETWEEN CANOPY REFLECTANCE AND TOTAL CHLOROPHYLL (CHL). The coefficients and equation resulting from these computations are shown for each available wavelength. The sample set in each case consisted of 40 of 1/4 square meter plots of blue grama (B. gracilis). Plots of r, r^2, F, Y, and m values versus wavelength occur in Figures D-11 and D-12.

Wave-Length (μm)	r Value	r^2 Value	Standard Error of Estimate	Degrees of Freedom	F Ratio	Regression Equation (y = b + mx)
.350	-.3861	.1491	.8742	1/38	6.6575	Y= 3.4467-.0015(CHL)
.355	-.6347	.4028	.6072	1/38	25.6332	Y= 3.6043-.0021(CHL)
.360	-.6603	.4360	.6010	1/38	29.3734	Y= 3.5454-.0022(CHL)
.365	-.6913	.4779	.5689	1/38	34.7821	Y= 3.5475-.0022(CHL)
.370	-.6872	.4723	.5933	1/38	34.0045	Y= 3.5952-.0023(CHL)
.375	-.6865	.4712	.5975	1/38	33.8633	Y= 3.6541-.0023(CHL)
.380	-.6802	.4627	.6105	1/38	32.7255	Y= 3.7356-.0023(CHL)
.385	-.7367	.5428	.5907	1/38	45.1128	Y= 4.3935-.0026(CHL)
.390	-.7530	.5671	.5397	1/38	49.7711	Y= 4.3232-.0025(CHL)
.395	-.7035	.4949	.6854	1/38	37.2346	Y= 4.6007-.0028(CHL)
.400	-.6748	.4553	.7013	1/38	31.7647	Y= 4.8306-.0026(CHL)
.405	-.7228	.5224	.6184	1/38	41.5699	Y= 4.9968-.0027(CHL)
.410	-.6955	.4837	.6234	1/38	35.6060	Y= 5.0703-.0025(CHL)
.415	-.6943	.4820	.6346	1/38	35.3595	Y= 5.2939-.0025(CHL)
.420	-.6911	.4776	.6454	1/38	34.7349	Y= 5.4714-.0025(CHL)
.425	-.6652	.4426	.7100	1/38	30.1680	Y= 5.7288-.0026(CHL)
.430	-.6527	.4260	.7830	1/38	28.2000	Y= 6.0320-.0028(CHL)
.435	-.5682	.3228	.8962	1/38	18.1171	Y= 6.2005-.0025(CHL)
.440	-.6221	.3870	.8235	1/38	23.9899	Y= 6.4756-.0027(CHL)
.445	-.6598	.4354	.8305	1/38	29.3019	Y= 6.7474-.0030(CHL)
.450	-.6803	.4628	.7720	1/38	32.7387	Y= 6.8714-.0029(CHL)
.455	-.6861	.4707	.7750	1/38	33.7905	Y= 7.0312-.0030(CHL)
.460	-.6881	.4735	.8039	1/38	34.1774	Y= 7.2202-.0031(CHL)
.465	-.6911	.4777	.8076	1/38	34.7519	Y= 7.4039-.0032(CHL)
.470	-.6777	.4593	.8616	1/38	32.2817	Y= 7.6005-.0033(CHL)
.475	-.6705	.4495	.9316	1/38	31.0322	Y= 7.8770-.0035(CHL)
.480	-.6652	.4425	.9517	1/38	30.1630	Y= 8.0958-.0035(CHL)
.485	-.7098	.5038	.9410	1/38	38.5848	Y= 8.4329-.0039(CHL)
.490	-.6767	.4579	.9452	1/38	32.0927	Y= 8.4746-.0036(CHL)
.495	-.6724	.4522	.9396	1/38	31.3670	Y= 8.5946-.0035(CHL)

Table D-6 - cont.

Wave-Length (μm)	r Value	r^2 Value	Standard Error of Estimate	Degrees of Freedom	F Ratio	Regression Equation (y = b + mx)
.500	-.6640	.4408	.9291	1/38	29.9592	Y= 8.7665-.0034(CHL)
.505	-.6450	.4160	.9312	1/38	27.0678	Y= 8.9620-.0032(CHL)
.510	-.5917	.3501	.9329	1/38	20.4675	Y= 9.1642-.0028(CHL)
.515	-.5732	.3285	.9089	1/38	18.5926	Y= 9.4446-.0026(CHL)
.520	-.5530	.3058	.8819	1/38	16.7386	Y= 9.8124-.0024(CHL)
.525	-.4977	.2477	.8908	1/38	12.5133	Y=10.1050-.0021(CHL)
.530	-.4205	.1768	.9776	1/38	8.1610	Y=10.3443-.0019(CHL)
.535	-.3896	.1518	.9852	1/38	6.8006	Y=10.6167-.0017(CHL)
.540	-.3801	.1445	1.0040	1/38	6.4172	Y=10.8734-.0017(CHL)
.545	-.3878	.1504	1.0419	1/38	6.7248	Y=11.1371-.0018(CHL)
.550	-.2658	.0706	1.2521	1/38	2.8888	Y=11.2887-.0014(CHL)
.555	-.3015	.0909	1.2245	1/38	3.7998	Y=11.4336-.0016(CHL)
.560	-.2995	.0897	1.2801	1/38	3.7433	Y=11.5552-.0017(CHL)
.565	-.3295	.1086	1.3153	1/38	4.6274	Y=11.6307-.0019(CHL)
.570	-.3361	.1340	1.3564	1/38	5.8818	Y=11.7164-.0022(CHL)
.575	-.4145	.1718	1.3656	1/38	7.8839	Y=11.8198-.0026(CHL)
.580	-.4467	.1995	1.3861	1/38	9.4708	Y=11.8969-.0028(CHL)
.585	-.4695	.2204	1.2879	1/38	10.7442	Y=11.8822-.0028(CHL)
.590	-.4479	.2007	1.3359	1/38	9.5391	Y=11.9318- 0028(CHL)
.595	-.4626	.2140	1.3263	1/38	10.3459	Y=11.9373-.0028(CHL)
.600	-.4069	.1656	1.3629	1/38	7.5412	Y=11.9322-.0025(CHL)
.605	-.4665	.2176	1.3381	1/38	10.5685	Y=12.0817-.0029(CHL)
.610	-.5174	.2677	1.4077	1/38	13.8917	Y=12.2484-.0035(CHL)
.615	-.5328	.2839	1.4183	1/38	15.0635	Y=12.3599-.0037(CHL)
.620	-.5223	.2728	1.4757	1/38	14.2545	Y=12.4423-.0037(CHL)
.625	-.5718	.3269	1.4791	1/38	18.4591	Y=12.6483-.0042(CHL)
.630	-.5610	.3148	1.4750	1/38	17.4544	Y=12.6604-.0041(CHL)
.635	-.5742	.3298	1.5066	1/38	18.6956	Y=12.8001-.0043(CHL)
.640	-.5900	.3481	1.5520	1/38	20.2882	Y=12.8828-.0047(CHL)
.645	-.5938	.3526	1.6001	1/38	20.6997	Y=13.1199-.0049(CHL)

Table D-6 - cont.

Wave-Length (μm)	r Value	r^2 Value	Standard Error of Estimate	Degrees of Freedom	F Ratio	Regression Equation (y = b + mx)
.650	-.5656	.3199	1.5905	1/38	17.8742	Y=12.9138-.0045(CHL)
.655	-.6038	.3646	1.5978	1/38	21.8034	Y=13.1071-.0050(CHL)
.660	-.5838	.3409	1.8528	1/38	19.6510	Y=13.4045-.0055(CHL)
.665	-.5986	.3583	1.9037	1/38	21.2204	Y=13.6089-.0059(CHL)
.670	-.6031	.3637	1.9924	1/38	21.7193	Y=13.9028-.0062(CHL)
.675	-.6335	.4013	1.9887	1/38	25.4727	Y=14.0242-.0067(CHL)
.680	-.6089	.3707	2.1497	1/38	22.3853	Y=14.0956-.0068(CHL)
.685	-.5328	.2838	2.1682	1/38	15.0597	Y=13.6668-.0056(CHL)
.690	-.5021	.2521	2.0992	1/38	12.8097	Y=13.8084-.0050(CHL)
.695	-.5017	.2517	2.1102	1/38	12.7828	Y=14.5263-.0050(CHL)
.700	-.3570	.1275	2.2961	1/38	5.5516	Y=15.2324-.0036(CHL)
.705	-.2558	.0654	2.2901	1/38	2.6603	Y=15.3891-.0025(CHL)
.710	-.2125	.0452	2.1426	1/38	1.7979	Y=15.9236-.0019(CHL)
.715	-.1807	.0327	1.8422	1/38	1.2833	Y=16.5915-.0014(CHL)
.720	-.0473	.0022	1.7439	1/38	.0851	Y=17.3071-.0003(CHL)
.725	.2205	.0486	1.4690	1/38	1.9425	Y=17.0276+.0014(CHL)
.730	.2932	.0860	1.6835	1/38	3.5752	Y=17.8671+.0021(CHL)
.735	.4784	.2288	1.6607	1/38	11.2760	Y=18.1174+.0037(CHL)
.740	.6994	.4892	1.6509	1/38	36.3872	Y=17.8808+.0067(CHL)
.745	.6936	.4811	1.8405	1/38	35.2297	Y=18.0450+.0073(CHL)
.750	.7203	.5189	1.8436	1/38	40.9848	Y=18.0506+.0079(CHL)
.755	.6887	.4743	2.1035	1/38	34.2867	Y=18.0472+.0083(CHL)
.760	.7305	.5337	2.2423	1/38	43.4851	Y=17.8926+.0099(CHL)
.765	.7730	.5975	2.1588	1/38	56.4069	Y=17.9486+.0109(CHL)
.770	.7644	.5843	2.1830	1/38	53.4013	Y=17.8774+.0107(CHL)
.775	.7793	.6074	1.9771	1/38	58.7799	Y=18.0345+.0102(CHL)
.780	.6683	.4467	2.2179	1/38	30.6752	Y=18.7645+.0082(CHL)
.785	.6834	.4670	1.9880	1/38	33.3006	Y=18.9900+.0077(CHL)
.790	.6805	.4631	1.9151	1/38	32.7767	Y=19.3652+.0074(CHL)
.795	.5977	.3572	2.2398	1/38	21.1180	Y=19.7108+.0069(CHL)
.800	.6074	.3690	2.2462	1/38	22.2182	Y=19.8409+.0071(CHL)

APPENDIX E

APPENDIX E

Selected Bibliography on Remote Sensing of Grasslands

The following computer generated bibliography has been included for use by persons interested in the broad scientific application of remote sensing to grasslands. The bibliography is broken down into four main sections: (1) Solar irradiance as it relates to productivity of vegetated surfaces; (2) Biological factors affecting the application of remote sensing to the measurement of vegetated surfaces; (3) Techniques for measuring and modeling the primary productivity of grasslands; and (4) Applications of remote sensing to grassland research and management.

The bibliography was generated from the REmote SEnsing of NAture Technical Document Library (RESEÑA) developed, organized, and maintained by Professor L. D. Miller. RESEÑA uses a computerized information storage and retrieval system which permits storage of large amounts of coded reference material in such a fashion that the system can be interrogated and manipulated from an interactive computer terminal. Typical user interaction produces a terminal character display or a printout of a set of citations in the American Institute of Biological Science Style Manual form which corresponds to either authors, titles, subjects and/or sources which have been input by the user at his remote terminal or through a search data card deck input by a batch mode method.

Computer assistance is required for general manipulation and searching of the RESEÑA data base due to the over 9000 library document citations currently cataloged in the library. Approximately one-half of the listed citations are contained in a microfilm format by the Colorado State University Libraries and a portion of the remaining half are available in the original publication contained in the CSU library.

The following sections are contained in appendix E.

Solar Irradiance as it Relates to Productivity of Vegetated Surfaces

Solar radiation and its distribution, attenuation, and exchange at a vegetative canopy are referenced in this section. Primary emphasis in the selection of these references was placed upon those dealing with energy exchange with vegetative materials and factors which cause variation in this exchange such as atmospheric conditions, solar angle, and time of the year.

Alderfer, R. G. and D. M. Gates. 1971. Energy exchange in plant canopies. Ecol. 52(5):855-861.

Allen, W. A. and A. J. Richardson. 1968. Interaction of light with a plant canopy. J. Opt. Soc. Am. 158(8):1023-1028.

Allen, W., T. Gayle and A. Richardson. 1970. Plant-canopy irradiance specified by the Duntley equations. J. Opt. Soc. Am. 60(3):372-376.

Anderson, M. C. and O. T. Denmead. 1969. Short-wave radiation on inclined surfaces in model plant communities. Agron. J. 61(6):867-872.

Anderson, M. C. 1970. Interpreting the fraction of solar radiation available in forest. Agr. Meteorol., 7(1):19-28.

Bartman, F. L., 1967. The reflectance and scattering of solar radiation by the earth. Univ. Mich., High Altitudes Eng. Lab., Feb. 284 p.

Bell, E. E., L. Eisner, J. Young and R. A. Oetjen. 1960. Spectral radiance of sky and terrain at wavelengths between 1 and 20 microns. II. Sky Measurements. J. Opt. Soc. Am. 50(12): 1313-1320.

Bemporad. A. 1907. Search for a new empirical formula for the representation of the variation of the intensity of solar radiation with zenith angle. Meteorologisch Zeitschrift. 24, July.

Bener, P. 1962. Comparison of measured and theoretical values of the spectral intensity of ultraviolet sky radiation. USDC, OTS, Defense Doc. Cnt., Sept.

Bener, P. 1963. The diurnal and annual variations of the spectral intensity of ultraviolet sky and global radiation on cloudless days at Davos. 1590 M.A.S.L. USDC. OTS. Defense Doc. Cnt., Contract AF 61 (052) 618.

Bener, P. 1969. Spectral intensity of natural ultraviolet radiation and its dependence on various parameters. Biol. Effects of Ultraviolet Radiat. Pergamon Press, N.Y., N.Y. p. 351-358.

Cialdea, R. and S. Sciaratta. 1968. The absorption of solar radiation by the earth. Geophy. Ann., 21:155-171.

Condit, H. R. and F. Grum. 1964. Spectral energy distribution of daylight. J. Opt. Soc. Am., 54(7):937-944.

Combe, D. E. 1957. The spectral composition of shade light in woodlands. J. Ecol., 45:823-830.

Cowan, I. R. 1968. The interception and absorption of radiation in plant stands. J. Appl. Ecol. 5(2):367-379.

DeBruin, J. P. 1961. Principles of ultraviolet light and some of its applications in photography. J. Biol. Photo. Assoc. 29(2):53-63.

DeSloover, J. and T. Marynen. 1963. An ecological measure of the amount of light and radiation. Compt. Rend. 257(18):2707-2710.

Denmead, O. T., L. J. Fritschen and R. H. Shaw. 1962. Spatial distribution of net radiation in a corn field. Agron. J. 54(6):505-510.

DeWitt, C. 1965. Agr. Res. Rep. 663. Inst. Biol. Chem. Res. on Field Crops and Herbage. Wageningen, Netherlands.

Doraiswamy, P. C. 1971. Energy balance and spectral properties of a reflectorized soybean canopy. Univ. Nebraska. Dept. Hort. and For., Hort. Progress Rep. 88, Lincoln, Nebraska. 189 p.

Dunkelman, L. and R. Scolnik. 1959. Solar spectral irradiance and vertical atmospheric attenuation in the visible and ultraviolet. J. Opt. Soc. Am. 49(4).

Egbert, D. and F. Ulaby. 1972. Effect of angles on reflectivity. Photogrammetric Engineering 38(6):556-564.

Eisner, L., E. E. Bell and J. Young. 1962. Spectral radiance of sky and terrain at wavelengths between 1 and 20 micron. III. Terrain Measurements. J. Opt. Soc. Am. 52(2):201-209.

Ekern, P. C. 1965. Fraction of sunlight retained as net radiation in Hawaii. J. Geophy. Res. 70(4).

Evans, G. C. 1969. The spectral composition of light in the field. J. Ecol. 57(1):109-125.

Federer, C. A. and C. B. Tanner. 1966. Spectral distribution of light in the forest. Ecol. 47:555-561.

Federer, C. A. 1968. Spatial variation of net radiation. Albedo and Surface Temperature of Forests. J. Appl. Meteorol. 7:789-795.

Federer, C. A. 1972. Solar radiation absorption by leafless hardwood forests. Agr. Meteorol. 9(1-2):3-20.

Filippov, V. L. and S. O. Minuntants. 1970. The variation of the spectral coefficients of radiation attenuation by hazes in the spectral region of .59 to 13 microns. Izvestiya. Atmos. and Oceanic Phys. No. 6. 4 p.

Freyman, S. 1968. Spectral distribution of light in forests of the Douglas fir zone of southern British Columbia, Can. J. Plant Sci. 48(3):326-328.

Friis-Nielson, B. 1966. Active leaf area index: a meteorological-plant physiological parameter for photosynthetic production. 1. Under conditions of optimal water supplies. Kgl. Ve. Lando Rohoejskole Arsskr. 49-60.

Fritschen, L. J. 1967. Net and solar radiation relations over irrigated field crops. Agr. Meteorol. 4:55-62.

Garnier, B. J. and A. Osmura. 1970. The evaluation of surface variations in solar radiation income. Solar Energy 13(1): 21-34.

Gates, D. M. 1962. Energy exchange in the biosphere. Harper and Row Biol. Monogr., N.Y.

Gates, D. M. 1963. Energy environment in which we live. Am. Sci. J., Oct.

Gates, D. M. 1966. Spectral distribution of solar radiation at the earth's surface. Sci., 152, Feb. 4.

Gates, D. M. 1968. Energy exchange in the biosphere. Nat. Res. Rev. 5:33-43.

Gay, L. W., K. R. Knoerr and M. O. Braaten. 1971. Solar radiation variability on the floor of a pine plantation. Agr. Meteorol. 8(1):39-50.

Grasovsky, A. 1929. Some aspects of light in the forest. Yale Univ. School For. Bull. No. 23. 53 p.

Green, A. E. S. 1964. Attenuation by ozone and the earth's albedo in the middle ultraviolet. Appl. Opt. 3(2)

Hennes, J. 1965. The ultraviolet solar spectrum and the earth's reflectivity. Proc. of the sym. on electromagnetic sensing of the earth from satellites. Polytechnic Press, Polytechnic Inst. of Brooklyn, Brooklyn, N.Y. 6 p.

Hennes, J. P., W. P. Fowler and L. Dunkelman. 1964. Middle ultraviolet day radiance of the atmosphere. J. Geophy. Res. 69(13).

Ho, P., P. Schwerdtfeger and G. Weller. 1968. The energy exchange within a vegetation layer. Arch. Meteorol. Geophy. Bioklimatol., Ser. B. 16(2-3):262-271.

Howard, J. N. 1959. The transmission of the atmosphere. Proc. of the IRE 47(9):1451-1457.

Hulburt, E. O. 1935. Attenuation of light in the lower atmosphere. J. Opt. Soc. Am. 25:125-130.

Hutchinson, B. A. 1971. Spatial and temporal variation in the distribution and partitioning of solar energy in a deciduous forest ecosystem. IBP. E. Deciduous For. Biome, Memo Rep. 71-82, Oak Ridge, Tenn. 40 p.

Idso, S. and C. Dewitt. 1971. Light relations in plant canopies. App. Opt. 9(1):177.

Impens, I. and R. Lemeur. 1969. The radiation balance of several field crops. Arch. Meteorol. Geophy. Bioklimatol. Ser. B. 17:261-168.

Impens, I., R. Lemeur and R. Moermans. 1970. Spatial and temporal variation of net radiation in crop canopies. Agr. Meteorol. 7(4):335-338.

Izotov, V. F. 1969. The penetration of solar radiation below the canopy (In Russian). Lesn. Zh. Archangel-Sk 12(4):20-23.

Kalma, J. D. and R. Badham. 1972. The radiation balance of a tropical pasture. I. The reflection of short-wave radiation. Agri. Meteorol. 10(4-5):251-259.

Kalma, J. D. 1972. The radiation balance of a tropical pasture. II. Net all-wave radiation. Agri. Meteorol. 10(4-5):261-275.

Kimball, P. P. 1928. The distribution of energy in the visible spectrum of sunlight, skylight, and total daylight. Proc. Internat. Congr. Illumination. p. 501-505.

Kubelka, P. and F. Munk. 1931. Ein Beitrag zur Optik der Farbanstriche. Z. Techn. Physic 12:593-601.

Lambert, C. J. 1970. Thermal response of a plant canopy to drifting cloud shadows. Ecol. 51(1):143-149.

Lemon, E., D. W. Stewart and R. W. Shawcroft. 1971. The sun's work in a cornfield. Sci 174(4007):371-378.

Lemon, E. R. and K. W. Brown. 1964. The energy budget at the earth's surface (Vertical fluxes within the vegetative canopy of a corn field). Cornell Univ., Aug.

Linacre, E. T. 1969. Net radiation to various surfaces. J. Appl. Ecol. 6(1):61-73.

Liu, B. Y. H. and R. C. Jordan. 1960. Interrelationship and characteristic distribution of direct, diffuse and total solar radiation. Solar Energy 4(3).

Lopukhin, Y. A. 1965. The spectral constitution of direct sunlight. Heliotechnology. 21 Dec. 1965. p. 40-44.

McCullough, E. C. and W. P. Porter. 1972. Computing clear day solar radiation spectra for the terrestrial ecological environment. Ecol. 52(6):1008-1015.

McPherson, H. G. 1969. Photo-cell filter combinations for measuring photosynthetically active radiation. Agr. Meteorol. 6(5): 347-356.

Miller, P. C. 1970. Tests of solar radiation models in three forest canopies. Ecol. 50(5):878-885.

Milthorpe, F. L. 1970. From the qualitative to the quantitative, with special reference ot the use of light by crops. Aust. J. Sci. 32(9):345-349.

Moon, P. 1940. Proposed standard solar-radiation curves for engineering use. J. Franklin Inst. 230(5):583-618.

Morowitz, H. J. 1968. Energy flow in biology. Academic Press, N.Y. 179 p.

Nilson, T. 1971. A theoretical analysis of the frequency of gaps in plant stands. Agri. Meteorol. 8:25-38.

Norman, J. M. and C. B. Tanner. 1969. Transient light measurements in plant canopies. Agron. J. 61(6):847-849.

Oetjen, R. A., E. E. Bell, J. Young and L. Eisner. 1960. Spectral radiance of sky and terrain at wavelengths between 1 and 20 microns. I. Instrumentation. J. Opt. Soc. Am. 50(12):1308-1313.

Parmelee, G. V. 1954. Irradiation of vertical and horizontal surfaces by diffuse solar radiation from cloudless skies. Heating, Piping, Air Conditioning. p. 129-137, Aug.

Rawcliffe. 1965. The ultraviolet earth background. Proc. of the sym. on electromagnetic sensing of the earth from satellites. Polytechnic Press, Polytechnic Inst. of Brooklyn, Brooklyn, N.Y. 17 p.

Reifsnyder, W. E. and H. W. Lull. 1965. Radiant energy in relation to forests. USDA For. Serv., Tech. Bull. No. 1344. Dec.

Reifsnyder, W. E., G. M. Furnival and J. L. Horowitz. 1972. Spatial and temporal distribution of solar radiation beneath forest canopies. Agr. Meteorol. 9(1-2):21-37.

Robertson, G. W. 1966. The light composition of solar and sky spectra available to plants. Ecol. 47:640-644.

Rose, C. W., J. E. Begg, G. F. Byrne, J. H. Gonoz and B. W. R. Torsell. 1972. Energy exchanges between a pasture and the atmosphere under steady and non-steady-state conditions. Agr. Meteorol. 9(5-6):385-403.

Schulze, R. and K. Grafe. 1969. Consideration of sky ultraviolet radiation in the measurement of solar ultraviolet radiation. Biol. Effects of Ultraviolet Radiation. Pergamon Press, N.Y., N.Y. p. 359-373.

Shirley, R. L. 1935. Light as an ecological factor and its measurement. Bot. Rev. 1:355-381.

Smith. J. A. and R. Oliver. 1972. Plant canopy models for simulating composite scene spectroradiance in the .4 to 1.05 μm region. Proc. of the Eighth Intern. Sym. on Remote Sensing of the Env., Univ. of Mich., Willow Run Labs., Ann Arbor. 21 p.

Suits, G. 1972. The calculation of the directional reflectance of a vegetative canopy. Remote Sensing of Environment 2:117-125.

Suits, G. H., G. Safir and A. Ellingbor. 1972. Prediction of directional reflectance of a corn field under stress. Fourth annual earth resources program review. NASA, Manned Spacecraft Cnt., Houston, Texas. 11 p.

Tanner, C. B., A. E. Peterson and J. R. Love. 1960. Radiant energy exchange in a corn field. Agron. J. 52:373-379.

Tanner, C. B. and A. E. Peterson. 1960. Light transmission through corn to interseeded alfalfa. Agron. J. 52:487-489.

Uchijama, Z. 1968. A newly devised solarimeter for measuring photosynthetically active radiation. Japan Agr. Res. 3(3): 20-22.

Utaaker, K. 1966. A study of the energy exchange at the earth's surface. Abok Univ. Bergen. Math. Nat. Ser. 199)1):37.

Vezina, P. E. and D. W. K. Boulter. 1966. The spectral composition of near ultraviolet and visible radiation beneath forest canopies. Can J. Bot. 1966(44):1267-1270.

Warren Wilson, J. 1967. Stand structure and light penetration. III. Sunlit foliage area. J. Appl. Ecol. 4:159-165.

Williams, C. N. 1967. A simple foliage model for studying light penetration. Ann. Bot. (London) 31:783-790.

Wright, J. L. and E. R. Lemon. 1962. Energy budget at the earth's surface--estimation of turbulent exchange within a corn crop at Ellis Hollow (Ithaca, N.Y.) 1961. Cornell Univ., N.Y. State Coll. Agr. July.

Yao, A. Y. M. and R. H. Shaw. 1964. Effect of plant population and planting pattern of corn on the distribution of net radiation. Agron J. 56(2).

Biological Factors Affecting the Application of Remote Sensing to the Measurement of Vegetated Surface

References dealing with the spectro-optical properties of vegetation were selected for this section of the selected bibliography. Emphasis was placed upon those studies dealing with leaf optical parameters such as pigment properties, pigment composition and concentration, leaf structure and its effect upon scattering, and optical properties of leaf water. Also selected were those which deal with the primary production or photosynthesis of vegetation, models of leaf optical systems, energy budget considerations, and basic physical and biological properties of leaf constituents.

Aboukhaled, A. 1966. Optical properties of leaves in relation to their energy balance, photosynthesis, and water use efficiency. Univ. Calif., Ph.D. thesis. Davis, Calif. 139 p.

Allen, M. B. 1964. Absorption spectra, spectrophotometry, and action spectra. In Photophysiology (1). Academic Press, New York. p. 83-110.

Allen, W. A., A. J. Richardson and H. W. Gausman. 1968. Reflectance produced by a plant leaf. NASA. Earth Res. Aircraft Program--Status rev. 13 p.

Allen, W. A., H. W. Gausman, A. J. Richardson and J. R. Thomas. 1969. Interaction of isotropic light with a compact plant leaf. J. Opt. Soc. Am. 59(10):1376-1379.

Allen, W. A., H. W. Guasman and C. L. Wiegand. 1970. Spectral reflectance of plant canopies. Spectral survey of irrigated region crops and soils. USDA. 1970 Ann. Rep., Weslaco, Texas. 20 p.

Allen, W. A., H. W. Gausman, A. J. Richardson and R. Cardenas. 1970. Water and air changes in grapefruit, corn, and cotton leaves with maturation. Spectral survey of irrigated region crops and soils. USDA. 1970 Ann. Rep., Weslaco, Texas. 11 p.

Allen, W. A., H. W. Gausman and A. J. Richardson. 1970. Mean effective optical constants of cotton leaves. Spectral survey of irrigated region crops and soils. USDA. 1970 Ann. Rep., Weslaco, Texas. 1 p.

Allen, W. A., H. W. Gausman, A. J. Richardson and C. L. Wiegand. 1970. Mean effective optical constants of thirteen kinds of plant leaves. Spectral surveys of irrigated region crops and soils. USDA. 1970 Ann. Rep., Weslaco, Texas. 10 p.

Allen, W. A., H. W. Gausman and A. J. Richardson. 1970. Discrimination among different kinds of plant leaves by spectral reflectance in the near infrared. Spectral survey of irrigated region crops and soils. USDA. 1970 Ann. Rep., Weslaco, Texas. 8 p.

Allen, W. A. 1970. Mean effective optical constants of thirteen kinds of plant leaves. App. Opt. 9:2573-2577.

Allen, W. A. and A. J. Richardson. 1971. A leaf cross section treated as an optical system. Spectral survey of irrigated region crops and soils. USDA. ARS. P. O. Box 267. Weslaco, Texas. 15 p.

Allen, W. A., H. W. Gausman and A. J. Richardson. 1971. Discrimination among different kinds of plant leaves by spectral reflectance in the near infrared. Spectral survey of irrigated region crops and soils . USDA, ARS. P. O. Box 267, Weslaco, Texas. 5 p.

Anderson, M. C. 1967. Photon flux, chlorophyll content and photosynthesis under natural conditions. Ecol. 48:1050-1053.

Arnold, W. and J. R. Oppenheimer. 1950. Internal conversion in the photosynthetic mechanism of blue-green algae. J. Gen. Physiol. 33(4):423-435.

Aston, A. R., R. J. Millington and D. B. Peters. 1969. Radiation exchange in controlling leaf temperature. Agron. J. 61(5): 797-800.

Backstrom, H. and E. Welander. 1953. En undersokning av remissionsformagan has blad och barr av olika tradslag (an investigation of the spectral remission power of leaves and needles of different tree species). Sartryck ur Norrlauds Skovsvardsforbunds Tidskrift. 1:141-169.

Balegh, S. E. and O. Biddulph. 1970. The photosynthetic action spectrum of the bean plant. Plant Physiol. 46:1-5.

Bartholic, J. F. and L. N. Namken. 1971. Canopy temperature as an indicator of plant water stress. Spectral survey of irrigated region crops and soils. USDA, ARS. P. O. Box 267, Weslaco, Texas. 4 p.

Bartholic, J. F., L. N. Namken and C. L. Wiegand. 1971. Temperature of soils and of crop canopies differing in water conditions. Spectral survey of irrigated region crops and soils. USDA, ARS. P. O. Box 267, Weslaco, Texas. 2 p.

Bazzar, F. A. and J. S. Boyer. 1972. A compensating method for measuring carbon dioxide exchange, transpiration, and diffusive resistances of plants under controlled environmental conditions. Ecol. 53(2):343-349.

Belov. S. V. and E. S. Artsybashev. 1957. A study of reflecting properties of arboreal species. Bontanicheskii Zhvr. 42:517-534.

Bement, R. P. 1968. Herbage growth rate and forage quality on shortgrass range. Ph.D. Dissertation. Colorado State Univ., Ft. Collins. 53 p.

Benedict, H. M. and R. Swidler. 1961. Nondestructive method for estimating chlorophyll content of leaves. Sci. p. 2015-2016.

Bennett, H. E. and J. O. Porteus. 1961. Relation between surface roughness and specular reflectance at normal incidence. J. Opt. Soc. Am. 51(2):123-127.

Benninghoff, W. S. 1963. Relationships between vegetation and frost in soils. Purdue Univ., Internat. Conf. Permafrost, Nov. p. 11-15.

Bierhuizen, J. F. and R. O. Slatyer. 1965. Photosynthesis relationships of cotton leaves. Agr. Meteorol. 2(4):259-270.

Biggs, W. W., A. R. Edison, J. D. Easton, K. W. Brown, J. W. Maranville and M. D. Clegg. 1971. Photosynthesis light sensor and meter. Ecol. 52(1):125-131.

Billings, W. D. and R. J. Morris. 1951. Reflection of visible and infrared radiation from leaves of different ecological groups. Am. J. Bot., Vol. 38.

Birkebak, R. 1964. Solar radiation characteristics of tree leaves. Ecol. 45(3):646-649.

Blevin, W. R. and W. J. Brown. 1961. Light-scattering properties of pigment suspensions. J. Opt. Soc. Am. 51(9):975-981.

Botkin, D. B. 1970. Prediction on net photosynthesis of trees from light intensity and temperature. Ecol.50(5):854-858.

Bray, J. R. 1960. The chlorophyll content of some native and managed plant communities in central Minnesota. Canadian J. Bot. 38:313-333.

Brock, T. D. and M. L. Brock. 1967. The measurement of chlorophyll. Primary productivity, photo-phosphorylation, and macromolecules in benthic algal mats. Limnol. and Oceanogr. 12:600-605.

Brock, T. D. and M. L. Brock. 1968. Measurement of steady-state growth rates of a thermophilic alga directly in nature. J. Bact. 95:811-815.

Brougham, R. W. 1960. The relationship between critical leaf area, total chlorophyll content, and maximum growth of some pasture and crop plants. Ann. of Bot. N.S. 24:463-474.

Brown, H. T. and F. Escombe. 1905. Researches on the physiological processes of green leaves with special reference to the interchange of energy between the leaf and its surroundings. Proc. Royal Soc. of Longon, Ser. B. 76:29-111.

Burns, G. R. 1942. Photosynthesis and absorption in blue radiation. Am. J. Bot. 29:381-387.

Butler, W. L. 1961. A Far-red absorbing form of chlorophyll 'In vivo' Arch. of Biochem. and Biophys. 93(2):413-422.

Butler, W. L. and K. H. Norris. 1963. Lifetime of the long-wavelength chlorophyll flourescence. Biochem. Et Biophys. Acta. 66:72-77.

Cardenas, R. and H. W. Gausman. 1971. Light reflectances, chlorophyll assays, and photographic film densities of isogenic barley lines. Spectral survey of irrigated region crops and soils. USDA, ARS. P. O. Box 267, Weslaco, Texas. 5 p.

Coblentz, W. W. and R. Stair. 1929. The infrared absorption spectrum of chlorophyll and xanthophyll. Phys. Rev., II, Vol. 33.

Comar, C. L. and F. P. Zscheile. 1942. Analysis of plant extracts for chlorophylls A and B by a photoelectric spectrophotometric method. Plant Physiol. 17:198-209.

Coulson, K. C., E. L. Gray and G. M. Bouricius. 1965. A study of the reflection and polarization characteristics of selected natural and artificial surfaces. Gen. Electric. Space Sci. Lab., Missile and Space Div., China Lake, Calif., May.

Curcio, J. A. and C. C. Petty. 1951. The near infrared absorption spectrum of liquid water. J. Opt. Soc. Am. 41(5):302-304.

Dadykin, V. D., V. P. Bedenko and A. Davydova, Jr. 1959. The relationship between optical properties of plant leaves and soil fertilizer. Dokl. Akad. Nauk, SSSR, 128(6):1305-1308.

Dadykin, V. P. 1960. Relation of optical properties of plant leaves to soil fertilization. Dokl. Biol. Sci. Sect., Vol. 218.

Dadykin, V. P. and V. P. Bedenka. 1960. Concerning the geographic variability of optical properties in plant leaves. Dokl. Biol. Sci. Sect. 130:6-8.

DeLoor, G. P. and A. A. Jurriens. 1971. The radar backscatter of vegetation. Physics Lab., Waalsdorp, The Hague, The Netherlands. 8 p.

DeWitt, C. T. 1965. Photosynthesis of leaf canopies, Inst. Biol. Chem. Res. on field crops and herbage, Agr. Res. Rep. 663, Wageningen. 57 p.

Devlin, R. M. and A. V. Baker. 1971. Photosynthesis. Van Nostrand Reinhold Company, New York. 304 p.

Denmead. O. T. 1964. Evaporation sources and apparent diffusivities in a forest canopy. J. Appl. Meteorol. 3:383-389.

Dinger, J. E. 1941. Absorption of radiant energy in plants. J. Sci. 16:44-45.

Dorsey, N. E. 1940. Properties of ordinary water-substances in all its phases--water-vapor, water, and all the ices. Am. Chem. Soc., Monog. Ser.

Dwornik, S. E. and D. G. Orr. 1961. Reflectance studies of vegetation damage. U.S. Army Eng. Dev. Lab., Tech. Sum. Rept. 1, Oct. 5, 1960 - March 15, 1961, Ft. Belvoir, Va.

Dye, A. J. 1972. Carbon dioxide exchange of blue grama swords in the field. Ph.D. dissertation, Colorado State University, Ft. Collins. 54 p.

Dye, A. J., L. F. Brown and M. J. Trlica. 1972. Carbon dioxide exchange of blue grama as influenced by several ecological parameters, 1971. U.S. IBP Grassland Biome Tech. Rep. No. 181. Colorado State Univ., Ft. Collins. 44 p.

Dye, A. J. and W. H. Moir. 1971. CO-2 exchange over shortgrass sods. IBP grassland biome, NREL. Tech. Rep. No. 81, Ft. Collins, Colo. 13 p.

Eglinton, G. 1962. Hydrocarbon constituents of the wax coatings of plant leaves--a taxonomic survey. Phytochemistry, Pergamon Press Ltd., England. 1:89-102.

Eik, K. and J. J. Hanway. Some factors affecting development and longevity of leaves of corn. Agron. J.

Esau, K. 1965. Plant Anatomy. John Wiley and Sons, New York. 767 p.

Escobar, D. E., R. R. Rodriguez and H. W. Gausman. 1971. Light reflectance, transmittance, and absorptance of nutrient sufficient and deficient squash leaves. Spectral survey of irrigated region crops and soils. USDA, ARS, P. O. Box 267, Weslaco, Texas. 5 p.

Finley, V. P. 1960. Photo interpretation of vegetation-literature and analysis. U.S. Army Corps of Eng., Snow, ice and permafrost res. EST., Tech. Rep. No. 69, Willmette, Ill., July.

Fuchs, M. and C. B. Tanner. 1966. Infrared thermometry of vegetation. Agron. J., 58:597-601.

Gates, D. M. and W. Tantraporm. 1952. Reflectivity of deciduous trees and herbaceous plants in the infrared to 25 microns. Sci. 115:613-616.

Gates, D. M. 1965. Energy, plants and ecology. Ecol. 46(1-2): 1-13.

Gates, D. M. 1965. Characteristics of soil and vegetated surfaces to reflected and emitted radiation. Proceedings of the third symposium on remote sensing of environment. Univ. Mich., cnt. for remote sensing info. and analysis, Ann Arbor, Mich. p. 573-600.

Gates, D. M., H. J. Keegan, J. C. Schleter and V. R. Weidner. 1965. Spectral properties of plants. Appl. Opt. 4(1):11-20.

Gausman, H. W., R. Cardenas, W. A. Allen and R. W. Leamer. 1968. Reflectance and structure of cycocel-treated cotton leaves. NASA, Earth Res. Aircraft Program - Status Rev. 9 p.

Gausman, H. W., W. A. Allen and R. Cardenas. 1969. Reflectance of cotton leaves and their structure. RSE 1(1):19-22.

Gausman, H. W., W. A. Allen, R. Cardenas and A. J. Richardson. 1969. Relation of light reflectance to cotton leaf maturity. Proceedings of the sixth symposium on remote sensing of environment. Univ. Mich. Cnt. for remote sensing info. and analysis, Ann Arbor, Mich. p. 1123-1141.

Gausman, H. W., W. A. Allen, R. Cardenas and M. Schupp. 1969. The influence of cycocel treatment of cotton plants and foot rot disease of grapefruit trees of leaf spectra in relation to aerial photographs with infrared color film. Proc. workshop on aerial color photo. In Plant Sci. Univ. Fla., Gainesville, Fla. p. 16-24.

Gausman, H. W., W. A. Allen, R. Cardenas and A. J. Richardson. 1970. Effects of leaf nodal position on absorption and scattering coefficients and infinite reflectance of cotton leaves. *Gossypium hirsutum* L. Spectral Survey of Irrigated Region Crops and Soils. USDA, 1970 Ann. Rep., Weslaco, Texas. 6 p.

Gausman, H. W., P. S. Bauer, Jr., M. P. Porterfield and R. Cardenas. 1970. Effects of salt treatments on cotton plants on leaf mesophyll, cell microstructure, and light transmittance of mitochondrial suspensions. Spectral survey of irrigated region crops and soils. USDA. 1970 Ann. Rep., Weslaco, Texas. 13 p.

Gausman, H. W., W. A. Allen, M. Schupp, C. L. Wiegand, D. E. Escobar and R. R. Ridriquez. 1970. Reflectance, transmittance, and absorptance of light of leaves for eleven plant genera with different leaf mesophyll arrangements. Spectral survey of irrigated region crops and soils. USDA. 1970 Ann. Rep., Weslaco, Texas. 22 p.

Gausman, H. W., W. A. Allen, D. E. Escobar, R. R. Rodriquez and R. Cardenas. 1970. Age effects of growth chamber-greenhouse-, and field-grown cotton leaves on light reflectance, transmittance, and absorptance and on water content and thickness. Spectral survey of irrigated region crops and soils. USDA Ann. Rep., Weslaco, Texas. 7 p.

Gausman, H. W., W. A. Allen, C. L. Wieband, D. E. Excobar and R. R. Rodriquez. 1971. Leaf light reflectance, transmittance, absorptance, and optical leaf mesophyll arrangements. Proc. of 7th internat. symp. of RSE. Vol. III. Univ. Mich. WRL. Infrared and Opt. Sensor Lab. CRSIA. Ann Arbor, Mich. p. 1599-1625.

Gausman, H. W., W. A. Allen, C. L. Wiegand, D. E. Escobar, R. R. Rodriquez and A. J. Richardson. 1971. The leaf mesophylls of twenty crops, their light spectra, and optical and geometrical parameters. Spectral survey of irrigated region crops and soils. USDA, ARS. P. O. Box 267, Weslaco, Texas. 33 p.

Gausman, H. W., W. A. Allen, R. Cardenas and A. J. Richardson. 1971 Effects of leaf age for four growth stages of cotton and corn plants on leaf reflectance, structure, thickness, water and chlorophyll concentrations and selection of wavelengths for

crop discrimination. Spectral survey of irrigated region crops and soils. USDA, ARS. P. O. Box 267, Weslaco, Texas. 2 p.

Gausman, H. W. 1971. Photomicrographic record of light reflected at 850 nanometers by cellular constituents of *Zebrina pendula* leaf epidermis. Spectral survey of irrigated region crops and soils. USDA, ARS. P. O. Box 267, Weslaco, Texas. 5 p.

Gausman, H. W., W. A. Allen, R. Cardenas and A. J. Richardson. 1972. Effects of leaf age for four growth stages of cotton and corn plants on leaf reflectance, structure, thickness, water and chlorophyll concentrations and selection of wavelengths for crop discrimination. Remote sensing of earth resources, Vol. 1, Univ. Tenn., Space Inst., Tullahoma, Tenn. p. 25-51.

Gerbermann, A. H., H. W. Gausman and C. L. Wiegand. 1969. Shadow and other background effects on optical density of film transparencies. Proc. workshop on aerial color photo. In plant sci. Univ. Fla., Gainesville, Fla. p. 127-129.

Goedheer, J. C. 1965. Fluorescence action spectra of algae and bean leaves at room and at liquid nitrogen temperatures. Biochem. Et. Biophys. Acta. 102:73-89.

Gold, V. M. 1969. Some ecological-physiological features of the action spectrum of photosynthesis at light saturation. Fiziol. Rast. 11:594-602 (In Russian).

Goldstein, R. A. and J. B. Mankin. 1971. Space-time considerations in modeling the development of vegetation. Workshop on tree growth, dynamics and modeling, Proc. IBP, E. Deciduous For. Biome, Oak Ridge Nat. Lab., Oak Ridge, Tenn. 18 p.

Grabau, W. E. and W. N. Rushing. 1968. A computer-compatible system for quantitatively describing the physiognomy of vegetation assemblages. Land evaluation. MacMillan Co. of Aust., 107 Moray St., S. Melborne, Victoria.

Gramms, L. C. and W. C. Boyle. 1971. Reflectance and transmittance characteristics of several selected green and blue-green unialgae. Proc. of 7th internat. symp. on RSE. Vol. III. Univ. Mich., WRL. infrared and opt. sensor lab. CRSIA, Ann Arbor, Mich. p. 1627-1650.

Grulois, J. 1968. Annual variation of reflection, interception and transmission of short wave radiation (In French). Bull. Soc. Roy. Bot. Belg. 102:13-25.

Harms, W. R. 1971. Estimating leaf-area growth in pine. Ecol. 52(5):931-934.

Heald, C. M., H. W. Gausman, L. N. Namken and C. L. Wiegand. 1970. Cotton plant response to nematocide treatments. Spectral survey of irrigated region crops and soils. USDA, 1970 Ann. Rep., Weslaco, Texas. 6 p.

Heinicke, D. R. 1963. The micro-climate of fruit trees. 2. foliage and light distribution patterns in apple trees. Proc. Am. Soc. Hort. Sci., Vol. 83.

Holdsworth, M. 1960. The spectral sensitivity of light-induced leaf movements. J. Exptl. Bot., 11(31):40-44.

Howard, J. A. 1971. The reflective foliaceous properties of tree species. Appl. of remote sensors in for. Joint rep. by working group. Intern. Union of For. Res. Organ., Sect. 25. p. 127-146.

Hughes, A. P., K. E. Cockshull and O. V. S. Heath, 1970. Leaf area and absolute leaf water content. Annu. Bot. 34:259-265.

Hundley, E. and J. H. G. Smith. 1957. Spectrophotometric analysis of foliage of some British Columbia conifers. Photo. Eng. 23:894-895.

Idso, S. B., R. D. Jackson, W. L. Ehrler and S. T. Mitchell. 1970. Infrared emittance determinations of leaves. USDA, ARS, Soil and Water Conserv. Div.

Idso, S. B. and D. G. Baker. 1968. The naturally varying energy environments and its effects upon net photosynthesis. Ecol. 49:311-315.

Idso, S. B., R. D. Jackson, W. L. Ehrler and S. T. Mitchell. 1970. A Method for the determination of infrared emittance of leaves. Ecol. 50(5):899-902.

Idso, S. B. and C. T. DeWit. 1970. Light relations in plant canopies. Appl. Optics 9:177-184.

Jeffers, D. L. and R. M. Shibles. 1969. Some effects of leaf area, solar radiation, air temperature and variety of net photosynthesis in field-grown crops. Crop Sci. 9(6):762-764.

Jordan, C. F. 1970. Derivation of leaf-area from quality of light on the forest floor. Ecol. 50(4):663-666.

Jordan, C. F. 1971. A world pattern in plant energetics. Am. Sci. 59(4):425-433.

Keegan, H. J. and H. T. O'Neill. 1951. Spectrophotometric study of autumn leaves. Proc. Opt. Soc. Am. 41:284.

Keegan, H. J., J. C. Schleter, W. A. Hall and G. M. Haas. 1955. Spectrophotometric and colorimetric study of foliage stored in covered metal containers. USDC, Nat. Bur. of Standards Rep. 4370.

Keegan, H. J., J. C. Schleter and W. A. Hall, Jr. 1955. Spectrophotometric and colorimetric change in the leaf of a white oak tree under conditions of natural drying and excessive moisture. USDC, NBS Proj. 0201-20-2325, NBS Rept. 4322.

Keegan, H. J., J. C. Schleter and W. A. Hall. 1956. Spectrophotometric and colorimetric record of some leaves of trees, vegetation and soil. USDC Nat. Bur. Standards. Rep. No. 4528, Wash., D.C.

Keegan, H. J. 1956. Spectrophotometric and colorimetric study of manually inoculated and field infected wheat rust. Nat. Bur. Standards. Rep. to Wright Air Dev. Cnt., Wright-Patterson AFB.

Keegan, H. J., J. C. Schleter, W. A. Hall, Jr., and G. M. Haas. 1956. Spectrophotometric and colorimetric record of some leaves of trees, vegetation and soil. USDC. NBS Proj. 0201-20-2325, NBS Rept. 4591.

Kleshin, A. F. and I. A. Sulgin. 1959. Ob opticskih svojstvah listev r rastenig (The optical properties of plant leaves). Dokl. Akad. Nauk., SSR. 125(5):1158-1161.

Knievel, D. P. and D. A. Schmer. 1971. Preliminary results of growth characteristics of buffalograss, blue grama, and western wheatgrass and methodology for translocation studies using 14-C as a tracer. IBP, Grassland biome, NREL. Tech. Rep. No. 86. Ft. Collins, Colo. 28 p.

Knipling, E. B. 1967. Physical and physiological basis for differences in reflectance of healthy and diseased plants. CRREL. Hanover, N.H. March 3. 26 p.

Knipling, E. B. 1970. Physical and physiological basis for the reflectance of visible and near-infrared radiation from vegetation. RSE. 1(3):155-159.

Knoeer, K. R. and L. W. Gay. 1965. Tree leaf energy balance. Ecol. 46(1.2):17-24.

Koltay, A. and w. Horvath. 1967. The effect of the spectral composition of light on the production and localization of dry matter (In Hungarian). Agrartud-Egyet. Merogazd. Tud Kar. Kozlemen, Godollo. p. 131-151.

Kondrat-yed, K. Y., Z. F. Mironowa and L. V. Dayeva. 1960. Spectral albedo of snow and the vegetative cover. Leningrad Universitet.

Krey, A. and G. Krey. 1964. Fluorescence changes in porphyridium exposed to green light of different intensity--a new emission band at 693 milimicrons and its significance to photosynthesis. Proc. Nas. 52(6):1568-1572.

Kumura, A. 1970. Studies on dry-matter production of soybean plant. G. changes in spectral composition of solar radiation penetrating through a leaf canopy and the photosynthetic rate of leaf as affected by light quality (In Japenese). Proc. Crop Sci. Soc. (Japan) 38(3):408-418.

Larson, W. E. and W. O. Willis. 1957. Light, soil temperature, soil moisture and alfalfa--red clover distribution between corn rows of various spacings and row directions. Agron. J. 49(7).

Latimer, P. 1959. Influence of selective light scattering on measurements of absorption spectra of chlorella. Plant Physiology 34:193-199.

Latimer, P. and E. Rabinowitch. 1956. Selective scattering of light by pigment containing plant cells. J. Chem. Phys. 24:480.

Lemon, E. 1963. Energy and water balance of plant communities. Env. control of plant growth. Acad. Press, N. Y. and London. p. 55-94.

Limperis, T. and D. George. 1966. Electromagnetic field signatures in the optical spectrum. Ann. N. Y. Acad. Sci. 140:175-189.

Lingova, S. and V. Stanev. 1969. Photosynthetically active radiation and maize plant development in relation to crop density (In Bulgarian). Khidrol. Meterol. 4:47-56.

Loomis, W. E. 1965. Absorption of radiant energy by leaves. Ecol. 46(1,2).

Macleod, N. 1972. Spectral reflectance measurements of plant-soil combinations. Fourth annual earth resources program review. NASA. Manned spacecraft cnt., Houston, Texas. 11 p.

McClellan, W. D., J. P. Meiners and D. G. Orr. 1963. Spectral reflectance studies on plants. Proceedings of the second symposium on remote sensing of environment. Univ. Mich., Cnt. for remote sending info. and analysis, Ann Arbor, Mich. p. 403-413.

McCree, K. J. and J. H. Troughton. 1966. Prediction of growth rate at different light levels from measured photosynthesis and respiration rates. Plant Physiol. 41:559-566.

McCree, K. J. 1972. The action spectrum, absorptance and quantum yield of photosynthesis in crop plants. Agr. Meterol. 9(3-4): 191-216.

Mestre, H. 1935. The absorption of radiation by leaves and algae. Cold Springs, Harbor Symposium on Quatative Biology 3:191-209.

Miller, P. C. and D. M. Gates. 1967. Transpiration resistance in plants. Am. Midland Natur. 77:77-85.

Moir, W. 1969. Green leaf area and leaf area display. No source.

Moir, W. H., Boratgis, R. Sherman and G. Paetsch. 1969. Photosynthesis of shortgrasses under field conditions. IBP Grasslands Biome, NREL. Tech. Rept. No. 31, Ft. Collins, Colo. 14 p.

Monteith, J. L. 1965. Light distribution and photosynthesis in field crops. Ann. Bot. 19:17-37.

Mooney, H. A. and M. West. 1964. Photosynthetic acclimation of plants of diverse origin. Am. J. Bot. 51:825-827.

Moss, R. A. and W. E. Loomis. 1952. Absorption spectra of leaves. I. The visible spectrum. Plant Physio., Vol. 27.

Mueller, I. E., P. H. Carr and W. E. Loomis. 1954. The submicroscopic structure of plant surfaces. Am. J. Bot. 41:593-600.

Musgrave, R. B. 1967. Factors limiting photosynthesis. Plant Food Rev. 13(2):5-7.

No Author. 1968. The solar radiation regime in the vegetative cover (In Russian). Acad. Sci. Estonian S.S.R., Inst. Phys. and Astr., Tartv. Russia. 148 p.

Oechel, W. C., B. R. Strain and W. R. Odening. 1972. Tissue water potential, photosynthesis. 14-C.-labeled photosynthate utilization, and growth in the desert shrub. Ecol. Monogr. 42(2):127-141.

Olson, C. D. and R. E. Good. 1962. Seasonal changes in light reflectance from forest vegetation. Photo. Eng., March. p. 107.

Olson, C. E. 1962. Seasonal trends in light reflectance from tree foliage. Photo-Interp., Delft, Neth.

Olson, C. E. and J. M. Ward. 1968. Remote sensing of changes in morphology and physiology of trees under stress. For. Remote Sensing Lab., Annu. Prog. Rep., Berkeley, Calif. 35 p.

Olson, C. E., Jr. 1963. Seasonal trends in light reflectance from tree foliage. Archives Internationalies de Photogrammetrie. 14:226-232.

Olson, C. E., Jr., R. E. Good, C. A. Budelsky, R. L. Liston and D. D. Munter. 1964. An analysis of light reflectance from tree foliage made during 1960 and 1961. Univ. Ill., Agr. Exp. Sta. 218 p.

Olson, C. E., Jr. 1969. Seasonal change in foliar reflectance of five broadleaved forest tree species. Univ. Mich., Dept. For. Ph.D. Diss., Ann Arbor, Mich. 112 p.

Olson, R. A., W. L. Butler and W. H. Jennings. 1962. The orientation of chlorophyll molecules, 'In vivo'--further evidence from dichroism. Biochem. Et Biophys. Acta 58:144-146.

Oster, G. 1948. The scattering of light and its applications to chemistry. Chemical Reviews 43:319-365.

Ovington, J. D., and D. B. Lawrence. 1967. Comparative chlorophyll and energy studies of prairie, savanna, oakwood, and maize field ecosystems. Ecol. 48:518-524.

Paleg, L. G. and D. Aspinall. 1970. Field control of plant growth and development through the laser activation of phytochrome. Nature. 228(5275):970-973.

Pearman, G. I. 1966. The reflection of visible radiation from leaves of some western Australian species. Aust. J. Biol. Sci. 19:97-103.

Pease, R. W. 1969. Plant tissue and the color infrared record. USGS. Interagency rep. NASA-147, Wash., D.C. 17 p.

Phillip, J. R. 1964. Sources and transfer processes in the air layers occupied by vegetation. J. Appl. Meteorol. 3:390-395.

Planet, W. G. 1970. Some comments on reflectance measurements of wet soils. RSE. 1(2):127-129.

Popp, H. W. and F. Brown. 1936. Effects of different regions of the visible spectrum upon seed plants. McGraw-Hill Book Co., N.Y., Chap. 22 In Biol. Effects of Radiat. Ed. by B. M. Duggar.

Rabideau, G. S., C. S. French and A. S. Holt. 1946. The absorption and reflection spectra of leaves. Chloroplast suspensions, and chloroplast fragments as measured in an Ulbright sphere. Am. J. Bot. 33:769-777.

Rauzi, F., and A. K. Dobrenz. 1970. Seasonal variation of chlorophyll in western wheatgrass and blue grama. J. of Range Manage. 23:372-373.

Riedacker, A. 1972. Measurement of different components of trees for physiological investigations. Forest biomass studies. Univ. Main. Coll. of Life Sci., Orono, Maine. p. 223-240.

Saeki, T. 1963. Light relations in plant communities. Env. control of plant growth. Acad. Press., N.Y. and London. p. 79-94.

Salisbury, F. B. and C. Ross. 1969. Plant physiology. Wadsworth Publishing Company, Belmont, Calif. 765 p.

Sanger, J. E. 1972. Quantitative investigations of leaf pigments from their inception in buds through autumn coloration to decomposition in falling leaves. Ecol. 52(6):1075-1089.

Sayn-Wittgenstein, L. 1970. Patterns of spatial variation in forests and other natural populations. Pattern Recognition. 2(4):245-253.

Schertz, F. M. 1929. Seasonal variation of the chloroplast pigments in several plants on the mall at Washington, D.C. Plant Physiol. 4:133-139.

Schieferstein, R. H. and W. E. Loomis. 1956. Wax deposits on leaf surfaces. Plant Physiol. 31:240-247.

Schieferstein, R. H. and W. E. Loomis. 1959. Development of the cuticular layers in angiosperm leaves. Iowa Agr. and Home Econ. Exp. Sta., J. Paper No. J-3584, Proj. No. 944 and 1139. p. 625-635, Ames, Iowa.

Shul-Gin, I. A., V. S. Khazanov, and A. F. Kleshnin. 1960. On the reflection of light as related to leaf structure. Dokl. Akad. Nauk. (SSSR), April.

Shul-Gin, I. A., A. F. Kleshins, M. I. Verbolora and V. Z. Podol-Nyi. 1960. An investigation of the optical properties of leaves of woody plants using the SF-4 spectrophotometer. Plant Physiol., (USSR) 7:247-252.

Shull, C. A. 1928. Reflection of light from the surfaces of leaves. Sci. 67:107-108.

Shull, C. A. 1929. Spectrophotometric study of reflection of light from leaf surfaces. Bot. Gazette, Vol. 87, June.

Sims, P. L., G. R. Lovell and D. F. Hervey. 1970. Seasonal trends in herbage and nutrient production of important sandhill grassis. IBP . Grasslands Biome, Reprint 12, Ft. Collins, Colo. 20 p.

Sinclair, T. R. 1968. Pathways of solar radiation through leaves. Purdur Univ., M.S. Thesis, Lafayette, Ind. 126 p.

Stair, R. and W. W. Coblentz. 1933. Infrared absorption spectra of some plant pigments. Nat. Bur. of Standards. J. Res. 11:703-711.

Stanhill, G. The effect of environmental factors on the growth of alfalfa in the field. Neth. J. Agr. Sci. 10:247.

Steg, L. and R. T. Frost. 1970. Visible polarization signature for remote sensing of soil surface moisture. COSPAR. Plenary Meeting, Leningrad, USSR. 15 p.

Steiner, Dieter Guterman and Thomas. 1966. Russian data on spectral reflectance of vegetation, soil, and rock types. U.S. Army, European Res. Off. 232 p.

Steiner, D. and T. Gutermann. 1966. Russian data on spectral reflectance of vegetation, soil, and rock types. Univ. Zurich, Switz., Dept. Geogr., Final Tech. Rep. on Contract No. DA-91-EUC-3863:10-652-0106. 232 p.

Tageeva, S. V., A. B. Brandt and V. G. Derevyanko. 1960. Changes in optical properties of leaves in the course of the growing season. Dokl. Akad. Nauk. SSSR. June.

Thomas, C. E., H. W. Gausman and R. Cardenas. 1970. Disease effects in the light reflectance of cantaloupe leaves. Spectral survey of irrigated region crops and soils. USDA, 1970 Ann. Rep., Weslaco, Texas. 1 p.

Thomas, J. R., V. I. Myers, M. D. Heilman and C. L. Wiegand. 1966. Factors affecting light reflectance of cotton. Univ. Mich., Proc. of the 4th symp. on RSE, June. p. 305-312.

Thomas, J. R., V. I. Myers, M. D. Heilman and C. L. Wiegand. 1966. Factors affecting light reflection of cotton. Proc. of the 4th symp. on RSE. Univ. Mich., Cnt. for remote sensing infor. and analysis. Ann Arbor, Mich. p. 305-312.

Thomas, J. R. 1970. Estimating leaf nitrogen content by reflectance measurements. USDA, ARS. P. O. Box 267, Weslaco, Texas, 78596.

Tranwuillini, W. 1964. Leaf temperature, evaporation and photosynthesis under different rates of air flow through the assimulation chamber with a note on evaporation at 200 m altitude. Ber. Deut. Bot. Ges. 77(6):204-218.

Tucker, C. J., and L. D. Miller. 1973. Spectro-Optical characteristics of selected plants of the Pawnee Intensive Site measured 'in situ'/ the flow of solar energy into the primary producers. IBP Tech. report (in preparation), Colorado State Univ., Ft. Collins. 70 p.

Tucker, C. J., L. D. Miller, and R. L. Pearson. 1973. Measurement of the combined effect of biomass, chlorophyll, and leaf water on canopy spectroreflectance of the shortgrass prairie. Proc. of the second annual Remote Sensing of Earth Resources conf. Univ. of Tennessee Space Institute, Tullahoma. 27 p. (in press).

Turrel, F. M. and S. W. Austin. 1965. Comparative nucturnal thermal budgets of large and small trees. Ecol. 46(1-2).

Uresk, D. M. 1971. Dynamics of blue grama within a shortgrass ecosystem. Ph.D. dissertation, Colorado State Univ., Ft. Collins. 52 p.

Van Bavel, C. H. M. 1967. Measuring transpiration resistance of leaves. Plant Physiol. 40:535-540.

Van Miegroet, M. 1965. Transmission and reflection of light by the leaves of some broadleaved species. Schweiz. Z. Forstwiss. 116(7):556-589.

Van Miegroet, M. and G. Vyncke. 1969. Transmission of light through tree leaves developed under artificial illuminations. Sylva Gandavensis, Gent. Vol. 13. 37 p.

Veress, S. A. 1972. Extinction coefficient. Photo. Eng. 38(2): 183-191.

Vernon, L. P. 1960. Spectrophotometric determination of chlorophylls and pheophytins in plant extracts. Analytical Chem. 32(9):1144-1150.

Waggoner, P. E. 1967. Moisture loss through the boundary layer. Internat. J. Biometeorol. 3:41-52.

Waggoner, P. E. and W. E. Reifsnyder. 1968. Simulation of the temperature, humidity, and evaporation profiles in a leaf canopy. J. Appl. Meteorol. 7:400-409.

Ward, J. M. 1969. The significance of changes in infrared reflectance in sugar maple, induced by soil conditions of drought and

salinity. Proc. of the Sixth Symp. on RSE. Univ. Mich., Cnt. for Remote Sensing Info. and Analysis. Ann Arbor, Mich. p. 1205-1226.

Watson, M. A. 1937. The estimation of leaf area in field crops. J. Agr. Sci., Vol. 27.

Weber, F. P. 1965. Exploration of changes in reflected and emitted radiation properties for early remote detection of tree vigor decline. Univ. Mich. Master's thesis.

Weigl, J. W. and R. Livingston. 1953. Infrared spectra of chlorophyll and related compounds. J. Am. Chem. Soc., Vol. 75, May.

West. N. E. 1972. Biomass and nutrient dynamics of some major cold desert shrubs. IBP. Desert Biome, Utah State Univ., Logan, Utah. 24 p.

Westlake, D. F. 1963. Comparisons of plant productivity. Biol. Rev. 38:385-425.

Weigand, C. L., H. W. Gausman, W. A. Allen and R. W. Leamer. 1969. Interaction of electromagnetic energy with agricultural crops. NASA. Earth Res. Aircraft Program - Status Rev. 14 p.

Willstätter, A. and K. Stoll. 1913. Untersuchungen über die-Assimilation der Kohlensäure, Verlag-Springer, Berlin.

Woolley, J. T. 1971. Reflectance and transmittance of light by leaves. Plant Physiol. 47:656-662.

Yentsch, C. S. 1971. The absorption and flourescence characteristics of biochemical substances in natural waters. Proc. of the Symp. on Remote Sensing in Marine Biol. and Fishery Res. Texas A & M Univ., Remote Sensing Cnt., Rep. TAMU-SG-71-106. College Station, Texas. p. 75-97.

Zscheile, F. P. 1934. An improved method for the purification of chlorophylls A and B-quantitative measurement of their absorption spectra-evidence for the existence of a third component of chlorophyll. Bot. Gazette 95:529-562.

Zscheile, F. P., J. W. White, Jr., B. W. Beadle and J. R. Roach. 1942. The preparation and absorption of five pure carotenoid pigments. Plant Physiol. 17:331-346.

Zunder, E. and K. Kreeb. 1970. Investigations into the potentiometric measurement of rates of photosynthesis (In German). Bericte der Deutschen Botanischen Gesellschaft 83(5-6):245-257.

Techniques for Measuring and Modeling the Primary Productivity of Grasslands

The references have been selected for inclusion over three topic areas:

1. The techniques and methods used for field data collection and analysis at the IBP Grassland Biome's Pawnee Intensive Site.

2. The methods of measuring herbage biomass and other vegetational characteristics.

3. The synthesis and management of grasslands is reviewed from a systems viewpoint.

Bledsoe, L. C. and G. M. Van Dyne. 1970. A compartment model simulation of secondary succession. IBP, Grasslands Biome, NREL, Reprint 4, Ft. Collins, Colo. 56 p.

Bonham, C. D. 1970. Statistical study of basic ecological variations in a shortgrass site. Univ. Ariz., Dept. of Watershed Mgt., Tech. Prog. Rep. Tucson, Aroz. 26 p.

Coleman. D. C., J. E. Ellis, J. K. Marshall and F. M. Smith. 1972. Basic field data collection procedures for the grassland biome. 1972 season. IBP, Grasslands Biome, NREL, Tech. Rep. No. 145, Ft. Collins, Colo. 86 p.

Crow, T. R. 1972. Estimation of biomass in an even-aged stand--regression and mean tree techniques. Forest Biomass Studies, Univ. Maine, Col. of Life Sci., Orono, Maine. p. 33-48.

Dickenson, C. E. 1972. Pawnee site plant live-dead separation. IBP, Grassland Biome, NREL, Tech. Rep. No. 140, Ft. Collins, Colo. 18 p.

Dickenson, C. E. and C. V. Baker. 1972. Pawnee site field plant list. IBP, Grassland Biome, NREL, Tech. Rep. No. 139, Ft. Collins, Colo. 44 p.

Dix, R. L. and R. G. Beidleman. 1969. The grassland ecosystem--a preliminary synthesis. IBP, Grasslands Biome, NREL, Range Sci. Series No. 2, Ft. Collins, Colo. 435 p.

Dixon, W. J., Ed. 1971. Biomedical computer programs. Univ. of Calif. Publications in Automatic Computation, No. 2. Calif. Press, Berkeley. p. 233-257.

Fletcher, J. E. and M. E. Robinson. 1956. A capacitance meter for estimating forage weight. J. Range Management. 9:96-97.

French, N. R. 1971. Basic field data collection procedures for the grassland biome. 1971 season. Colo. State Univ., NREL. Tech. Rep. No. 85, Ft. Collins, Colo. 87 p.

French, N. R., Ed. 1971. Preliminary analysis of structure and function in grasslands. IBP, Grassland Biome, NREL, Range Sci. Ser. No. 10, Ft. Collins, Colo. 387 p.

Hammond, A. L. 1972. Ecosystem analysis/biome approach to environmental research. Sci. 175(4017):46-48.

Harris, W. F., R. A. Goldstein and P. Sollins. 1971. Net aboveground production and estimates of standing biomass CN Walker Branch Watershed. IBP, E. Deciduous For. Biome, Memo Rep. 71-80, Oak Ridge, Nat. Lab., Oak Ridge, Tenn. 12 p.

Heilman, M. D., C. L. Gonzalez, W. A. Swanson and W. J. Rippert. 1968. Adaptation of a linear transducer for measuring leaf thickness. Agron. J. 60:578-579.

Hitchcock, A. S. 1935. Manual of the grasses of the United States. USDA. Misc. Pub. No. 200. Wash., D.C.

Hulett, G. K. and G. W. Tomanek. 1971. Herbage dynamics on a mixed prairie grassland near Hays, Kansas. IBP Grasslands Biome, NREL. Tech. Rep. No. 108, Ft. Collins, Colo. 34 p.

Jameson, D. A. 1970. Land management policy and development of ecological concepts. IBP, Grasslands Biome, NREL, Reprint 8, Ft. Collins, Colo. 22 p.

Jameson, D. A., Ed. 1970. Modeling and systems analysis in range science. Colo. State Univ., Range Sci. Dept., Sci. Ser. No. 5, Ft. Collins, Colo. 134 p.

Kinerson, R., Jr. and L. J. Fritxchen. 1971. Modeling a coniferous forest canopy. Agr. Meteorol. 8(6):439-445.

Knight, D. H. 1971. Some measurements of vegetation structure of the Pawnee Grassland. 1970. IBP, Grassland Biome, NREL, Tech. Rep. No. 72, Ft. Collins, Colo. 43 p.

Knight, D. H. 1972. Leaf area dynamics of the Pawnee Grasslands. IBP, Grassland Biome, NREL, Tech. Rep. No. 164, Ft. Collins, Colo. 22 p.

Lieth, H. 1972. Modeling and primary productivity of the world. Nature and Res. 8(2):5-10.

Love, R. M. 1970. The rangelands of western U.S. Sci. Am. 222(2): 89-96.

Milner, C. and R. E. Hughes. 1968. Methods for the measurement of the primary production of grasslands. IBP Handbook No. 6. Blackwell Sci. Pub., Oxford and Edinburgh. 70 p.

Mitchell, J. E. 1972. An analysis of the beta-attenuation technique for estimating standing crop of prairie range. J. Range Mgt. 25:300-304.

No Author. 1969. General description of the Pawnee Site. IBP, Grasslands Biome, NREL, Tech. Rep. No. 1, Ft. Collins, Colo. 31 p.

Owens, M., M. A. Learner and P. J. Maris. 1967. Determination of the biomass of aquatic plants using an optical method. J. Ecol. 55(3):671-676.

Pearson, R. L. and L. D. Miller. 1971. Design of a field spectrometer laboratory. Dept. of Watershed Sci., Sci. Ser. 2, Colo. State Univ., Ft. Collins. 102 p.

Pearson, R. L., L. D. Miller and K. J. Ranson. 1971. A field light quality laboratory--initial experiment/the measurement of percent of functioning vegetation in grassland areas by remote sensing methodology. IBP, Grasslands Biome, NREL, Tech. Rep. No. 90, Ft. Collins, Colo. 24 p.

Pearson, R. L., L. D. Miller and C. J. Tucker. 1973 (in preparation). Field spectrometer experimental data--1971; spectroradiance, spectroreflectance, spectroabsorptance, and spectrotransmittance of shortgrass prairie vegetation. Internal. Biol. Prog., Grassland Biome Prog., Tech. Rep., Colo. State Univ., Ft. Collins. 1600 p.

Philip, J. R. 1965. The distribution of foliage density with foliage angle estimated from inclined point quadrat observations. Australian J. of Bot. 13:357-366.

Preisendorfer, R. W. 1965. Radiative transfer on discrete spaces. Pergamon Press, New York. 459 p.

Ramsey, D. M., Ed. 1968. Image processing in biological science. Univ. Calif. Press.

Sims, P. L., D. W. Uresk, D. L. Bartos and W. K. Lauenroth. 1971. Herbage dynamics on the Pawnee Site/aboveground and below ground herbage dynamics on the four grazing intensity treatments/and preliminary sampling on the ecosystem stress site. IBP, Grassland Biome, NREL, Tech. Rep. No. 99, Ft. Collins, Colo. 95 p.

Smith, F. M. 1971. Growing season precipitation records, Central Plains Experimental Range A.R.S., Nunn, Colorado. IBP Grasslands Biome, NREL, Tech. Rep. No. 74, Ft. Collins, Colo. 73 p.

Smith, J. H. G. 1972. Bases for sampling and simulation in studies of tree and stand weights. Forest biomass studies. Univ. Maine. Coll. of Life Sci., Orono, Maine. p. 137-149.

Stickler, F. C., S. Wearden and A. W. Pauli. 1961. Leaf area determination in grain surghum. Agron J. 53(4):187-188.

Swartzman, G., Ed. 1970. Some concepts of modeling. IBP Grasslands Biome, NREL, TEch. Rep. No. 32, Ft. Collins, Colo. 143 p.

Teare, I. D., G. O. Matt and J. R. Eaton. 1966. Beta atteunation--a technique for estimating standing crop of prairie range. J. Range Mgt. 25:300-304.

Thilenius, J. F. 1966. An improved vegetation sampling quadrat. J. Range Mgt. 19(1):40.

Tucker, C. J., L. D. Miller, and R. L. Pearson. 1973 (in preparation). Field spectrometer experimental data--1972: spectroradiance, spectroreflectance, spectroabsorptance, and spectrotransmissance of shortgrass prairie vegetation. Internat. Biol. Prog., Grassland Biome Prog., Tech. Rep., Colo. State Univ., Ft. Collins. 2000 p.

Uresk, D. W. and P. L. Sims. 1969. Preliminary methodology and results for aboveground herbage biomass sampling of the Pawnee Site. IBP, Grasslands Biome, NREL, Tech. Rep. No. 33. Ft. Collins, Colo. 14 p.

Van Atta, G. F. 1936. Filters for the separation of living and dead leaves in monochromatic photographs with a method for determination of photographic filter factors. J. Biol. Photo. Assoc. 4(4):177-191.

Van Dyne, G. M., F. M. Glass and P. A. Opstrup. 1968. Development and use of capactiance meters to measure standing crop of herbaceous vegetation. Oak Ridge Nat. Lab., Rep. No. ORNL-TM-2247.

Van Dyne, G. M. 1969. Grasslands management, research and training viewed in a systems context. Colo. State Univ., Range Sci. Dept., Sci. Ser. No. 3. 39 p.

Van Dyne, G. M. 1971. Analysis of structure function, and utilization of grassland ecosystems. IBP, Grassland Biome, NREL, Prog. Rep. and Proposal, Ft. Collins, Colo. 363 p.

Van Wyk, J. J. P. 1972. A preliminary report on new separation techniques for live-dead aboveground grass herbage and roots from dry soil cores. IBP, Grassland Biome, NREL, Tech. Rep. No. 144, Ft. Collins, Colo. 16 p.

Warren Wilson, J. 1959. Analysis of the spatial distribution of foliage by two dimenstional point quadrats. New Phytol. 58: 92-101.

Warren Wilson, J. 1960. Inclined point quadrats. New Phytol. 59:1-8.

Warren Wilson, J. 1963. Estimation of foliage denseness and foliage angle by inclined point quadrats. Aust. J. Bot. 11:95-105.

Wear, J. F. 1968. The development of spectro-signature indicators of root disease impacts on forest stands. For. Remote Sensing Lab., Annu. Proc. Rep., Berkeley, Calif. 27 p.

Wells, K. F. 1971. Measuring vegetation changes on fixed quadrats by vertical ground sterophotography. J. Range Mgt. p. 233-236.

Wendlandt, W. W. and R. G. Hecht. 1966. John Wiley and Sons, Inc., 605 3rd Ave., N.Y., N.Y. 10016. Cragg, J. B., Ed.

Young, H. E. 1972. Biomass sampling methods for puckerbrush stands. Forest biomass studies, Univ. Maine, Coll. of Life Sci., Orono, Maine. p. 177-190.

Applications of Remote Sensing to Grassland Research and Management

Various studies of the applications of remote sensing technology to the measurement of types of grasslands, their productivity, and their management are referenced in this section. Major emphasis is given to the spectral methods for measuring herbage biomass and the estimation of other biological parameters of grassland vegetation such as species type, soil and plant moisture, status, etc.

Burke, G. F. and R. C. Wilson. 1939. A vegetation inventory for aerial photographs. Photo. Enc. 5(1):30-42.

Carneggie, D. M. and D. T. Lauer. 1966. Uses of multiband remote sensing in forest and range inventory. Photogrammetria. 21:115-141.

Carneggie, D. M. 1968. Analysis of remote sensing data for range resource management. For. Remote Sensing Lab., Annu. Prog. Rep., Berkeley, Calif. 24 p.

Carneggie, D. M. 1964. Remote-sensing applications for the inventory of range resources. NASA, Earth Res. Aircraft Program, Status Rev. 27 p.

Carneggie, D. M. 1968. Large scale 70mm photography - A potential tool for improving range resource inventories. Papers on the 34th annual meeting. ASP. Falls Church, Va.

Carneggie, D. M. 1970. Remote sensing/Review of Principles and Research in Range and Wildlife Management. USFS. Misc. Pub. no. 1147. GPO. Wash., D.C. 165-178 p.

Chase, M. E. 1969. Airborne remote sensing for groundwater studies in prairie environment. Can. J. of Earth Sci. 6(4):737-741.

Clouston, J. G. 1950. The use of aerial photographs in range inventory work on the national forests. Photo. Eng. 16(3).

Colwell, R. and W. Draeger. 1969. Vegetation resource - user requirements versus remote sensing capabilities. NASA. Earth Res. Aircraft program - Status Rev. 71 p.

Colwell, R. N. 1961. Aerial photographs show range conditions. Univ. of Calif., Calif. Agr., Berkeley, Div. Agr. Sci. 15(12):12-13.

Colwell, R. N. and D. L. Olson. 1965. Thermal infrared imagery and its use in vegetation analysis by remote aerial reconnaissance. Proc. of the third symp. on remote sensing of environment. Univ. Mich., Cnt. for Remote Sensing Inf. and Analysis. Ann Arbor, Mich. p. 607-621.

Colwell, R. N. 1972. The future for remote sensing of agricultural, forest and range resources. U.S. House of Representatives 13th panel on sci. and tech. GPO. Rep. 71-749. Wash., D.C. 14 p.

Condon, R. W. 1968. Estimation of grazing capacity on arid grazing lands. Land evaluation. MacMillan Co. of Aust., 107 Moray St., S. Melborne, Victoria.

Ceullar, J. A. 1971. Correlation of ground cover estimated from aerial photos with ground observations. Spectral survey of irrigated region crops and soils. USDA, ARS. P. O. Box 267. Weslaco, Texas. 5 p.

Draeger, W. C. 1968. The interpretation of high altitude multi-spectral imagery for the evaluation of range resources. For. Remote Sensing Lab., Annu. Prog. Rep., Berkeley, Calif.

Driscoll, R. S. and J. N. Reppert. 1968. The identification and quantification of plant species, communities and other resource features in herbland and shrubland environments from large scale aerial photography. For. Remote Sensing Lab., Annu. Prob. Rep., Berkeley, Calif. 52 p.

Driscoll, R. S. 1969. Aerial color and color infrared photography--some applications and problems for grazing resource inventory. Proc. workshop on aerial color photo. in Plant Sci., Univ. Fla., Gainesville, Fla. p. 140-149.

Driscoll, R. S. 1970. Identification and measurement of shrub type vegetation on large-scale aerial photographs. Third annual earth resources program review. NASA, Manned Space-craft Cng., Houston, Texas. 15 p.

Driscoll, R. S. and R. E. Francis. 1971. Multistage, multiband and sequential imagery to identify and quantify non-forest vegetation resources. USFS, R.M. For. and Range Exp. Sta., Ft. Collins, Colo. 75 p.

Driscoll, R. S. 1972. Pattern recognition of native plant communities--Manitou Colorado test site. Fourth annual earth resources program review. NASA. Manned Spacecraft Cnt., Houston, Texas. 28 p.

Dwornik, S. F., L. M. Young and J. Grande. 1962. Reflectance studies of vegetation damage and soil density changes. Project gnome. U.S. Army Eng. Res. Dev. Lab., Tech. Sum. Rept. 1, Nov. 17, 1961 - March 15, 1962. Ft. Belvoir, Va.

Egan, W. G. 1970. Optical remote sensing of bioresources. Grumman Aerospace Corp., Bethpage, N.Y. p. 303-316.

Falkner, E. H. 1960. Applying photogrammetry to range allotment planning. Photo. Eng. 26(4):672-674.

Frank. C. R. 1970. Management of grazing lands by earth resources satellites. Proc. Princeton Univ. Conf. on Aeros. Methods for Revealing and Evaluating Earth's Res. Princeton Univ. Conf., Princeton, N.J. 21 p.

Gittins, W. J. 1970. The determination of vegetal cover using multiband aerial photography. Internat. Symp. on photointerpretation. Univ. of Melbourne, Sch. For., Melbourne, Ast. p. 267-280.

Jameson, D. A., R. K. Gierisch, S. Wallace and R. Robinson. 1970. Range condition evaluation by discriminant analysis. Colo. State Univ., Range Sci. Dept. Sci. Ser. No. 8. Ft. Collins, Colo. 26 p.

Kuchler, A. W. 1967. Vegetation mapping. Ronald Press, N.Y.

Lent, J. D. and J. D. Nichols. 1970. Machine-aided photo interpretation techniques for vegetation analysis. AIAA earth resources observation and information system meeting. March 2-4. Am. Inst. Aeron. Astr., Rep. 70-308, N.Y., N.Y. 8 p.

Leontyeva, Y.V. 1964. The use of photosurveying materials in large scale mapping of the forest-steppe and steppe vegetation of northern Kasakhstan. Aerial photo. used in mapping vegetation and soils. Sci. Pub. House, Moscow, Russ. p. 40-65.

McDonald, R. B. and D. Landgrebe. 1967. Remote sensing for agriculture and natural resources from space. AAAS, Proc. 1967 Nat. Symp. 6:14.

Miller, L. D. and R. L. Pearson. 1971. Aerial mapping program of the IBP grassland biome/remote sensing of the productivity of the shortgrass prairie as input into biosystem models. Proc.

of 7th internat. symp. on RSE, Univ. Mich., WRL. Infrared and Opt. Sensor Lab. CRSIA. Ann Arbor, Mich. p. 165-205.

Morain, S. A. and D. S. Simonett. 1966. Vegetation analysis with radar imagery. Proceedings of the fourth symposium on remote sensing of environment. Univ. Mich., Cnt. for remote sensing info. and analysis. Ann Arbor, Mich. p. 605-622.

No Author. 1967. Potential benefits to be derived from applications of remote sensing of agriculture, forest and range resources. Cornell Univ., Cnt. for Aerial Photo. Studies. Hollister, all. No. 3.

No Author. 1971. Analysis of remote sensing data for evaluating vegetation resources. Univ. of Calif. Sch. of For. and Conserv. Berkeley, Calif. 197 p.

Null, W. S. 1969. Photographic interpretation of canopy density--a different approach. J. For. 67(3):175-177.

Orshan, G. 1969. Use of vegetation as an indicator for soil properties under desert conditions. Hebrew Univ. Jerusalem, Dept. of Bot. Israel. 67 p.

Paulsen, H. A., Ed. and E. H. Red., Ed. 1970. Range and wildlife habitat evaluation/aresearch symposium. USFS, Misc. Pub. No. 1147. GPO. Wash., D.C.

Pearson, R. L. and L. D. Miller. 1972. Remote spectral measurements as a method for determining plant cover. Technical report 167, Grassland Biome, IBP, Colorado State Univ., Ft. Collins, Colorado.

Pearson, R. L. and L. D. Miller. 1972. Remote mapping of standing crop biomass for estimation of the productivity of the shortgrass prairie, Pawnee National Grassland, Colorado. Proc. of the Eighth Intern. Symp. on Remote Sensing of Environment, Univ. of Michigan, Ann Arbor, Michigan.

Pettinger, L. R. 1970. The application of high altitude photography for vegetation resource inventories in southeastern Arizona. Univ. of Calif. For. Remote Sensing Lab., Final rep., Berkeley, Calif. 148 p.

Poulton, C. E., R. J. Schrumpf and E. Garcia-Moya. The feasibility of inventorying native vegetation and related resources from space photography. For. Remote Sensing Lab. Ann. Prog. Rep. Berkeley, Calif. 27 p.

Poulton, C. E. 1968. The feasibility of inventorying native vegetation and related resources from space photography. NASA Earth Res. Aircraft Program - Status Rev. 24 p.

Poulton, C. E. 1970. Practical application of remote sensing in range resources development and management. USFS, Misc. Pub. No. 1157. GPO. Wash., D.C. p. 179-189.

Poulton, C. E., D. P. Faulkner and B. J. Schrumpf. 1970. A vegetational inventory and ecological resource analysis from space and high flight photography. Third annual earth resources program review. NASA. Manned Spacecraft Cnt., Houston, Texas. 14 p.

Reid, E. H. and G. D. Pickford. 1942. An appraisal of range survey methods from the standpoint of effective range management. P.N.W. For. and Range Exp. Sta., Portland, Oregon. Range Res. Rep. No. 2. 66 p.

Reid, E. H. and G. D. Pickford. 1944. An appraisal of range survey methods. J. For. 42:47;-479/

Schulte, O. W. 1951. The use of panchromatic infrared, and color aerial photography in the study of plant distribution. Photo. Eng., Dec.

Stellingwerf, D. A. 1966. Practical applications of aerial photographs in forestry and other vegetation studies Series B. No. 36. ITC for aerial Surv., Delft, Neth. 60 p.

Stellingwerf, D. A. 1968. Practical applications of aerial photographs in forestry and other vegetation studies. IIases, Ser. B, No. 46. Delft, Neth. 68 p.

Tueller, P. T. and G. Lorain. 1972. Application of remote sensing techniques for analysis of desert biome validation studies. IBP. desert biome. Renewable Res. Cent., Univ. Nevada, Reno, Nevada. 5 p.

Turner, R. M. 1970. Measurement of plant community cover from aerial photographs using Ektachrome infrared aero film. Third annual earth resources program review. NASA. Manned Spacecraft Cnt., Houston, Texas. 8 p.

Vinogradov, B. V. 1964. The classification and mapping of desert vegetation combinations in central Turkmenia according to the materials of aerial surveying. Aerial photo. used in mapping vegetation and soils. Sci. Pub. House, Moscow, Russ. p. 69-93.

Vinogradow, B. V. and Y. N. Kudryavteseva. 1964. The experience of interpreting and mapping fodder land on deserts and semi-deserts from aerial photographs. Aerial photo. used in mapping vegetation and soils. Sci. Pub. House, Moscow, Russ. p. 140-181.

Vinogradov, B. V. 1966. Aerial analysis of vegetation in arid zones. Aerometody izucheniya rastitelnosti arionykh zon. navka., Moskow. 503 p.

Vinogradov, B. V. 1968. Experience in large-scale landscape interpretation and mapping of key sectors in the arid and subarid zones of central Asia and Kazakhstan. Army For. Sci. and Tech. Center. Wash., D.C. 37 p.

Vinogradov, B. V. 1969. Remote sensing of the arid zone vegetation in the visible spectrum for studyin g the productivity. Proc. of the Sixth Symp. on Remote Sensing of Environment. Univ. Mich., Cnt. for remote sensing info. and analysis. Ann Arbor, Mich. p. 1237-1250.

Wagner, T. W. and J. E. Colwell. 1969. An investigation of grassland resources using multispectral processing and analysis techniques. Univ. Mich., WRL. Rep. 34795-1-F, Ann Arbor, Mich. 77 p.

Weber, F. P. 1966. Multi-spectral imagery for species identification. USDA. P.S.W. For. and Range Exp. Sta., Annual Prog. Rep., Sept. 30th.

Wenderoth, S. and E. Yost. 1969. Applications of multispectral false-color photography to the plant sciences. Proc. Workshop on Aerial Color Photo. In Plant Sci. Univ. Fla., Gainesville, Fla. p. 53-68.

Warren Wilson, J. 1959. Analysis of the distribution of foliage in grassland. The measurement of grassland productivity. Acad. Press. N.Y., N.Y.